THE MOLECULAR MECHANISMS UNDERPINNING METABOLIC REPROGRAMMING IN INNATE IMMUNITY AND CARCINOGENESIS: INSIGHTS FROM TOLL-LIKE RECEPTOR SIGNALLING

by

PHILEMON NJENDE UBANAKO

Student Number: 456991

Thesis submitted in fulfilment of the requirements for the degree of Doctor of Philosophy in Molecular and Cell Biology

FACULTY OF SCIENCE

at the

UNIVERSITY OF THE WITWATERSRAND

JOHANNESBURG

SOUTH AFRICA

Supervisor: Prof. M.M. NTWASA

Co-supervisor: Prof. R. VEALE

April 2019

DECLARATION

I declare that this thesis is my own, unaided work. It is being submitted for the degree of Doctor of Philosophy (PhD) to the Faculty of Science, University of the Witwatersrand, Johannesburg, South Africa. This thesis has not been submitted to any other Institution for any degree or examination.

_____

Philemon Njende Ubanako

April 2019

SUMMARY

Tumour cells reprogram their metabolism by boosting glycolysis and suppressing oxidative phosphorylation despite adequate oxygen levels; a phenomenon known as the Warburg effect. Innate immune cells such as macrophages and dendritic cells also mimic the Warburg effect following infection for immune activation. Up to 20% of all lethal cancers are associated with infection. Microbial oncogenic transformation has been shown to be elicited by chronic inflammation because of prolonged infection. Nonetheless, metabolic reprogramming associated with infection has received little attention as a possible promoter in microbial carcinogenesis.

THP-1 (acute monocytic) and K562 (chronic myelogenous) leukaemia cells were treated with TLR4 agonist, bacterial lipopolysaccharides at 5, 10 and 20 ng/ml for 24 and 48 hours. To evaluate cytokines synthesized, a multi-analyte ELISA array kit was used to investigate the expression of 12 pro-inflammatory cytokines. To further validate cytokine expression at the transcriptional level, reverse RT-PCR using gene-specific primers of upregulated cytokines observed in ELISA was performed. L-lactate and mitochondrial membrane potential assays were used to investigate metabolic reprogramming. Cell cycle analysis and cell viability assays were done. Finally, two *in silico* tools (GeneMANIA and IMP) were used to investigate gene interaction pathways and biological processes using upregulated cytokines and some glycolytic genes.

In the present study, it is demonstrated that, in THP-1 monocytes, LPS can enhance the glycolytic phenotype in a TLR4-dependent manner. Although this has also been demonstrated in macrophages, this is the first time in undifferentiated monocytes. LPS also caused a decline in mitochondrial membrane potential which is characteristic decreased OxPhos. Furthermore, THP-1 monocytes were shown to upregulate pro-inflammatory chemokines; RANTES, IL8, MIP-1 and MDC at mRNA and protein levels in a TLR4-dependent manner. Interestingly, this study showed that RANTES, which was highly upregulated in THP-1 monocytes was not expressed in another myeloid-derived line – the K562 erythroleukaemia cell line even after LPS stimulation. Furthermore, LPS-mediated glycolytic phenotype in THP-1 monocytes which is reminiscent of the Warburg effect, is not accompanied by increased cell proliferation in this study and instead cell death is noticed upon LPS treatment. Furthermore, this study showed that the upregulated cytokines can be co-expressed and/or co-localised with certain glycolytic genes and glucose

transporters (GLUT1 and GLUT3) suggesting a pathway for the observed enhancement for the glycolytic phenotype. Most importantly, all the upregulated cytokines were co-expressed with HK3, an enzyme that catalyses the first, irreversible step of glycolysis and has been shown to be instrumental in leukaemia pathogenesis.

These findings show that infection-induced cytokines may interact with glycolytic genes to upregulate a glycolytic phenotype. However, glycolysis is dispensable for cell proliferation in THP-1 cells given that induction of the Warburg effect is insufficient to drive cell proliferation in THP-1 cells. These results indicate that innate immune cells express important chemokines which may influence their metabolic program. Furthermore, the study proposes that chemokines influence the metabolic programme in THP-1 monocytes likely through mechanisms that involve the glucose transporters (GLUT1 and GLUT3), HK3 and other glycolytic proteins.

DEDICATION

This thesis is dedicated to God Almighty.

Who has put wisdom in the inward parts? Who has given understanding to the heart?

Job 38:36.

For the LORD gives wisdom; from his mouth come knowledge and understanding.

Proverbs 2:6

PRESENTATIONS

Meeting	Presentation Title	Authors	Venue	Date	Type of Presentation
South African Society for Biochemistry and molecular biology (SASBMB) congress 2016	Mechanisms of Apoptosis in ovarian cancer	Philemon Ubanako, Lesetja Motadi	East London The East London International Convention Centre Eastern Cape	10th to 14th July 2016	Oral
Molecular Biosciences Research Trust (*MBRT*) Research Day-MBRT 2016	Elucidating molecular mechanisms of metabolic reprogramming in innate immunity and carcinogenesis	Philemon Ubanako, Monde Ntwasa	WITS Club, West campus, University of Witwatersrand	08-12-2016	Poster
Wits Cancer symposium 2017	Mechanisms of metabolic reprogramming in innate immunity and carcinogenesis: Insights from TLR signalling	Philemon Ubanako, Monde Ntwasa	Faculty of health sciences, University of Witwatersrand.	09-02-2017	Poster

PUBLICATIONS

Articles

1. **Ubanako, P.N**, Choene, M. and Motadi, L., 2015. Mechanisms of apoptosis in ovarian cancer: The small molecule targeting. *International Journal of Medicine and Medical Sciences*, *7*(3), pp.46-60.
2. **Ubanako**, **P.N**, Xelwa, N and Ntwasa, M. LPS induces inflammatory chemokines via TLR-4 signalling and enhances the Warburg Effect in THP-1 cells
   In preparation
3. Elumalai, R., **Ubanako, P.N**, Tichaona, N. Ntwasa, M., Raichur, A.M, and Mamba, B. Sericin-Heparin microcapsules for Dox delivery in leukemia
   In preparation

Book chapter

4. Ntwasa, M and **Ubanako, P.N** (2018). Glucose Metabolism and Carcinogenesis: The Impact of the Tumor Suppressor p53. In Neoplasm (Rijeka: IntechOpen), p. 109 Ch. 5. Book title & ISBN: *"Neoplasm,"* 978-1-78923-778-8. DOI: 10.5772/intechopen.75976

ACKNOWLEDGEMENTS

To God, Almighty for a vision, wisdom, strength and courage.

My supervisor, Prof. Monde Ntwasa for all his guidance, mentorship, encouragement throughout my project.

My elder brother, Valentine Ubanako, for his love, encouragement, financial, moral and spiritual support.

To my parents Godfred and Christina Ubanako, and all my siblings: Gideon, Clarise, Ralph and Blaise for their love, support and encouragement.

The “FlyLab” family, Emmanuel, Bernice, Ntombi, Zanele, Charmy: you guys have been very supportive throughout my studies.

My co-supervisor, Prof. R. Veale for his encouragement and support.

To MCB staff and postgraduates: I am grateful for all your help.

To Dr. Heather Hong, Dr. Leonie Harmse and Zeenat Ismael: thank you for your support.

To Pastor France Khawulela for his spiritual support and encouragement.

To the South African National Research Foundation and Financial Aid Office for the Postgraduate Merit Award: Thank you for financial support.

LIST OF ABBREVIATIONS

Akt- Protein Kinase B

ATP-Adenosine triphosphate

Bax-Bcl-2-associated X protein

Bcl_2-B-cell lymphoma 2 protein

BSA- Bovine serum albumin

DMEM-Dulbecco's modified eagle medium

DNA- Deoxyribonucleic acid

DNase- Deoxyribonuclease

EDTA- Ethylenediaminetetraacetic acid

EGFR- Epidermal Growth Factor Receptor

$FADH_2$-flavin adenine dinucleotide-hydroquinone form

FCCP- carbonyl cyanide-p-trifluoromethoxyphenylhydrazone

GeneMANIA- Gene Multiple Association Network Integration Algorithm

GPCR-G-protein-coupled receptor

HIF-1α-Hypoxia-inducible factor 1α

IFN-interferon

IKK- IκB kinase

IMP- Integrative Multi-species Prediction

IRAK- Interleukin-1 receptor-associated kinase

IRF- IFN regulatory factor

K-RAS- Kirsten rat sarcoma

LPS-Lipopolysaccharide

MD2- myeloid differentiation protein 2

MHC- Major Histocompatibility complex

ml-millilitre

mRNA- Messenger RNA

mTOR- mammalian target of rapamycin

MyD88-Myeloid differentiation factor 88

NADH-reduced nicotinamide adenine dinucleotide

NCBI- National center for biotechnology information

NFκB-Nuclear factor kappa B

PAMP-pathogen-associated molecular pattern

PFKFB3-6-phosphofructo-2-kinase/fructose-2,6-biphosphatase 3

PI3K-phosphatidylinositol-3-kinase

PCR- Polymerase chain reaction

PDGF- Platelet-Derived Growth Factor

PPI- Protein-protein interaction

PRR-pattern recognition receptor

Ras-Rat sarcoma protein

RNA- Ribonucleic acid

RNase- Ribonuclease

Rpm- Revolutions per minute

RPMI-Roswell Park Memorial Institute medium

SARM-sterile α and hydroxyphenyl-ethyl-aminomethyl-tetralone-armadillo motif

siRNA-small interfering RNA

SLC15A4- Solute Carrier Family 15 member 4

Src-Sarcoma protein

TAG-Transient axonal glycoprotein

TBE- Tris borate EDTA buffer

THP-1- Tohoku Hospital Pediatrics-1

TIR-Toll/IL1 receptor domain

TLR4- Toll-like receptor 4

TNF-Tumour-necrosis factor

TNFR- Tumour-necrosis factor receptor

TRAF- TNFR-associated factor

TRAM- TRIF-related adaptor molecule

TRIF- (TIR) domain-containing adaptor inducing IFN-β

VDAC-Voltage-dependent anion channels

VEGF- Vascular epidermal growth factor

α- Alpha

β- Beta

κ-Kappa

µL-microlitre

TABLE OF CONTENTS

LIST OF FIGURES

LIST OF TABLES

Chapter 1 –Literature review

1.1 Cancer overview

Cancer is a group of diseases characterised by unrestrained cell proliferation, invasion and metastasis, caused by genetic and epigenetic abnormalities (Bender et al., 1998; Hanahan and Weinberg, 2000). It is the second main cause of mortality worldwide according to the World Health Organisation (WHO); with approximately 9.8 million deaths in 2018 (WHO, 2018). According to the WHO, about 70% of cancer-related deaths occur in middle- and low-income countries. Most worryingly, about 14 million new cancer cases are diagnosed every year worldwide, with more than 100 thousand South Africans diagnosed per annum. According to the Cancer Association of South Africa (2018), the global mortality rate for cancer exceeds that of HIV/AIDS, tuberculosis and malaria combined. About 20% of cancers worldwide are caused by micro-organisms, with a staggering 12% caused by oncoviruses and more than 80% of cases occurring in the developing world (Parkin, 2006). About 90% of all cancers are of epithelial origin (carcinomas) and it is known that infectious agents first come in contact to their host by adhering to epithelial surfaces.

Carcinogenesis is a multi-stage process by which normal cells are transformed into cancer cells. It exhibits the following phases: initiation, promotion, progression and metastasis (Siddiqui et al., 2015). The challenge with cancer remains our limited understanding of the molecular mechanisms involved in carcinogenesis. Even though our knowledge of such mechanisms and pathways is on the rise, the mortality from cancer does not seem to be slowing down. A faster pace of knowledge acquisition on molecular mechanisms involved in carcinogenesis and a corresponding boost in translational medicine is therefore imperative to combat cancer.

1.2 Hallmarks of cancer

Cancer hallmarks are phenotypic changes that differentiate cancer cells from normal cells. They were first proposed by Hanahan and Weinberg (2000) who suggested that cancers are characterised by hallmarks that are acquired during the multi-stage process of tumour development. These hallmarks include: Resisting cell death, sustaining proliferative signals, evading growth

suppression, activating invasion and metastasis, inducing angiogenesis, enabling replicative immortality, avoiding immune destruction, genomic instability, tumour-promoting inflammation and metabolic reprogramming (Warburg effect) (Colotta et al., 2009; Hanahan and Weinberg, 2011). These hallmarks are depicted in **Figure 1.1**.

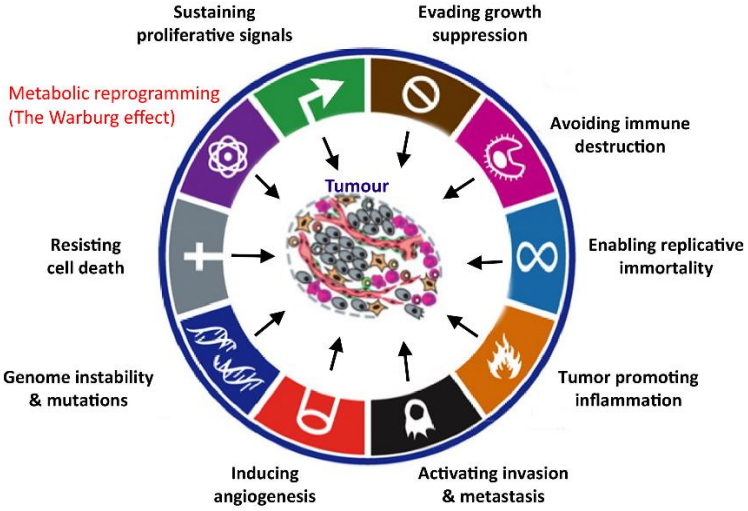

Figure 1.1. **The hallmarks of cancer**. Modified from Hanahan and Weinberg (2000). The Warburg effect—the hallmark investigated in this study, is written in red. Tumours are characterised by several phenotypic changes (hallmarks) which differentiate them from normal cells.

It appears that the process of drug discovery and development is dependent on our understanding of the mechanisms that underpin the hallmarks of cancer; given that these hallmarks differentiate normal from cancer cells. For example, the hallmark, "sustaining proliferative signals", can be targeted using a tyrosine kinase inhibitor, imatinib mesylate in chronic myeloid leukaemia (CML) patients. Imatinib mesylate targets a constitutively active tyrosine kinase known as Bcr-Abl protein caused by a mutation which is common in more than 90% of patients suffering from CML (Dagher et al., 2002; Savage and Antman, 2002). Other examples include the use of angiogenesis inhibitors and chemotherapy-induced apoptosis which target the hallmarks "inducing angiogenesis" and "resisting cell death" respectively (El-Kenawi and El-Remessy, 2013; Kaufmann and Earnshaw, 2000).

This study will focus on the Warburg effect and its potential impact on infection-associated carcinogenesis. As a bioenergetic hallmark, the Warburg effect describes altered cellular ATP-synthesising machinery in many cancers which shows upregulated glycolysis and suppressed

oxidative phosphorylation (OxPhos), despite adequate oxygen levels. It has been proposed that rapidly-dividing cells require enough energy and metabolites for biosynthesis and optimized energy supply. Hence, these metabolic changes are geared toward improving energy supply and metabolite synthesis which are required for proliferation (Heiden et al., 2009). However, it is important to review ATP synthesis mechanisms in normal cells before reviewing metabolic reprogramming in carcinogenesis.

1.2.1 Metabolism of ATP synthesis: focusing on glycolysis and OxPhos

Glycolysis is activated when glucose is transported into the cell by glucose transporters, known as the GLUT/SLC2A receptors (James et al., 1988). The glucose molecule binds to the receptor on the extracellular surface of the cell, leading to a conformational change in the transporter which enables the import of glucose into the cell (Cloherty et al., 1995, 1996; Oka et al., 1990). **Figure 1.2** summarises the process of glycolysis.

The process of glycolysis, which occurs in the cytosol through a series of enzyme-catalysed reactions, generates two 3-carbon molecules of pyruvate from a 6-carbon glucose molecule with a net production of 2 ATP molecules, and 2 NADH molecules. In the presence of oxygen, pyruvate enters the mitochondrion and is oxidised to acetyl-CoA, while reducing NAD+ to NADH in the reaction and releasing carbon dioxide. Acetyl-CoA, a 2-carbon molecule, is then fed into the citric acid cycle and combines with oxaloacetic acid (4-carbon molecule) to form citrate (Cox et al., 2013). The citric acid cycle is a series of enzyme-catalysed reactions that essentially oxidise acetyl-CoA into carbon-dioxide (CO_2) and generate ATP. In addition, the TCA cycle generates precursors for the synthesis of certain amino acids, reducing equivalents, NADH (three molecules per cycle) and one $FADH_2$ molecule which get utilised subsequently in the electron transport chain (ETC) as electron acceptors for the synthesis of ATP. In most cancer cells, most of the pyruvate molecules are converted into lactate and exported out of the cell via monocarboxylate transporters (MCTs) (**Figure 1.2**) despite adequate oxygen supply. This lactate efflux leads to extracellular acidification of the tumour microenvironment which may stimulate immune evasion by cancer cells (Calcinotto et al., 2012; Lardner, 2001).

Following glycolysis, the preparatory phase and the citric acid cycle, 10 NADH and 2 $FADH_2$ molecules are produced per molecule of glucose. These high-energy electron carriers get reduced by sequentially donating their electrons to protein complexes (Complex I to Complex IV for NADH and Complex II to Complex IV for $FADH_2$) studded in the mitochondrial inner membrane. The transfer of electrons from NADH, for example, to NADH dehydrogenase (Complex I), causes protons to be taken up from the mitochondrial matrix and pumped to the mitochondrial intermembrane space. In summary, the mitochondrial inter-membrane space becomes highly positively charged following the pumping of protons from electron transport chain protein complexes (Mitchell, 1974, 2011). Complex IV then transfers its electrons to molecular oxygen, the final electron acceptor, and reduces it to water. The high potential difference across the mitochondrial inner membrane (mitochondrial membrane potential (MMP)) causes protons to flow back through ATP synthase, a multi-subunit complex, into the matrix. This proton motive force drives ATP synthase which couples ADP via mechanical action to inorganic phosphate to generate ATP. The pumping of protons to the mitochondrial inter-membrane space creates a potential difference across the mitochondrial inner membrane which is critical for the chemiosmotic synthesis of ATP (Mitchell, 1974, 2011; Mitchell and Moyle, 1967).

The mitochondrial membrane potential (MMP) is not only relevant for the chemiosmotic synthesis of ATP but is also an important parameter in overall cell viability. It is imperative that the inner mitochondrial membrane of eukaryotic cells be maintained at a hyperpolarised state. In the event of the dissipation of the positive charge in the intermembrane space, voltage-sensitive permeability transition pores will be triggered to open, causing the release of pro-apoptotic mediators such as cytochrome C to the cytoplasm, eventually leading to apoptosis (Zamzami and Kroemer, 2001). Reactive oxygen species (ROS) such as superoxides, hydroxyl radicals, peroxides, and the singlet oxygen are generated primarily by the reaction of electrons with oxygen mainly at Complex I and Complex III. ROS are potentially DNA- and membrane-damaging molecules. This makes it necessary for the cell to convert ROS to less harmful intermediates.

The MMP is tightly regulated by uncoupling proteins that are sensitive to excessive levels of reactive oxygen species (Boss et al., 2000). High levels of ROS, indicative of high OxPhos activity trigger uncoupling proteins to reduce the MMP by pumping protons back into the mitochondrial

matrix. This, in turn, leads to a drop in OxPhos, thereby protecting the cells from the damaging effects of excessive ROS (Boss et al., 2000; Valle et al., 2010).

In the absence of glucose, however, fatty acids and certain amino acids (especially glutamine) can be converted and fed into the citric acid cycle at specific stages. Fatty acids can be converted by beta oxidation to yield acetyl-CoA. Glutamine, on the other hand, can be converted into glutamate and further converted to α-ketoglutarate, an intermediate in the TCA cycle. These provide substrates for the citric acid cycle for further generation of electron carriers, NADH and $FADH_2$ which will be oxidised to generate ATP in the electron transport chain. Glutamine metabolism is deregulated in several cancers (Dang, 2010; Huang et al., 2014; Liu et al., 2014; Wise and Thompson, 2010).

OxPhos is an efficient mechanism for generating ATP through protein complexes embedded in the mitochondrial inner membrane. Glycolysis which occurs in the cytosol is not as efficient; owing to the incomplete breakdown of glucose to large amounts of lactate. Glycolysis yields 2 ATP molecules per molecule of glucose, compared to 36 ATP generated from OxPhos and the citric acid cycle. However, cancer cells and other proliferating cells prefer glycolysis to OxPhos, despite adequate oxygen levels, making them highly dependent on glucose availability. This frequently leads to rapacious glucose uptake via glucose transporters such as GLUT1 and GLUT3, whose expression is usually upregulated (Barron et al., 2012; Younes et al., 1997). This metabolic signature has been exploited in cancer diagnosis by using positron emission tomography (PET) imaging with fluorodeoxyglucose to monitor increased glucose uptake in cancer patients (Almuhaideb et al., 2011). **Figure 1.2** summarises the process of glycolysis and OxPhos and highlights certain glucose transporters and glycolytic genes that are upregulated in several cancers.

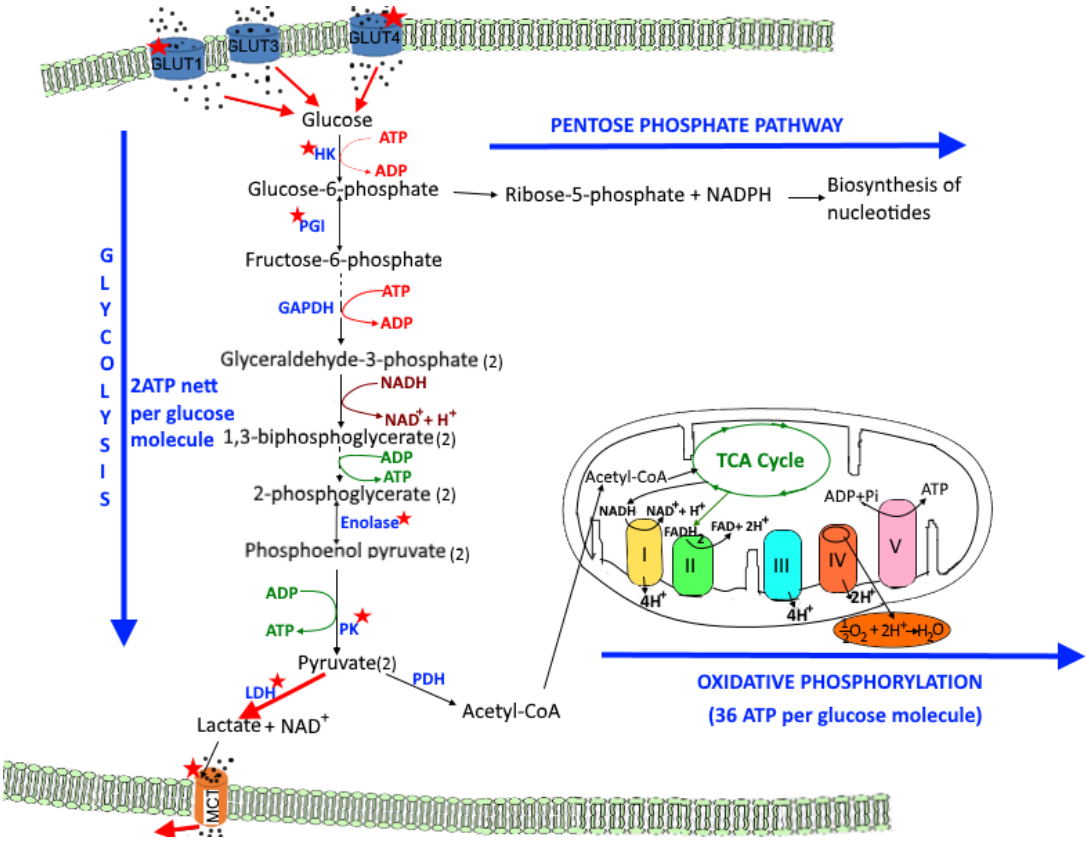

Figure 1.2. Glycolysis and OxPhos: comparing normal and cancer cells. Modified from Pelicano et al. (2006) and Vousden and Ryan (2009). Glucose is taken up from the systemic circulation by glucose transporters (such as GLUT1, 3 and 4). The glucose molecule is phosphorylated by HK (hexokinase). A series of glycolytic steps continue, culminating in the production of 2 molecules of pyruvate per glucose molecule. Pyruvate is either converted to acetyl Co-A and fed into the tricarboxylic acid (TCA) cycle, which generates reducing equivalents NADH and $FADH_2$. NADH and $FADH_2$ are oxidised in the electron transport protein complexes, generating protons which are pumped across the inner mitochondrial membrane (IMM). At complex IV, where the final electrons are received, molecular oxygen is converted to water. The potential difference across the IMM generates a proton motive force which mechanically drives ATP synthase (Complex V) enabling it to produce ATP from the ADP and inorganic phosphate (Pi). Alternatively, and as preferred by most cancer cells, most of the pyruvate is converted into lactate and exported out of the cell via monocarboxylate transporters (MCTs). The red stars show some glycolytic genes that are upregulated in numerous cancers: HK (hexokinase), PGI (phosphoglycerate isomerase, enolase, and LDH (Lactate dehydrogenase). GAPDH (Glyceraldehyde-3-phosphate dehydrogenase, PDH (pyruvate dehydrogenase).

The Warburg effect, also known as aerobic glycolysis, is a cancer hallmark which describes elevated glycolysis and reduced OxPhos by cancer cells and other proliferating cells even in the presence of ample oxygen and healthy mitochondria.

The Warburg effect was previously thought to occur as a result of impaired OxPhos due to malfunctioning mitochondria (Koppenol et al., 2011), which compelled the cell to boost glycolysis as a compensatory strategy to augment ATP synthesis. Growing evidence showed that, despite ample oxygen supply and properly functioning mitochondria, many cancer cells still prefer glycolysis to OxPhos for the synthesis of ATP (Fantin et al., 2006; Weinhouse, 1976).

Contrarily, it is noteworthy that mitochondrial defects are also characteristic of some cancers (Alam et al., 2005; Baysal et al., 2000). This is not surprising, given that mitochondria are responsible for the synthesis of most of the energy required for cellular life processes, and at the same time mediators of the machinery of cell death (apoptosis). Why do cancer cells prefer a rather inefficient glycolytic mechanism, producing only 2 ATP molecules per glucose molecule, compared with OxPhos which generates up to 36 ATP molecules of ATP? The following have been suggested as the reasons cancer cells rewire their metabolism, preferring aerobic glycolysis.

1.2.2 Why do cancer cells reprogram their metabolism?

Despite reduced ATP synthesis in glycolysis compared with OxPhos, the speed at which ATP is generated in glycolysis is faster (Lodish et al., 2000; Pfeiffer et al., 2001). This faster rate is essential for cancer cells and other proliferating cells such as embryonic cells due to their high rate of cell division (Berridge et al., 2010; Pfeiffer et al., 2001).

It is worthy of note that not all cell types that display a high rate of glycolysis are proliferative. Innate immune cells such as dendritic cells and macrophages also display high glycolytic rates in response to infectious agents such as bacterial lipopolysaccharides from Gram-negative bacteria (Krawczyk et al., 2010). However, this temporal surge in glycolysis is not accompanied by cell proliferation. It is required for immune activation which demands temporal bursts of energy in response to infection (Kelly and O'Neill, 2015). Furthermore, sites of inflammation are usually characterised by hypoxia (Bartels et al., 2013). This suggests that the predominant use of glycolysis for ATP synthesis may be an adaptive mechanism of innate immune cells which usually carry out their functions in hypoxic microenvironments. Tumour microenvironments are also sometimes

hypoxic in nature, usually owing to rapid tumour growth that exceeds angiogenesis. This causes a tumour to rapidly deplete its oxygen supply and likely to rely more on glycolysis for ATP synthesis (Brown, 2007).

Meeting the biosynthetic demand

Increased glycolysis may also serve to generate biosynthetic molecules that are required for cell proliferation. These include nucleotides synthesized via the pentose phosphate pathway which branches off at glucose-6-phosphate in the glycolytic pathway. The precursors of several nonessential amino acids are glycolytic intermediates. For example, alanine, valine, isoleucine, and leucine can be synthesised from pyruvate; while serine is synthesised from 3-phosphoglycerate.

The role of lactate in carcinogenesis

Furthermore, enhanced glycolysis is also accompanied by increased lactate secretion in cancer cells; as pyruvate is preferentially metabolised to lactate rather than acetyl co-A. Lactate is not merely a waste product of glycolysis but has several roles in carcinogenesis. The conversion of lactate to pyruvate is catalysed by lactate dehydrogenase-A (LDH-A) which is highly upregulated in many cancers (Girgis et al., 2014; Le et al., 2010; Miao Ping et al., 2013). In this reaction, pyruvate reacts with NADH to generate lactate, NAD^+ and H^+ catalysed by LDH-A. The NAD^+ refuels glycolysis by converting glyceraldehyde-3-phosphate to 1,3-biphosphoglycerate.

The excess lactate is exported along with H^+ ions through proton-linked monocarboxylate transporters (MCTs) such as MCT1 and MCT4 (Andersen et al., 2016; Pinheiro et al., 2010). This lactate efflux leads to extracellular acidification of the tumour microenvironment which is known to stimulate immune evasion by cancer cells (Calcinotto et al., 2012; Lardner, 2001). Furthermore, Shime and colleagues (2008) also showed that lactate export fuels a local inflammatory reaction leading to the secretion of growth factors and cytokines by attracted inflammatory cells. These stimulate tumour proliferation and metastasis (Shime et al., 2008). It appears, therefore, that tumour cells may upregulate glycolysis owing to the tumour-promoting consequences of lactate.

Protection from reactive oxygen species (ROS)

Furthermore, decreasing the amount of ATP generated via OxPhos may serve as a protective mechanism against reactive oxygen species (Heiden et al., 2009). ROS (superoxides, peroxides and the singlet oxygen anion) may cause damage to biological membranes and genetic material

which can lead to programmed cell death (Higuchi et al., 1998; Simon et al., 2000). Therefore an increased dependence of cancer cells in glycolysis, while avoiding OxPhos may serve to protect the cells against oxidative stress which could result to cell death (Heiden et al., 2009).

Warburg effect-induced resistance to apoptosis

Resistance to apoptosis has been attributed to enhanced glycolytic flux observed in cancer cells. The permeabilisation of the mitochondrial outer membrane which is mediated by pro-apoptotic BCl_2 family of proteins is a key step in the intrinsic apoptotic process. Overexpression of hexokinase 2 (HK2) is observed in several tumours. HK2 is not only involved in the catalytic phosphorylation of glucose in the first step of glycolysis. It is known to inhibit apoptosis by binding to VDAC protein and preventing Bax-mediated cytochrome C release (Pastorino et al., 2002). Moreover, Akt-mediated antiapoptotic activities have been shown to rely on hexokinase-catalysed glucose phosphorylation in glycolysis. Hence mitochondrial membrane integrity which is important for cell viability is preserved by Akt and dependent on glucose availability and glycolysis (Gottlob et al., 2001). It is therefore not surprising that HK2 confers chemo- and radio-resistance in various cancers (Zhang et al., 2018; Zhong and Zhou, 2017). Hence, targeting HK2 is a promising therapeutic strategy in cancer (Krasnov et al., 2013).

1.2.3 How cells reprogram their metabolism: Mechanisms involved in metabolic reprogramming

As alluded to previously, cancer is a genetic disease at the cellular level. This implies that the cancer phenotype, expressed as several characterised hallmarks, has roots at the genetic level. The primary goal of the genetic defects which translate to cancer hallmarks is for cell survival, proliferation, and metastasis. Cancer is a complex and heterogeneous disease; with several mechanisms implicated in the carcinogenic process. In the same vein, the Warburg effect is caused by several mechanisms. However, the key mechanisms seem to be oncogene-driven deregulation of glycolytic genes.

Oncogene-mediated upregulation of glycolytic genes

The tumour suppressor p53, well known for its apoptotic, cell cycle arrest and senescence induction strategies for tumour suppression, surprisingly also plays a metabolic regulatory role in carcinogenesis (Li et al., 2012; Valente et al., 2013). For example, p53 represses glucose uptake

by cells by blocking the expression of glucose transporters GLUT1 and GLUT4 (Schwartzenberg-Bar-Yoseph et al., 2004). In addition, the p53 protein transcriptionally activates TIGAR (TP53-induced glycolysis and apoptosis regulator). TIGAR directly decreases intracellular fructose-2,6-biphosphate levels, hence suppressing glycolysis and thereby shunting glycolysis via the pentose phosphate pathway (Bensaad et al., 2006). The first rate-limiting enzyme in glycolysis, HK2 which catalyses glucose phosphorylation is also suppressed by p53 (Mathupala et al., 1997). p53 enhances OxPhos by transcriptional activation of the *synthesis of cytochrome* c oxidase 2 (SCO2), a complex IV enzyme of the electron transport chain (Matoba et al., 2006). This is probably the reason some cancer cells with mutant p53 show diminished OxPhos (Levine and Puzio-Kuter, 2010). Over 50% of cancers in humans have mutations in the TP53 gene (Petitjean et al., 2007; Vogelstein et al., 2000). This underscores its relevance as a tumour suppressor. Its impaired role is not limited deregulated apoptosis, cell cycle arrest, and senescence but also a metabolic reprogramming that promotes carcinogenesis.

Oncogenes such as the phosphatidylinositol-3-kinase/protein kinase B (PI3K/Akt), and c-Myc play vital roles in inducing the Warburg effect in carcinogenesis. The PI3K/Akt pathway controls the cell cycle, proliferation, and cellular metabolism. The PI3K/PκB pathway is deregulated in several tumours (Elstrom et al., 2004; Shukla et al., 2007; Yoeli-Lerner and Toker, 2006). PI3K activates Akt which induces the expression of GLUTs, HK2 and phosphofructokinase (DeBerardinis et al., 2008). The activity of Akt directly upregulates glycolysis; with a higher activity correlating with a more aggressive tumour phenotype in glioblastoma cells *in vivo* (Elstrom et al., 2004).

The c-Myc phosphoprotein is a multi-functional transcription factor that controls numerous aspects of cell physiology including apoptosis, cell cycle progression and cell is involved in oncogenic transformation. c-Myc is constitutively expressed and often deregulated in many cancers (Dang, 2012) and has even been shown to be a hallmark involved in cancer initiation and maintenance (Gabay et al., 2014). c-Myc activation enhances glycolytic gene expression in many cancer cells (Dang et al., 1997). For example, c-Myc increases the expression of pyruvate dehydrogenase kinase-1 (PDK1) (Kim et al., 2007). PDK1 is known to phosphorylate pyruvate dehydrogenase

(PDH) hence blocking the synthesis of acetyl CoA from pyruvic acid. Furthermore, it was shown that c-MYC transcriptionally upregulates lactate dehydrogenase-A isoform (LDH-A) in cancer cells (He et al., 2015; Shim et al., 1997). Glutamine metabolism plays a significant role in carcinogenesis (Yuneva et al., 2007). c-Myc boosts glutamine metabolism as well as NADPH synthesis which are needed for anabolism. HIF-1α cooperates with c-Myc to promote the Warburg effect; enabling cancer cells to thrive in hypoxic tumour microenvironments (Dang et al., 2008; Gordan et al., 2007).

1.3 Metabolic and non-metabolic functions of glycolytic genes

According to the public database for expression of genes and Expressed Sequence Tags (dbESTs) from the NIH (National Institutes of Health) (Boguski et al., 1993), glycolytic genes are upregulated in about 70% of all cancers globally (Altenberg and Greulich, 2004). This observation accentuates the importance of increased glycolysis and the Warburg effect in cancer cells. Furthermore, glycolytic genes are involved in several tumour-promoting activities besides increasing glycolytic rate. It has been recently shown that some glycolytic enzymes can translocate into the nucleus and transcriptionally upregulate genes involved in survival, epigenetic modifications, protein kinase activity and control of transcription factors and co-factors (Yu and Li, 2016). A typical example is the M2 isoform of pyruvate kinase (PKM2) in which I highlight both metabolic and non-metabolic functions in carcinogenesis. Pyruvate kinase (PK) catalyses the last step of glycolysis: the transfer of a phosphate group from phosphoenolpyruvate to ADP, yielding pyruvate and ATP. The expression of the M2 isoform of PK, PKM2 is upregulated in cancer, making it an attractive target for therapy (Christofk et al., 2008). It was also shown that PKM2 can lead to the Warburg effect and promote tumour growth. Switching from the M2 to the M1 isoform was shown to reverse the Warburg effect and slow tumour growth in mouse xenografts (Christofk et al., 2008).

Furthermore, mTOR-mediated transactivation of PKM2 has also been shown to activate the Warburg effect and promote tumour growth; showing how important PKM2 is in carcinogenesis (Sun et al., 2011). PKM2 was also shown to be a poor prognostic marker and also a therapeutic target in ovarian and hepatocellular carcinomas (Chao et al., 2017; Wong et al., 2014).

With regards to non-metabolic roles of PKM2 in carcinogenesis, recent findings show another mechanism by which PKM2 promotes carcinogenesis in a p53-dependent manner in MCF7 breast carcinoma cells exposed to a DNA-damaging agent. It was shown that PKM2 transcriptionally co-represses p53; preventing it from binding to the p21 gene promoter, thereby stimulating a continuous G1 phase (Xia et al., 2016). This mechanism provided favourable growth conditions to cancer cells exposed to a DNA-damaging drug (Xia et al., 2016). It is likely that such a strategy could confer PKM2-mediated resistance to chemotherapy in PKM2 expressed cancer cells. Moreover, it has been recently shown that shRNA-mediated knockdown of PKM2 resulted in a marked decrease in resistance to cisplatin in bladder cancer (Wang et al., 2017). Xia and colleagues (2016) also showed that PKM2 inhibits p53 phosphorylation at serine 15 which is critical for p53 activation and stability by serine/threonine kinase, ATM.

Another example is hexokinase 2 (HK2). HK2 is a highly expressed enzyme in numerous cancers which are poorly differentiated and highly glycolytic (Altenberg and Greulich, 2004; Smith, 2000). In addition to its role in phosphorylating glucose, it stimulates tumour initiation, promotes cell proliferation and metastasis; induces resistance to chemotherapeutics, confers resistance to apoptosis and correlates with poor prognosis in certain cancers (Ho and Coomber, 2016; Patra et al., 2013; Wolf et al., 2011).

HK2 interferes with outer mitochondrial membrane (OMM) permeability by binding to voltage-dependent anion channel (VDAC) proteins. This effect prevents VDAC from interacting with t-Bid, a proapoptotic member which helps in permeabilising the OMM. These actions culminate in preventing the release of cytochrome *C,* a key initiating step in apoptosis (Pastorino et al., 2002). In a nutshell, the properties of glycolytic enzymes which encompass glycolytic and non-glycolytic roles are important in carcinogenesis. It is therefore not surprising that cancer cells may incorporate high expression and activity of glycolytic enzymes in their arsenal to maintain survival, proliferation, and invasiveness.

1.4 Metabolic reprogramming in innate immune cells

It is important to note that metabolic reprogramming is not limited to cancer cells. Innate immune cells such as macrophages and dendritic cells, in response to infection, also display metabolic

reprogramming reminiscent of the Warburg effect seen in tumour cells (Krawczyk et al., 2010; West et al., 2011). Moreover, glycolysis, fatty acid metabolism, and TCA cycle reactions have an important role to play in the activation and function of innate immune cells such as macrophages and dendritic cells (O'Neill and Pearce, 2016). These innate immune cells are important in protecting the body from invasion by microorganisms.

1.4.1 Infection and cancer: an intimate relationship

The burden of infection-associated cancers is highest in Africa when compared with other continents (Plummer et al., 2016). South Africa has one of the highest prevalence rates of HIV/AIDS which is known to increase the risk of several cancers (AIDS-defining malignancies) especially Kaposi's sarcoma, non-Hodgkin lymphoma, cervical cancer and primary central nervous system lymphoma (Rubinstein et al., 2014). Parasitic infestations such as schistosomiasis are associated with high risk in bladder carcinomas (Mostafa et al., 1999; Rambau et al., 2013). The Epstein - Barr virus is a causative agent of Burkitt's lymphoma (Brady et al., 2007; Pannone et al., 2014), a common cancer in children that affects B lymphocytes. Furthermore, chronic malarial infection induced by *Plasmodium chabaudi* in mice was also shown to favour the development of mature B cell lymphomas lacking p53 (Achtman et al., 2003). Still, most cervical cancers are caused by the human papillomavirus (HPV). About 70% of cervical cancers that are related to the Human papillomavirus (HPV) are caused by 2 strains: HPV-16 or HPV-18 (Braaten and Laufer, 2008). The HPV vaccine was the first vaccine developed for the prevention of cervical cancer among adolescent females (Basu et al., 2013). The uses of certain vaccines such as those against HPV have shown a reduction in the incidence of cervical cancer (Basu et al., 2013; Hestbech et al., 2015). This has led to the approval by the WHO and several international organisations as a preventive strategy against cervical cancer (Basu et al., 2013). This directly implicates the HPVs as the cause of cervical cancers. Furthermore, several reports show that Hepatitis B and C viruses are involved in hepatocellular cancer (Cho et al., 2011; Liao, 2006; McLaughlin-Drubin and Munger, 2008). In a similar vein, Hepatitis B vaccines are effective in combating hepatocellular carcinomas (Chang et al., 2000; Kao, 2015). The afore-mentioned examples directly incriminate HPV and hepatitis B virus as causative agents of cervical cancer and hepatocellular cancer respectively. However, the link between bacterial infections and cancer is poorly understood. Several mechanisms have been proposed in *Helicobacter pylori*-induced gastric cancer and some virus-induced cancers. Interestingly, recent studies show that certain FDA-approved antibiotics

are effective in killing cancer cells, even though the mechanisms still remain elusive (De Francesco et al., 2017; Lamb et al., 2015).

How does the human body respond to the invasion of microbes? The innate immune system is the first line of defense against invading pathogens. These infectious agents such as viruses and bacteria stimulate chronic inflammation which has been described recently as one of the hallmarks of carcinogenesis (Coussens and Werb, 2002; Parkin, 2006). Furthermore, inflammation is associated with several types of cancer (Vetrano et al., 2010). A typical example is *Helicobacter pylori*-mediated gastritis which represents the important risk factor in stomach adenocarcinomas (Peek and Crabtree, 2006). Importantly, up to one in five cancers are caused by infection, making it crucial to understand the mechanisms of infection-induced carcinogenesis.

1.4.2 Mechanisms of infection-associated carcinogenesis

Inflammation is at the core of mechanisms that drive infection-related cancer (Colotta et al., 2009; Coussens and Werb, 2002; Wu et al., 2014). For example, chronic inflammation may lead to the activation of redox-related transcription factors such as NF-κB and STAT3 (signal transducer and activator of transcription 3) which stimulate the constitutive expression of inflammatory cytokines, production of ROS, reactive nitrogen species (RNS) and growth factors to the tumour microenvironment. These molecules with neoplastic consequences are largely responsible for infection-mediated carcinogenesis (Wu et al., 2014).

Inflammation-induced STAT3 and NF-κB activation

NF-κB is a heterodimeric transcription factor protein which shows constitutive expression in several tumours. STAT3 is a redox-sensitive transcription factor that can be activated by phosphorylation at tyrosine 705 (Tyr705) following specific stimuli such as cytokines. This activation causes the protein to dimerise and translocate to the nucleus where transactivates genes involved in cell cycle progression, inflammation, angiogenesis, and metastasis. STAT3 can be activated by numerous cytokines and growth factors such as, including IL-6, EGFs (epidermal growth factors), VEGF (vascular endothelial growth factor), PDGF (platelet-derived growth factor), IL-23, and IL-21(Akira et al., 1994; Yoshimura et al., 2007; Yu et al., 2009a). Oncogenic

proteins (including Ras, and Src) can also activate STAT3. STAT3 activation has been observed in many cancers such as colon, gastric and breast (Yuan et al., 2004).

Role of ROS and NADPH oxidases in carcinogenesis

Partial reduction of oxygen results in the generation of ROS and RNS which include hydrogen peroxide (H_2O_2), the superoxide anion (O_2^-) and hydroxyl radical (OH^-). Inflammatory tumour microenvironments are usually characterised by the increased generation of ROS (Mittal et al., 2014; Wiseman and Halliwell, 1996). An oxidative tumour microenvironment is usually observed in several solid tumours due to many factors: a hypoxic milieu, increased basal metabolic rate of cancer cells, overexpression of NADPH oxidase (Nox) and COX enzymes which generate ROS and deregulated cytokine/growth factor signalling. Furthermore, downregulated expression of antioxidant enzymes also contributes to increased ROS generation and subsequent oxidative stress which is characteristic of carcinogenesis.

ROS and RNS can lead to DNA damage and genomic instability which can promote initiation and progression of tumours (Wiseman and Halliwell, 1996). Second, it can promote cell survival and proliferation signalling pathways (Gupta et al., 2012; Waris and Ahsan, 2006). Third, ROS can stimulate tumour cell metastasis, angiogenesis, and invasiveness (Reczek and Chandel, 2017; Ushio-Fukai and Nakamura, 2008). Fourth, chemotherapeutic resistance has been attributed to ROS release in cancer cells (Kim et al., 2017).

Immunosuppression-induced tumour progression

Chronic inflammatory microenvironments are characterised by constitutive cytokine and chemokine synthesis. Inflammatory cytokines such as IL-5, IL-6, IL-7, IL-13, TNF-α, and chemokines such as IL8, RANTES (CCL5) are involved in oncogenesis. These cytokines recruit monocytes, T cells, mast cells, and eosinophils to the tumour microenvironment, stimulating tumour proliferation (Foss et al., 1993, 1995; Samoszuk and Nansen, 1990; Tedla et al., 1999). Furthermore, viruses (such as Herpes virus) synthesise viral homologues of human proteins important in carcinogenesis. For example viral IL6 and viral FLIP (Fas-associated death domain-like IL-1-converting enzyme inhibitory protein) (Holzerlandt et al., 2002).

Role of specific bacterial and viral oncogenic proteins

Bacterial and viral oncogenic proteins play an important role in infection-associated carcinogenesis. For example, the product of the Cag A gene (cytotoxin-associated gene A) is a cytotoxic protein produced from *H. pylori* which is known to induce peptic ulcer, gastritis, and poses a high risk of gastric cancer (Backert and Blaser, 2016; Blaser et al., 1995). Furthermore, the E6 oncoprotein synthesised by HPV is believed to drive cell proliferation by stimulating p53 degradation through the formation of a complex comprised of E6, E6-AP (a cellular ubiquitination enzyme) and p53. E6-induced p53 degradation suppresses p53 tumour suppressor functions such as apoptosis, cell cycle arrest and metabolic regulation (Crook et al., 1991). Another oncoprotein from HPV, E7, binds to the pocket domains of Rb a tumour suppressor thereby abrogating the interaction between Rb and E2F. Activated E2F unbound to Rb induces unrestrained replication and cell division characteristic of transformed cells (Chellappan et al., 1992).

Infection-mediated epigenetic modification: methylation

Chronic inflammation induced by viral and bacterial infections has been also shown to inactivate tumour suppressors by inducing aberrant DNA hypermethylation at CpG islands. Examples include some patients with Epstein-Barr- and *H. pylori*-associated cancers (Kang et al., 2002, 2003).

Infection-associated cancers

Table 1. shows the diversity of cancers that are associated with infection, brief mechanisms involved and references. Virtually all groups of micro-organisms are involved. They include bacteria, viruses, and protozoa.

Table 1. Infection-associated cancers

Infection	Cancer	Mechanism(s)	References
Helicobacter pylori	Gastric cancer	Inflammation Oncogenic protein: Cag A	(Backert and Blaser, 2016; Ding et al., 2010; Peek and Crabtree, 2006)
Gut pathogens (Inflammatory bowel disease)	Colorectal cancer	Inflammation	(O'Connor et al., 2010)
Human papilloma virus (Strains: HPV 16 and HPV 18)	Cervical cancer	Oncogenic viral proteins: E5, E6, E7 Inflammation	(Ishiji, 2000; Münger et al., 2004)
Schistosoma haematobium	Bladder cancer	Inflammation	(Mostafa et al., 1999; Rambau et al., 2013)
Hepatitis B and C viruses	Hepatocellular carcinoma	Inflammation	(Chang et al., 2000; Cho et al., 2011; McLaughlin-Drubin and Munger, 2008)
HIV/AIDS	Kaposi sarcoma Non-Hodgkin lymphoma Invasive cervical cancer.	Immunosuppression Inflammation	(Franceschi et al., 1998; Goedert et al., 1998)
Epstein-Barr virus	Burkitt's lymphoma Non-Hodgkin lymphoma	Oncogenic viral proteins Inflammation	(Brady et al., 2007; Pattle and Farrell, 2006; Thompson and Kurzrock, 2004)
Kaposi's sarcoma-associated herpesvirus (KSHSV)	Kaposi's sarcoma	Oncogenic viral proteins Co-infection with HIV dramatically increases the risk	(Delgado et al., 2010; Mesri et al., 2010)

1.5 Pathogen recognition in innate immunity

Upon exposure to infectious pathogens, the immune system responds aptly to protect the host. The immune system is divided into the innate and adaptive arms. While the innate immune system responds rapidly to the immediate threat of a pathogen invasion, the adaptive immune system takes longer to develop pathogen-specific, lasting effects. Innate immune cells include macrophages, monocytes, dendritic cells, neutrophils, basophils, mast cells, and eosinophils. Their primary roles include phagocytosis, antigen presentation and cytokine production (Janeway et al., 2001).

During infection, innate immune cells respond to specific signature molecules on pathogens known as pathogen-associated molecular patterns (PAMPs). This critical response is effected by specific

evolutionarily-conserved host receptors known as pattern-recognition receptors (PRRs). Binding of PRRs with their cognate PAMPs rapidly elicits a cascade of signalling events which culminate in the expression of pro-inflammatory cytokines, chemokines and type 1 interferons. These effector molecules are also used for the initiation of pathogen-specific, long-term adaptive immunity via B and T lymphocytes. PRRs, which are critical for host defence, are classified into a few families: Nucleotide oligomerisation domain (NOD)-like receptors (NLRs) (recognise bacterial peptidoglycan), Retinoic acid-inducible gene-I (RIG)-like receptors (RLRs) (respond to dsRNA), C-type lectin receptors (CLRs) (recognise fungal pathogens) and Toll-like receptors (TLRs) (recognise a wide variety of PAMPs). TLRs are the most extensively studied of all PRR families.

1.5.1 Toll-like receptors in innate immunity

The TLRs have attracted a lot of attention because of their diverse roles in numerous immune disorders, metabolic diseases and cancer. TLRs remain the most explored and characterised PRRs in innate immunity, with up to 11 TLR homologs found.

Discovery of TLRs

The Toll protein was first discovered in Drosophila and was shown to be responsible for dorsoventral patterning in embryonic development (Morisato and Anderson, 1994; Schneider et al., 1994). It was later shown to be involved in protection against fungal infection (Lemaitre et al., 1996). The discovery that the Drosophila Toll protein controls anti-fungal immune responses was pivotal in identifying Toll-like receptors as important regulators of host defence against infection in mammals (Lemaitre, 2004).

Structure and diversity of TLRs

Toll-like receptors are type I transmembrane pattern recognition receptors containing an N-terminal with a leucine-rich repeat extracellular domain forming a horseshoe structure, a transmembrane domain and a highly conserved intracellular C-terminal Toll/interleukin 1 (TIR) domain which is shared by TLRs and interleukin-1 receptor (Medzhitov, 2001; Takeda et al., 2003). The LRR of TLRs forms a horseshoe structure, on whose concave surface pathogens are thought to bind during the recognition process. Remarkably, even though LLR domains in TLRs are highly conserved, different TLRs are able to recognise various ligands that are structurally

unrelated (Janeway and Medzhitov, 2002; Medzhitov, 2001). Based on their ability to recognise different ligands leading to a cascade of signalling events, TLRs have been segregated into different groups as shown in **Table 2**.

Table 2. Diversity of TLRs, adaptor proteins, transcription factors, and effector cytokines

TLR	PAMP	Adaptor molecule recruited	Transcription factors activated	Effector molecules	References
TLR1/TLR2	Bacterial lipopeptides	Mal/MyD88	NFκB	Proinflammatory cytokines	(Takeuchi et al., 2002)
TLR2/TLR6		Mal/MyD88		Proinflammatory cytokines	(Takeda et al., 2003)
TLR3	dsRNA	TRIF	NFκB/IRF3	IFNβ and IFN inducible genes/ Proinflammatory cytokines	(Alexopoulou et al., 2001)
TLR4	Bacterial lipopolysaccharides	MyD88/MAL/TRAM/TRIF	NFκB/IRF3	Proinflammatory cytokines/ IFNβ and IFN inducible genes	(Takeda et al., 2003)
TLR5	Bacterial flagellin	MyD88	NFκB	Proinflammatory cytokines	(Hayashi et al., 2001)
TLR7	ssRNA/imiquimod	MyD88	IRF7/ NFκB	IFNα and IFN inducible genes/ Proinflammatory cytokines	(Diebold et al., 2004) (Jurk et al., 2002)
TLR8	Viral and bacterial ssRNA	MyD88	IRF7/ NFκB	IFNα and IFN inducible genes/ Proinflammatory cytokines	(Jurk et al., 2002)
TLR9	Unmethylated CpG dinucleotides from bacterial and viral DNA	MyD88	IRF7/ NFκB	IFNα and IFN inducible genes/ Proinflammatory cytokines	(Hemmi et al., 2000) (Hemmi et al., 2000)
TLR10	Influenza A virus, Listeria, H. pylori LPS	MyD88	Unknown	Unknown	(Lee et al., 2014)

TLR signalling mechanisms

Following receptor binding to their cognate ligands, a cascade of signalling events ensues, depending on which TLR was activated. **Figure 1.3** shows the diversity of PAMPs and the TLR signalling pathways which they activate.

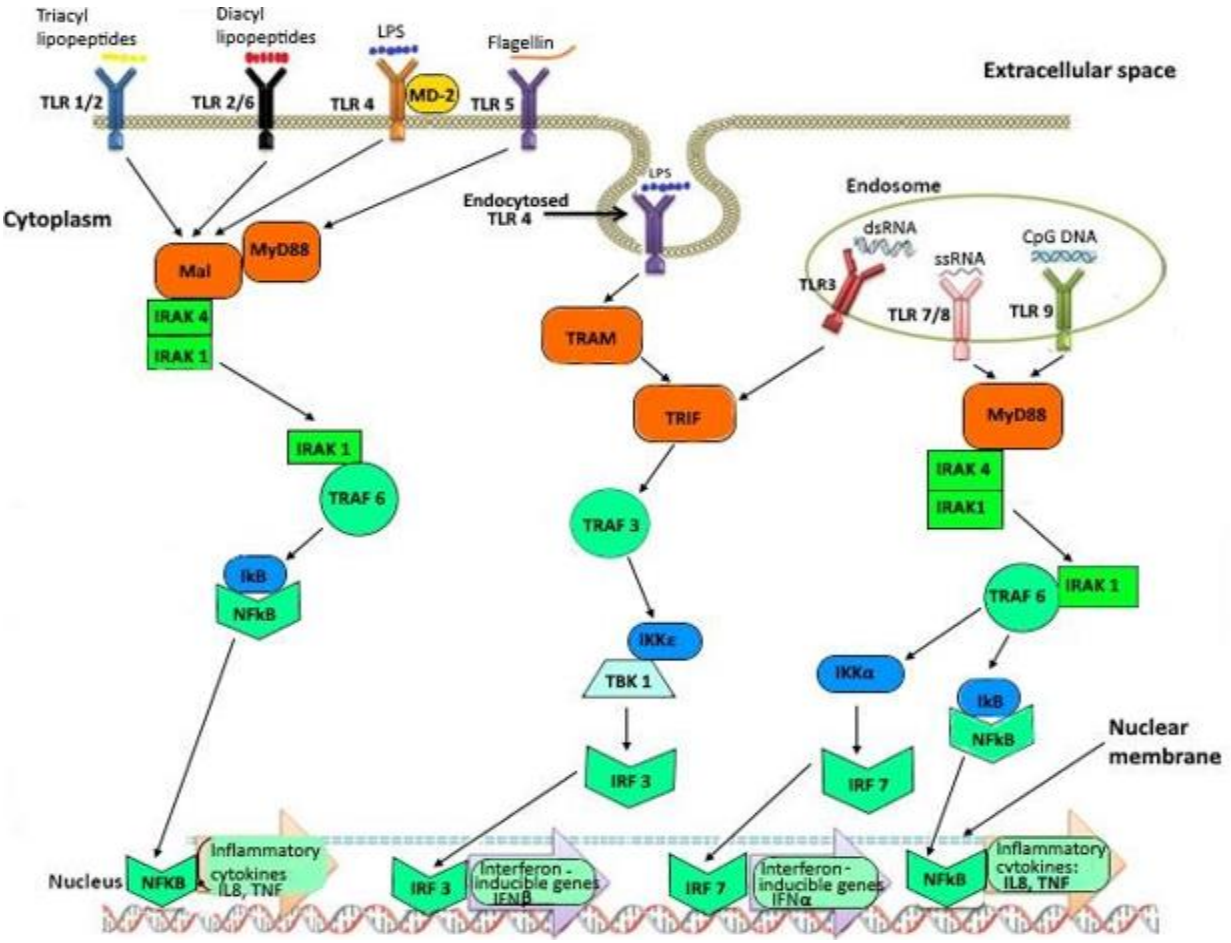

Figure 1.3. TLR signalling. Adapted from Takeda and Akira (2005) and Wang et al. (2014). The binding of microbial structures to the extracellular leucine-rich repeat region of their cognate TLRs leads to a homo-dimerisation of the intracellular Toll/Interleukin 1 receptor (TIR) domain which recruits specific adaptor proteins such as MyD88, TRAM, Mal or TRIF. These adaptor proteins bind to IRAK kinases which trigger a suit of signalling cascades, culminating in the translocation of transcription factors such as NF-κB, IRF3 or IRF7 to the nucleus. These transcription factors activate the expression of specific cytokines which neutralise the infection and prompts the adaptive arm of the immune system.

As shown in **Figure 1.3**, TLRs initiate signalling by forming homo-, or heterodimers after binding to their respective cognate ligands. MyD88 is recruited via its TIR domain to the TIR domain of TLRs. The TIR-TIR interaction causes a conformational change in the adaptor which recruits IRAK4 via homophilic death domain-death domain interaction. IRAK4 phosphorylates IRAK1, leading to IRAK1 autophosphorylation and subsequent recruitment of TRAF6. The IRAK1-TRAF6 complex disengages from the receptor and translocates to the cell membrane where it

associates with TAK1, TAB1, TAB2/TAB3. This large protein complex dissociates from the cell membrane and translocates to the cytosol. Activated TAK1 phosphorylates IKKs. The IKKs are a group of kinases that phosphorylate inhibitory kB (IkB) molecules. The IKK complex is made up of IKKα, IKKβand IKKγ. IKK-mediated IκB phosphorylation results in conformational changes that expose the nuclear localization signal of NF-κB. NF-κB is normally sequestered in the cytoplasm by IkB proteins. The exposure of the nuclear localisation (NLS) of NF-κB results in its nuclear translocation allowing NF-κB to bind to specific response elements on DNA and induce gene transcription of cytokines (Medzhitov, 2001; Takeda and Akira, 2005; Takeda et al., 2003). The expressed cytokines through interaction with their cognate receptors, ward off the infection by activating innate immune cells to attack the infectious agents or stimulate the adaptive arm of the immune system which may produce antibodies from B cells or activate T cells (helper or cytotoxic) which leads to T-cell-mediated cell death (Medzhitov, 2001).

The recognition mechanism of TLR4 is rather complex compared with the others. This is because accessory proteins are required before signalling through TLR4 can occur. In summary, bacterial lipopolysaccharides from Gram-negative bacteria following an infection, are recognised and bound to by LPS-binding protein (LBP) (Pugin et al., 1993). The LBP transports LPS to CD14 (a protein which could either be soluble or membrane-bound). CD14 then transports the LPS to the interface of MD2 (a small accessory protein), and the leucine-rich repeat extracellular domain of a TLR4 monomer (Pugin et al., 1993). TLR4, with the aid of MD2, recognises LPS. LPS recognition leads to dimerization of two TLR4 monomers. The dimerized TIR-TIR domains lead to the recruitment of adaptor proteins and further downstream signalling as described above.

Also, unique about TLR4 signalling is the fact that it can recruit different adaptor proteins for signalling which leads to the activation of different transcription factors. TLR4 signals through the Myd88-dependent pathway and the TRIF-dependent (Takeda et al., 2003).

Regulation of TLR signalling

Excessive TLR-dependent cytokine signalling could lead to deleterious effects such as inflammatory and autoimmune disorders. Stringent control mechanisms exist for cytokine signalling. Negative regulatory molecules such as ST2825 and suppressor of cytokine signalling 1 (SOCS1) inhibit MyD88-dependent TLR signalling (Loiarro et al., 2007; Prêle et al., 2008) while

SARM and TAG can suppress the TRIF-dependent pathway (Belinda et al., 2008; Palsson-McDermott et al., 2009).

1.5.2 Cytokines and cytokine signalling

The effector molecules from TLR signalling are mainly cytokines. Cytokines are low molecular weight proteins (>30 kDa) which have a high affinity for specific receptors in the picomolar range. The term is used to incorporate interleukins, interferons and chemokines and other similar molecules. Cytokines signal via autocrine, paracrine and endocrine mechanisms depending on cytokine receptor expression, cell type, and cell context. Cytokines could be pleiotropic, redundant, are often produced in a cascade, and may display synergistic or antagonistic activity with other cytokines (Zhang and An, 2007). The mode of signalling is usually dependent on the type of receptors expressed by the intended target cells. Following the binding of a cytokine ligand to its cognate receptor, the Janus activation kinases (JAKs) are activated. Following signalling cascades, STATs (signal transducers and activators of transcription) are activated, causing them to dimerise and translocate to the nucleus to activate transcription (Kisseleva et al., 2002). Chemokines (chemotactic cytokines) on the other hand, signal through G-protein-coupled receptors.

Cytokines are involved in a diverse array of physiological functions including growth, differentiation, and apoptosis. Mechanisms by which cytokines are involved in carcinogenesis have been discussed in chapter four. However, of interest to this study is their ability to influence the metabolic program, thereby stimulating the Warburg effect. The following table shows examples of cytokines that can boost cellular glucose intake and glycolysis, presenting a possibility to boost the Warburg effect:

Table 3. Glycolysis-inducing cytokines

Cytokine	Glycolytic function	References
TNF-α	Lactate transport, GLUT1 expression and increased glycolysis in MCF7	(Taylor et al., 1992; Vaughan et al., 2013)
IL-1β	Glucose influx and glycolysis rat ovaries	(Ben-Shlomo et al., 1997; Taylor et al., 1992)
IL6	Enhances expression of hexokinase 2 and 6-phosphofructo-2-kinase/fructose-2,6-bisphosphatase-3	(Ando et al., 2010; Han et al., 2016)
IL17A	In association with TNF-α, stimulates glucose metabolism and growth factor production in colorectal cells. Stimulates HK2	(Straus, 2013)
IL22	Upregulates HK2 in colon cancer cells	(Liu et al., 2017)

1.6 Rationale of study

Bacterial infection may cause constitutive expression of pro-inflammatory cytokines and chemokines by TLR-dependent pathways. The sustained expression of cytokines has been associated with carcinogenesis, albeit the possibility of cytokines inducing metabolic reprogramming and promoting carcinogenesis has received little attention. The main drivers of metabolic transformation are mutations of tumour suppressors and oncogenes, which stimulate increased expression of glycolytic genes (DeBerardinis et al., 2008; Ward and Thompson, 2012). In a similar vein, innate immune cells such as dendritic cells and macrophages also rewire their metabolism following infection in a TLR-dependent manner, by boosting glycolysis and inhibiting OxPhos (Krawczyk et al., 2010b**).** Nevertheless, the metabolic shift observed in normal innate immune cells is for immune activation and not cell proliferation as seen in cancer cells. If the innate immune cells were cancerous or transformed, would they proliferate following a further reprogramming of their metabolism? It is therefore imperative to examine the metabolic phenotypes and growth profiles of transformed innate immune cells following infection. The molecular basis by which infection and the metabolic program are mediated, along with the impact of the metabolic state on cell viability, will be the basis of this study. This study further probes the likelihood of a "double metabolic reprogramming" following infection of cancer cells (given that most cancer cells already show metabolic reprogramming and infection can induce metabolic reprogramming). Elucidating the potential pathways that connect oncogenesis and innate immunity would serve as the groundwork for future studies in these subjects. LPS has been shown to reprogram metabolism in normal macrophages and dendritic cells to the Warburg-like phenotype. However, this metabolic reprogramming did not induce cell proliferation or cell cycle progression. It is postulated that this metabolic reprogramming in transformed innate immune cells may aggravate the Warburg effect and lead to cell cycle progression and proliferation.

1.7 Aim

To investigate the molecular mechanisms involved in the metabolic reprogramming of infected immune cancer cells in the context of TLR4 signalling, and further probe the impact on carcinogenesis.

1.8 Objectives

1. To investigate the expression of TLR4 on THP-1 and K562 cells using RT-PCR
2. To probe the role of TLR4 in metabolic reprogramming by inhibiting LPS-TLR4 interaction using polymyxin B.
3. To investigate the cytokines profile results following LPS stimulation using an ELISA array and RT-PCR.
4. To investigate LPS-induced glycolytic flux by colorimetric lactate measurements.
5. To assess LPS-induced mitochondrial membrane potential using JC-10 staining and flow cytometry.
6. To investigate LPS-induced cell cycle changes of THP-1 and K562 cells using flow cytometry and assess proliferation by computing proliferative indices.
7. To evaluate molecular information obtained using *GeneMANIA* and *IMP* webservers thereby underpinning molecular pathways.

Chapter 2 –Materials and Methods

2.1 Background

This chapter describes the materials and methods used to acquire results in this study, in as much detail as possible to allow for reproducibility. I succinctly explain the principles involved in each method or technique that was used and highlight any modifications where necessary. Thereafter, the detailed protocol is outlined. The following techniques were used:

i) Reverse transcription polymerase chain reaction (RT-PCR)
ii) Enzyme-linked immunosorbent assay (ELISA) arrays
iii) Cell cycle analyses and calculation of proliferative indices
iv) Cell viability assay
v) Glycolysis (Lactate) assay
vi) Mitochondrial membrane potential assay
vii) Bioinformatic gene interaction analysis using GeneMANIA and IMP

2.2 Summary of materials and methods

Two cell lines were used in this study: THP-1 cells (acute monocytic leukaemia cells) and K562 cells (chronic myeloid leukaemia cells). The expression of Toll-like receptor 4 (TLR4), at different LPS concentrations (5, 10 and 20 ng/ml) was investigated using RT-PCR. Next, an ELISA array was used to assay the cytokine expression profile of the cells following stimulation of TLR4 agonist, LPS. The differential expression of the cytokines of interest was further confirmed by RT-PCR. To investigate the potential effects of the overexpressed cytokines on energy metabolism, a glycolysis (L-lactate) assay was performed. Thereafter, bioinformatic pathway analysis was done using GeneMANIA and IMP to ascertain possible associations between upregulated cytokines and glycolytic genes *in silico.* To investigate mitochondrial health, the mitochondrial membrane potential was assessed using the JC-10 dye in flow cytometry. To evaluate the impact of altered metabolism following treatment with 5, 10 and 20 ng/ml LPS over 24- and 48-hour time points on the cell cycle and proliferation, cell cycle analysis using propidium iodide in flow cytometry was done. The proliferation index was finally computed by considering the average percentages of cells in various phases of the cycle. **Figure 2.1** shows a summary of methods used in this study.

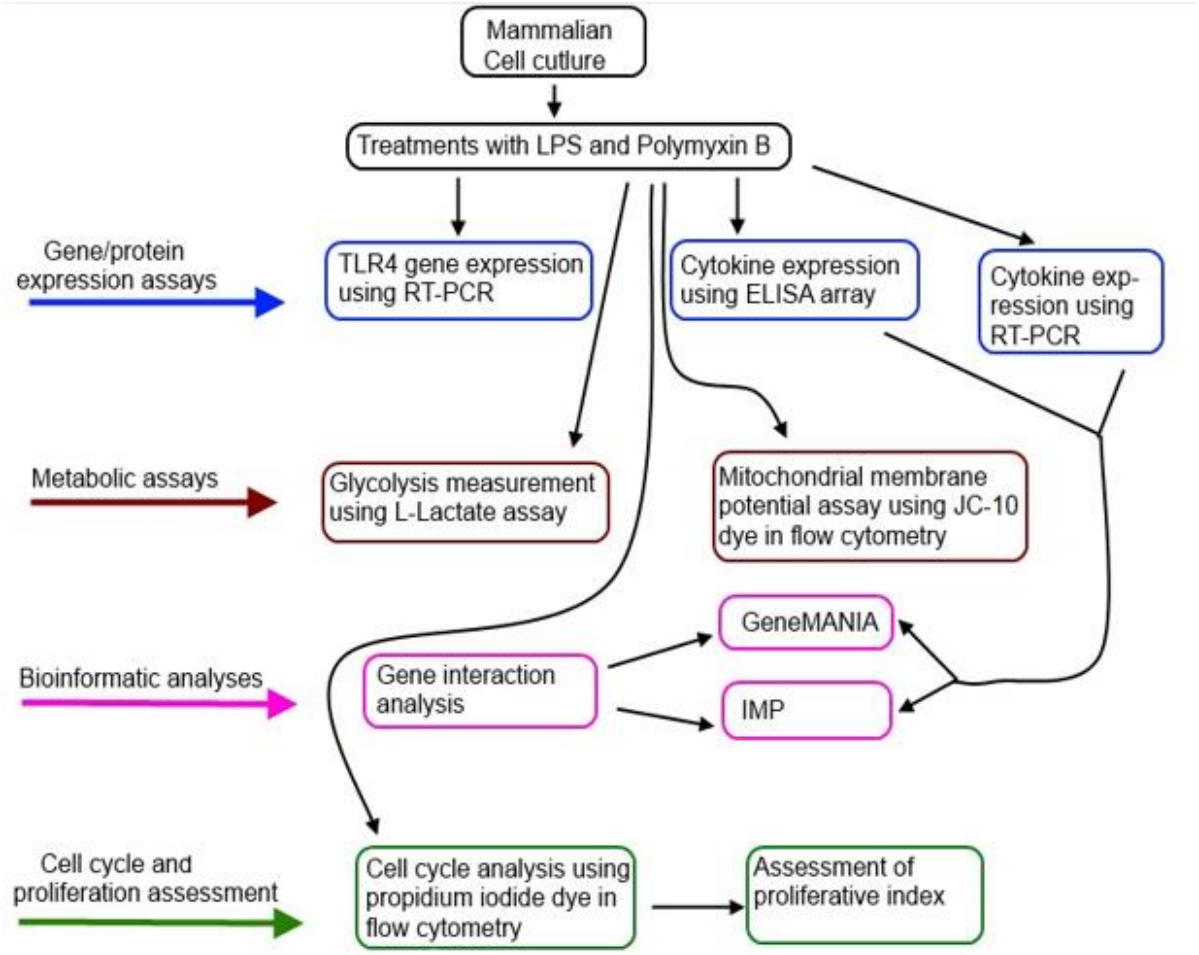

Figure 2.1. Summary flow chart of methods used in this study. Gene/protein expression assays, metabolic assays, bioinformatic analysis, and cell cycle assays and cell proliferation assessment were used to address the aim of this study.

2.3 Materials

Materials used in this study are shown in the appendix section, including kits (**Table A2.1**), instruments (**Table A2.2**), reagents and chemicals (**Table A2.3**). All manufacturers and catalogue numbers accompany the tables. **Table A2.4** shows web servers, and software used. The main cell stimulant treatments and controls are discussed in section **2.3.1**

2.3.1 Cell stimulation and treatments

Bacterial lipopolysaccharide (LPS)

Bacterial lipopolysaccharides (LPS) from *Escherichia coli* was used in this study mimic bacterial infection and as a TLR4 agonist. LPS is a potent endotoxin which is known to activate TLR4 (Chow et al., 1999). In this study, LPS was dissolved in 1X phosphate-buffered saline (PBS) by vortexing intermittently for about 5 minutes. Final concentrations of 5, 10 and 20 ng/ml were used.

Polymyxin B sulphate

Polymyxin B sulphate (hereafter referred to as polymyxin B) was used to block the effects of LPS. Polymyxin B is a potent cyclic cationic polypeptide antibiotic, particularly active against Gram-negative bacteria (Viljanen and Vaara, 1984). Polymyxin B inhibits the biological effects of Gram-negative LPS by binding to the toxic, negatively charged component of LPS known as Lipid A (Morrison and Jacobs, 1976; Cardoso et al., 2007). Hence, polymyxin B was used because of its ability to inhibit LPS-induced TLR4 signalling through its binding to LPS. Polymyxin B sulphate was dissolved in deionised water. All LPS-polymyxin B co-treatments were first pre-incubated at 37°C for 2 hours before cells were treated. Polymyxin B was used at a final concentration of 10 µg/ml.

Carbonyl cyanide-4-(trifluoromethoxy)phenylhydrazone (FCCP)

FCCP was used as a positive control for the mitochondrial membrane potential assay. FCCP is an ionophore uncoupling agent that inhibits ATP synthesis by transporting hydrogen ions through the mitochondrial membrane back to the mitochondrial matrix by causing proton leaks, thereby disrupting OxPhos (Heytler and Prichard, 1962). FCCP effectively depolarises the mitochondrial membrane making it a good positive control in measuring the mitochondrial membrane potential. Since the FCCP was dissolved in 95% ethanol, a vehicle-only control (cells treated with 95% ethanol only) was used.

2.3.2 Cell lines

Acute monocytic leukaemia (THP-1 ATCC® TIB-202™) and chronic myeloid leukaemia (K-562 ATCC ® CCL-243™) cell lines were obtained from American Type Culture Collection (ATCC), Virginia, USA.

2.4 Methods

2.4.1 Cell culture conditions

THP-1 cells were cultured in Roswell Park Memorial Institute (RPMI) 1640 Medium, supplemented with 10% foetal bovine serum (FBS) and 1% Penicillin/Streptomycin. K-562 cells were cultured in a 50:50 mixture of Dulbecco's Modified Eagle's Medium (DMEM) and Hams F-12; supplemented with 10% FBS and 1% Penicillin/streptomycin. Both cell lines were cultured at 37°C, at 5% CO_2 and at 95% relative humidity. THP-1 cells were seeded at $1X10^5$ cells/ml while K562 cells were seeded at $5X10^4$ cells/ml; unless otherwise stated.

2.4.2 Investigation of Toll-like receptor 4 (TLR4) expression

RNA Extraction

RNA was extracted using the acid guanidinium thiocyanate-phenol-chloroform method adapted from Chomczynski and Sacchi (1987). The suspension cells were transferred into 15 ml tubes and pelleted by centrifugation at 1500 rpm for 5 minutes. The supernatant was carefully discarded and 350 µL of Trizol reagent was added to each pellet and resuspended several times for cell lysis.

The cell lysates were transferred to 2 ml microcentrifuge tubes and incubated on ice for 5 minutes for complete cell lysis. Sixty microliters of chloroform was added to each cell lysate and samples were shaken vigorously until a milky pink suspension was formed. The samples were then incubated for 10 minutes at room temperature for initial phase separation. The samples were then centrifuged at 12000 g for 15 minutes at 4°C for phase separation. The aqueous phase (which contained nucleic acids) was carefully aspirated and transferred into new 2 ml microcentrifuge tubes. Isopropanol (250 µL) was added to the aqueous phase, tubes shaken vigorously and then incubated for 10 mins at room temperature RT. The samples were centrifuged at 12000 g for 10 mins at 4°C to pellet the RNA. The supernatant was then discarded. The RNA pellet was washed by resuspension in 500 µL of 75% ethanol and vortexed briefly. The samples were centrifuged at 10000 g for 5 mins at 4°C.

The supernatant was discarded, and RNA pellet was air-dried for 10 mins at RT. The RNA pellet was resuspended in 50 µL of nuclease-free water and incubated at 60°C on a heating block for 10 minutes for complete solubilisation of the RNA. The samples were then chilled on ice and RNA concentrations and purity accessed using a Nanodrop spectrophotometer. The samples were then stored at -70°C until further use.

Reverse transcriptase polymerase chain reaction (RT-PCR)

RNA yield was determined using the Nanodrop spectrophotometer (Thermofischer Scientific, CA, USA). Complementary DNA was synthesized from 1 µg of total RNA per sample, using the Revert Aid first strand cDNA synthesis kit. Oligo (dT) primers, which prime at the poly A tail of mRNA molecules, were used in the reaction. The reaction was run in a PCR thermal cycler at 42°C for 1 hour. After cDNA synthesis, the TLR4 PCR reaction was carried out in a final volume 25 µL containing: 200 nM forward and reverse primers (Forward primer: CCAGTGAGGATGATGCCAGAAT, reverse primer: GCCATGGCTGGGATCAGAGT), 1.5 uL of cDNA, 12.5 µL of 2X PCR Mastermix and 10 µL of nuclease-free water. Thermal cycling parameters were set as follows: Initial denaturation at 94°C for 30 seconds, followed by 30 cycles of 94°C (30 seconds), 60°C (60 seconds), and 68°C (30 seconds). Finally, the product was subject to extension at 68°C for 5 minutes.

The PCR products were run, alongside a 1kb DNA ladder, on a 1% agarose gel containing 0.5 µg/ml of ethidium bromide at 110 volts for one hour. The gels were imaged using the ChemiDoc™ MP Imaging machine. Densitometric analysis was performed on the bands using MyImageAnalysis™ software. The bands were normalized against GAPDH and RPL01 used as reference genes.

2.4.3 Analysis of cytokine expression using ELISA array

Enzyme-linked immunosorbent assays (ELISAs) is a technique that combines the sensitivity of enzyme assays with the specificity of antibodies for qualitative and quantitative detection of a protein of interest in biological samples such as serum, plasma, tissue culture supernatant, tissue homogenate, and others. In an ELISA assay, an antigen is immobilised to a solid surface and then complexed with an enzyme-linked antibody. The detection is carried out by measuring the activity of the conjugated enzyme through incubation with a suitable substrate which produces a measurable product. The absorbance of the product is finally measured at a specific wavelength by spectrophotometry.

The Human, bacterial Toll-like receptor Multi analyte ELISA array kit was used to assess cytokine production following LPS treatment. The kit is used for the concurrent detection of 12 cytokines or chemokines in several biological samples using an ELISA assay. The kit contains screened and

certified capture and detection antibodies, shows high sensitivity and linearity and uses standard ELISA equipment. All the buffers used for the ELISA array were supplied by the manufacturer.

Sample collection and processing

After 24 hours treatment, 1 mL of cell culture medium was pipetted from LPS-treated and untreated samples and dispensed into 1.5 mL centrifuge tubes and centrifuged at 1500 rpm at 4°C for 10 minutes. The supernatants were immediately aliquoted into 1.5ml centrifuge tubes and stored at -80°C until required.

Reagent preparation

Five-hundred millilitres of 1X wash buffer was prepared by diluting 50 mL of the wash buffer in 450 mL of dH_2O to a final. The 1X wash buffer was transferred to a wash bottle and kept at room temperature. A working solution of BSA was prepared by diluting 0.6 ml of 10% BSA into 30 mL of assay buffer stock solution and kept at room temperature. Sample dilution buffer (1X) was prepared by diluting 2 ml of 10% BSA into 18 ml of sample dilution buffer stock to a final volume of 20 mL.

Sample addition and assay

The wells of rows 1 to 12 contained antibodies that were pre-coated by the manufacturer. Fifty microliters of assay buffer was loaded into each well. Fifty microliters of each sample was added to appropriate ELISA array microtitre plate wells onto which specific monoclonal antibodies had been coated. Using a multi-channel pipettor, 50 µL of sample dilution buffer was added to all the wells of row A to set up the negative control. The microplate was then covered, gently agitated for 10 seconds and incubated for 2 hours at room temperature on a bench top. The stop solution was thawed at room temperature, in a drawer protected from light. At this time, the 12 secondary/detection antibodies were thawed on ice for 30 minutes and prepared by adding 855 µL of sample dilution buffer and gently mixed. Each diluted detection antibody was then transferred to its corresponding tube in a strip of 12 tubes. The ELISA plate was washed by adding 350 µL of 1X wash buffer into each well, shaken gently for 10 seconds and the contents of each well were gently aspirated. The plate was then blotted up-side-down to remove any residual buffer. The process was repeated twice for a total of three washes.

Using a 12-channel pipettor, 100 µl of the dilute detection antibody from the strip of 12 tubes were added to their corresponding rows in the ELISA plate. The plate was covered, gently agitated for

10 seconds and incubated for an hour at room temperature. Just before the second wash following the one-hour incubation, Avidin-HRP conjugate was thawed on ice for 20 minutes and gently vortexed to mix properly. Eleven microlitres of the Avidin-HRP conjugate was added to 11 ml of assay buffer and kept in the dark. The ELISA plate was washed as previously described. The Avidin-HRP conjugate (100 µL) was added to all wells. The plate was then covered, gently tapped for ten seconds to mix, and incubated for 30 mins at room temperature in the dark.

The plate was washed as previously described; however, the number of washes was increased to four. Twelve millilitres of the development solution was transferred to a multi-channel pipettor reservoir and 100 µL the solution was added to all wells and the plate was incubated in the dark for 15 mins at room temperature. One hundred microlitres of stop solution was added to each well and a colour change was observed from blue to yellow. The absorbance was read at a wavelength of 450 nm and at 570 nm after about 20 minutes of stopping the reaction. The readings at 570 nm were subtracted from those at 450 nm for wavelength correction. For each antigen, the corrected absorbance values were calculated by subtracting the absorbance of the negative control from the absorbance of test samples and the results were plotted on a bar graph.

2.4.4 RT-PCR for cytokine expression

To further validate ELISA array cytokine screening, gene-specific primers for upregulated cytokines were designed (NCBI Primer Blast, NCBI) and synthesized (Inqaba Biotec, Pretoria, South Africa). **Table 4** shows the primers used and their predicted PCR product sizes in base pairs.

Table 4. PCR primers used and predicted product sizes

Gene	Forward primer	Reverse primer	Product size (base pairs)
IL8 (CXCL8)	5'-AAGGTGCAGTTTTGCCAAGG-3'	5'-CAACCCTCTGCACCCAGTTT-3'	204
RANTES (CCL5)	5'-CTGCCTCCCCATATTCCTCG-3'	5'-TCGGGTGACAAAGACGACTG-3'	137
MIP-1β (CCL4)	5'-GCACCAATGGGCTCAGAC-3'	5'-GCTCAGTTCAGTTCCAGGTC-3'	211
MDC (CCL22)	5'-GCGTGGTGTTGCTAACCTTC-3'	5'-AGGGCCAGGGGACATCTAAT-3'	649
RPL01	5'-GGCAAGAACACCATGATGCG-3'	5'-TCGAACACCTGCTGGATGAC-3'	416
GAPDH	5'-GAA GGT GAA GGT CGG AGT C-3'	5'-GAAGATGGTGATGGGATTTC-3'	226

cDNA synthesis and RT-PCR reactions were carried out as previously described in section 2.4.1.

2.4.5 L-Lactate assay

Naturally, lactate exists in two stereoisomers: L-lactate and D-lactate. L-lactate is the main stereoisomer of lactate produced during glycolysis and more pathophysiologically significant. This is due to the abundant presence of L-lactate dehydrogenase enzyme, producing almost exclusively L-lactate. Both stereoisomers of lactate are produced from the metabolism of pyruvate by the enzyme lactate dehydrogenase. L-lactate, the end product of glycolysis provides a reliable method of assessing the rate of glycolysis as shown in several studies (Elstrom et al., 2004; TeSlaa and Teitell, 2014; Zhao et al., 2009) making it the method of choice used in this study.

After 48-hour treatments with LPS and polymyxin B, 10 µL of cell culture supernatant was carefully aspirated from samples to be used for the assay. A glycolysis reaction solution (6 ml) was made containing 60 µL each of glycolysis assay substrate and co-factor into 5.82 ml of assay buffer. L-lactate standards (10, 5, 2.5, 1.25, 0.625, 0.313, 0.156 and 0 mM) were prepared from the 10mM stock solution to generate a standard curve. Ten microlitres of each sample, in duplicates, were transferred into appropriate wells in a clear, flat-bottomed 96-well plate. Two wells were allocated for the blank, into which culture medium was transferred. An equal volume of L-lactate standards was also transferred into appropriate wells on the 96-well plate in duplicates. One hundred microliters of the reaction solution was added using a multi-channel pipette to all wells. The plate was incubated at room temperature on an orbital shaker for 30 minutes. The absorbance was read at 490 nm using a Multiskan™ GO Microplate spectrophotometer. The average absorbance values were computed, and the blank absorbance was subtracted from all values to obtain the corrected absorbance values. The corrected absorbance values for each of the standards were plotted against their corresponding concentration values to obtain a standard curve. The L-lactate concentrations for experimental samples were finally computed using the formula below:

$$[L-Lactate] = (Absorbance/Slope) - y\_intercep\text{t}$$

2.4.6 Gene interaction analysis

In order to investigate possible relationships between upregulated cytokines and enhanced glycolysis observed from increased lactate levels following LPS treatment, pathway analysis was

done using GeneMANIA (Mostafavi et al., 2008; Warde-Farley et al., 2010) and IMP (Wong et al., 2012, 2015). GeneMANIA and IMP predict the function of genes of interest as well as possible protein-protein interaction networks.

IMP enables the analysis of candidate gene sets in the setting of functional networks. The functional interactions are predicted from integrated high-throughput data. IMP also further investigates enriched biological processes from the input gene set (Wong et al., 2012). GeneMANIA on the other hand, analyses a set of input genes and finds other genes that are related to it, by means of a large set of functional association data. These data include protein domain similarity, protein, and genetic interactions, co-expression, pathways and protein co-localization (Mostafavi et al., 2008).

GeneMANIA was shown to be the most accurate when compared with other web servers, and also generally faster in analysing inputs (Mostafavi et al., 2008; Peña-Castillo et al., 2008). The default settings for both web servers were used after entering the input genes. **Table 5** shows the input genes in both web servers:

Table 5. Input genes for GeneMANIA and IMP pathway analysis webservers

NCBI Gene ID	**Gene**	**Common name**
Upregulated cytokines		
3576	CXCL8	Interleukin 8 (IL8)
6352	CCL5	Regulated Upon Activation Normal T-cell Expressed Sequence (RANTES)
6351	CCL4	Macrophage inflammatory protein-1 beta (MIP-1β)
6367	CCL22	Macrophage-Derived Chemokine (MDC)
Glycolytic genes investigated		
NCBI Gene ID	**Gene**	**Common name**
3099	HK2	Hexokinase, isoform 2
3101	HK3	Hexokinase, isoform 3
3939	LDHA	Lactate dehydrogenase A
5224	PGAM2	Phosphoglycerate mutase, isoform 2
6513	SLC2A1	Glucose transporter 1 (GLUT1)
6517	SLC2A4	Glucose transporter 4 (GLUT4)
2023	ENO1	Enolase 1
5163	PDK1	Pyruvate dehydrogenase kinase1
5315	PKM	Pyruvate kinase
3091	HIF-1α	Hypoxia-inducible factor 1 alpha
5209	PFKFB3	6-phosphofructo-2-kinase/fructose-2,6-biphosphatase 3

2.4.7 Investigation of biological processes

Gene Ontology (GO) is defined as "a structured, precisely defined, common, controlled vocabulary for describing the roles of genes and gene products in any organism" (Ashburner et al., 2000). GO comprises three ontologies: cellular component, molecular function, and biological process. A biological process is a recognised chain of molecular functions which is essential for life. It was observed from GeneMANIA gene interaction networks that certain cytokines may co-express or be co-localised with glycolytic proteins (See **Figure 3.8** and **Table 6**). I postulated that the upregulated cytokines in this study could be involved in similar biological processes with certain glycolytic proteins. Each upregulated cytokine was used as an input gene in the IMP web server alongside the glycolytic proteins previously investigated. Next, "process network" was selected. Under the "network filters", "Only show shared processes' box was checked and "only show predictions" was unchecked. The prediction confidence cutoff was left at the default 0.5 value. The resulting images were processed and saved.

2.4.8 Mitochondrial membrane potential assay using JC-10 dye

Flow cytometric use of JC-10 dye provides a robust method for observing variations in mitochondrial membrane potential. This test is based on the detection of the mitochondrial membrane potential changes in cells by the lipophilic, cationic dye, JC-10. In healthy cells, JC-10 concentrates in the mitochondrial matrix where it forms aggregates with red fluorescence. However, during mitochondrial depolarisation, JC-10 disperses out of mitochondria. This causes the dye to change to its monomeric form and stain cells in green fluorescence.

Following 48-hour treatments, cells were pelleted by centrifugation at 1500 rpm for 5 minutes. Positive control and negative control samples were FCCP (Sigma-C2920) - and 95% ethanol-treated samples respectively.

The supernatant was discarded, and the pellet resuspended gently in 400 µL of JC-10 dye-loading solution (MAK160-1KT). The cells were incubated at 37°C, 5% CO_2, and 95% humidity for 60 minutes. Fluorescence intensity was monitored using FL1 (green) and FL2 (orange) fluorescent channels in a BD Acuri C6 flow cytometer (BD Biosciences, CA, USA). Fluorochrome spillover between FL1 and FL2 channels was corrected by fluorescence compensation. FL1 was corrected

by subtracting 3.2 units from FL2, while FL2 was corrected by subtracting 7.5 from FL1. All samples were run in triplicates.

2.4.9 Cell cycle analysis

Cell cycle analysis assesses the percentage of cells at sub G0/G1, G0/G1, S and G2M phases of the cell cycle. In this study, propidium iodide (PI), a fluorescent and DNA-intercalating dye was used to assess DNA content in ethanol-fixed cells following treatments at 24 and 48-hour time points. Firstly, the cells had to be fixed and permeabilised using 70% ethanol, permitting PI to enter the cells and bind to DNA. DNA contents change as a cell progresses from one phase of the cell cycle to another. At G0/G1 the DNA content is 2n (where n denotes the haploid DNA content of the genome). As S-phase during which DNA synthesis occurs, cellular DNA content ranges between 2n and 4n. At G2/M phase where DNA is fully synthesised, and cells are ready for mitosis, the DNA content is 4n. Any cells undergoing death would have DNA content less than the diploid number, 2n (Evan and Vousden, 2001). This means that cells at G2/M are about twice as fluorescent as those at the G0/G1 phase since PI binds proportionately to the amount of DNA present.

Somatic cells proliferate through mitosis which is determined by cell cycle progression (Alenzi, 2004). Given that a glycolytic flux, characteristic of the Warburg effect was observed following LPS treatments, I decided to investigate any possible changes in the cell cycle following LPS treatments at 24- and 48-hour time points. It was expected that, since the Warburg effect observed is a hallmark of cancer, LPS-induced metabolic reprogramming could lead to cell proliferation.

Cell fixation

Following treatment with LPS and Polymyxin B for 24 and 48 hours, cells were transferred from 6 well plates into 15 ml falcon tubes and centrifuged to pellet at 1500 rpm for 5 minutes. The supernatants were discarded, and 1 ml of PBS was added to the pellets. The pellets were then resuspended, and mixture transferred to labelled 1.5 ml Eppendorf tubes. The cells were then washed by centrifuging at 1500 rpm for 5 minutes. The supernatant was discarded and 1 ml of

70% prechilled (at -20°C) ethanol was added to each cell pellet slowly, while gently vortexing. The cells were then stored at -20°C for 24 hours.

Propidium iodide (PI) staining

A PI in RNase solution was used in this study. RNase was used because PI is a nucleic acid-binding dye. However, since only DNA content is representative of the different phases of the cell cycle, RNase was used to degrade all RNA present and give an accurate assessment of DNA content.

The cell suspensions were centrifuged at 3000 rpm for 5 minutes to pellet the cells. The ethanol supernatant was discarded, and the pellet washed by adding 1 ml of 1X PBS to the cell pellet, resuspending and centrifuging for 5 minutes. The wash step was repeated, to completely remove any ethanol which may interfere with the staining procedure. Three hundred microliters of FxCycle™PI/RNase solution was added to each pellet. Each tube was vortexed gently to resuspend the pellet. The samples were incubated at room temperature in the dark for 30 minutes. Thereafter, samples were analysed using a BD FACS Aria III flow cytometer with wavelength set at 488 nm. The sample flow rate was set to 'slow', for proper interrogation at the flow cell. Ten thousand events were acquired, and the sample population was gated by identifying singlet populations on the forward scatter versus side scatter plot. PI intensity was read on an FL3 channel at a wavelength of 488 nm.

2.5 Statistics

A two-tailed student t-test was used on the GraphPad Prism web server. Significance was calculated by comparing the means and standard deviations of three or two independent experiments at 95 % confidence interval ($p<0.05$). *p*-values less than 0.05 were considered statistically significant.

Chapter 3 -Results

Overview

This study showed that TLR4 was expressed in both THP-1 and K562 cells. However, there was a dose-dependent change in TLR4 expression following LPS treatments in THP-1, and not K562 cells. Furthermore, it was observed that RANTES, IL8, MIP-1β, and MDC, were upregulated following LPS treatment at both mRNA and protein levels. Moreover, LPS induced increased lactate production, indicative of enhanced glycolysis in THP-1 cells. This enhanced lactate production was inhibited by polymyxin B. Hence, glycolytic flux observed in THP-1 cells was TLR4 dependent, given that polymyxin B is an inhibitor of LPS-induced TLR4 signalling. Nevertheless, LPS was not able to induce an increase in glycolysis with 5, 10 and 20 ng/ml concentrations in K562 cells.

The function of proteins is largely determined by protein-protein co-expression and subcellular co-localisation. Analysis of possible relationships between upregulated cytokines and glycolysis, using IMP and GeneMANIA suggested that the upregulated cytokines in this study are co-expressed and co-localised with key glycolytic proteins. This shows that receptors for the upregulated cytokines are expressed, suggesting that the cytokines utilise an autocrine mechanism to induce LPS-mediated upregulation of glycolysis in THP-1 cells. It was found that Interleukin-8, MIP-1β, and RANTES showed co-expression with Hexokinase 3 (HK-3). IL8 in addition being co-expressed with HK-3 also showed co-expression with GLUT1 (SLC2A1) and PGM and co-localised with enolase 1 (ENO1). MDC showed co-expression with the LDHA, which is usually upregulated in several types of cancer. Both IL8 and MIP-1β are co-expressed with PFKFB3. Furthermore, both HIF-1α, GLUT3 (SLC2A3) are co-expressed and co-localised with IL8. The afore-mentioned protein-protein co-expression and co-localisation are presented in **Table 6**. Still, an investigation of the biological processes shared by the upregulated cytokines (IL8, RANTES, MDC, and MIP-1β) with glycolytic proteins, using IMP web server showed that several processes are shared; most of which are innate and adaptive immune responses.

Assessment of mitochondrial health using the JC-10 dye showed that LPS induced mitochondrial membrane depolarisation in both cell lines. Following an increase in glycolysis after LPS treatment, it was expected that the cells would proliferate, given that glycolytic flux is a metabolic

signature of the Warburg effect. After 24 hours of LPS treatments, a G0/G1 cell cycle arrest was observed, accompanied by a decrease in S-phase populations. However, after 48 hours, THP-1 cells showed an accumulation of sub/G0/G1 cell populations following LPS treatments. No cell cycle progression was observed. In K562 cells, an increase in G0/G1 was observed following 24 hours of treatment with LPS, however, after 48 hours, no significant change was observed between cell subpopulations. Proliferative indices are important determinants of cell proliferation. Following computation of proliferative indices of cell cycle sub-populations, no proliferation was observed in both cell lines. Overall, THP-1 displayed LPS-induced elevated glycolysis, mitochondrial membrane depolarisation, and upregulated chemokines; IL8, RANTES, MIP-1β, and MDC. Bioinformatic predictions showed that the upregulated chemokines are co-expressed with glucose transporters and glycolytic proteins. Especially, all upregulated chemokines were co-expressed with HK3.

3.1 TLR4 is expressed in both THP-1 and K562 cells

TLR4 plays an important role in pathogen recognition and innate immune activation; making its expression in innate immune cells critical for their functions. TLR4 responds to bacterial LPS, a PAMP which is present on the cell wall of Gram-negative bacteria, as well as other endogenous molecules released from tissue damage. Following TLR4 recognition of LPS, the receptor mediates the production of inflammatory cytokines necessary for mediating innate and subsequently influencing adaptive immunity. This work investigated the effects of LPS-induced TLR4 signalling on the metabolic program of THP-1 and K562 cells.

Since bacterial LPS was used to simulate infection in transformed innate immune cells (THP-1 and K562), it became necessary to investigate the expression of its cognate receptor, TLR4 in these cells. To investigate LPS-induced TLR4 receptor expression, the cells were treated with varying doses (5, 10 and 20 ng/ml) of LPS for 24 hours. It was observed that TLR4 was expressed in both THP-1 and K562 cell lines (**Figure 3.1**). However, LPS treatment of THP-1 cells for 24 hours showed a maximal expression of TLR4 at the lowest concentration of LPS (5 ng/ml), compared with higher concentrations (10 and 20 ng/ml). On the other hand, the lowest expression of TLR4 was observed at the highest concentration of LPS (20 ng/ml); suggesting an inverse relationship between the dose of LPS and TLR4 expression in THP-1 cells (**Figure 3.1A**). In contrast, in K562

cells, the highest expression was observed at 20 ng/ml of LPS concentration. Compared with the untreated cells, there was only a slight increase in TLR4 expression in K562 cells following treatment. Unexpectedly, there was a marked downregulation of TLR4 in K562 cells after treatment with 10 ng/ml LPS for 24 hours.

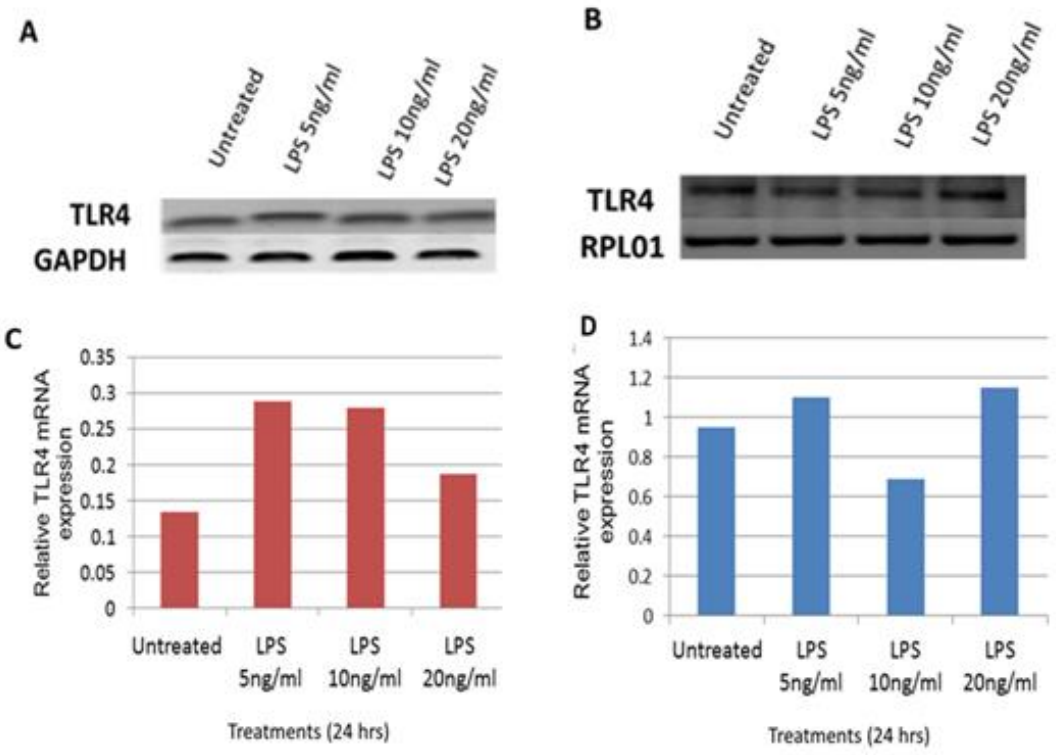

Figure 3.1. THP-1 and K562 cells express Toll-like receptor 4. THP-1 and K562 cells were treated with 5, 10 and 20 ng/ml LPS for 24 hours, total RNA was extracted, 1 µg of RNA was reverse-transcribed and TLR4 was amplified by PCR. The PCR products were run, on a 1% agarose gel. The gels were imaged using the ChemiDoc™ MP Imaging machine. Densitometric analysis was performed using MyImageAnalysis™ software. **A** and **B** show RT-PCR gel images for THP-1 and K562 respectively while and **C** and **D** show THP-1 and K562 densitometry results, respectively. TLR4 was normalised with reference genes (GAPDH and RPL01).

3.2 LPS upregulates IL8, RANTES, MIP-1β, and MDC protein expression THP-1 cells

After confirming the expression of TLR4, the function of TLR4 signalling pathway was investigated following LPS treatment. LPS, the main structural constituent of the cell wall of Gram-negative bacteria is a macromolecule having a molecular mass between 10 and 20 kDa. LPS is made up of lipid A, which is a hydrophobic lipid component responsible for its endotoxic properties. It also possesses a hydrophilic polysaccharide chain in the core region and a repeating hydrophilic oligosaccharide side chain which confers bacterial specificity (Rietschel et al., 1994).

To further investigate the signalling pathway activated by LPS in THP-1 cells, the cells were stimulated with LPS (5 ng/ml) and polymyxin B (10 μg/ml) for 24 hours and measured downstream effector cytokine expression using a TLR-induced multi-analyte ELISA array kit. The array simultaneously profiled the expression of 12 inflammatory cytokines namely: TNF-α, IL1β, IL6, IL12, IL17A, IL8, MCP-1, RANTES, MIP-1α, MIP-1β, MDC and eotaxin in a single detection experiment. It was found that IL8 and RANTES were highly upregulated after treatment with LPS. MIP-1β and MDC were slightly upregulated when compared with the untreated and samples co-treated with polymyxin B **(Figure 3.2).** When compared to LPS-treated cells, these findings also showed that the expression of RANTES, IL8, MIP-1β, and MDC were abrogated by polymyxin B. Interestingly, all upregulated cytokines in this study were chemokines. Surprisingly, TNF-α and IL-1β, which are known to be induced by LPS in monocytes and macrophages, were not detected in this study. Notably, untreated cells appear to secrete basal amounts of chemokines prior to LPS-mediated stimulation which may be required for other housekeeping functions.

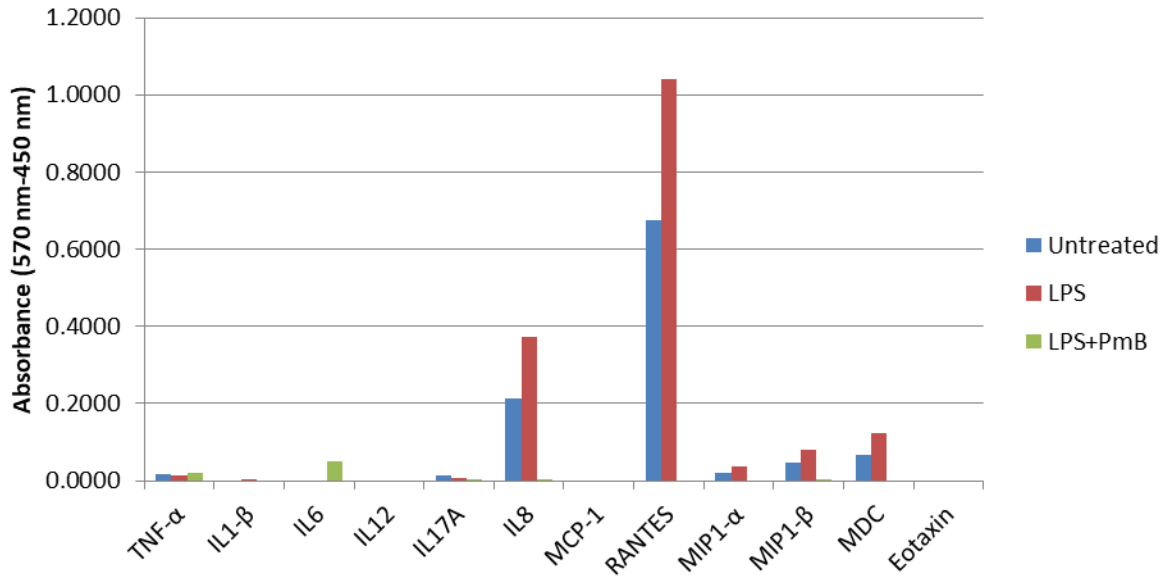

Figure 3.2. RANTES (CCL5) and interleukin 8 are highly upregulated following LPS treatment. Expression of 12 cytokines in THP-1 cells following LPS (5 ng/ml) treatment for 24 hours in a single detection ELISA array experiment. Polymyxin B (PmB) was used at 10 µg/ml to inhibit LPS-induced TLR4 signalling. Absorbance was read using a microplate spectrophotometer (Multiskan™ GO) at 450 nm and 570 nm. The readings at 570 nm were subtracted from those at 450 nm for wavelength correction. The Key insert shows various treatments.

3.2.1 RT-PCR validation of cytokine expression

Upon LPS binding to TLR4, conformational changes in TLR4 leads to the recruitment of intracellular adaptor proteins, subsequent activation of kinases (IRAK4 and IRAK1), followed by a cascade of signalling events which culminate in the translocation of transcription factors such as NF-κB to the nucleus (Chen et al., 2007; Medzhitov, 2001; Takeda and Akira, 2005). Next, NF-κB triggers the expression of specific cytokines by binding to their DNA promoter regions. To validate the ELISA, RT-PCR was performed on highly upregulated cytokines. Samples were treated for 24 and 48 hours with LPS alone and LPS and polymyxin B in biological duplicates. Gene-specific primers for RANTES, IL8, MIP-1β, and MDC were designed using the NCBI Primer blast software. In THP-1 cells, it was observed that there was an increased expression of RANTES, IL8, MIP-1β, and MDC which could be inhibited partially by polymyxin B (**Figure 3.3)**. In K562 cells, IL8, MDC, and MIP-1β were upregulated. But, no RANTES was detected in K562 cells prior to and post LPS stimulation (**Figure 3.4)**.

The lowest concentration of LPS, 5 ng/ml (compared with 10 and 20 ng/ml of LPS), showed the highest expression of mRNA for upregulated cytokines in both cell lines after 24-hour treatment as seen in **Figures 3.3** and **3.4**. Furthermore, there was a constitutive expression of IL8, RANTES, MIP-1β, and MDC in THP-1 cells as evidenced by mRNA expression in the untreated samples. Additionally, polymyxin B inhibited LPS-induced cytokine synthesis at 24 hours when 5 ng/ml of LPS was used, but not a clear inhibitory pattern when higher concentrations (10 ng/ml and 20 ng/ml) were used. At 48-hour treatments in THP-1 cells, both IL8 and RANTES mRNA were upregulated following LPS treatments (**Figure 3.3 E** and **F**), albeit apparently not inhibited by polymyxin B. Moreover, there was no apparent change in IL8 mRNA expression in K562 cells at 48-hour treatments with LPS (**Figure 3.4 B**), when compared with the untreated, and independent of co-treatment with polymyxin B. As seen in **Figure 3.4 C**, MDC expression in K562 cells was the same at all LPS treatment concentrations and showed polymyxin B-mediated inhibition. MDC mRNA levels in K562 at 48-hour LPS treatments only showed an increase in expression when the highest concentration (20 ng/ml) of LPS was used (**Figure 3.4 D**).

TLR4 expression results that were obtained showed that 5 ng/ml of LPS showed maximal TLR4 expression. ELISA array using 5 ng/ml of LPS indicated that IL8 and RANTES were highly upregulated at protein levels while MIP-1β and MDC were moderately upregulated. All upregulated cytokines were confirmed both at mRNA and protein levels. However, further comparing the pattern of expression between cytokines indicated that there was a lack of similarity. For example, it would have erroneously been expected IL8 mRNA expression levels in THP-1 to be highest when compared with MDC and MIP-β, judging from their protein expression levels. By contrast, the relative mRNA expression of MDC was higher than that of IL8 as seen in **Figure 3.3 A** and **3.3 C** respectively. Furthermore, even though RANTES protein expression was dramatically higher than that of MDC, their mRNA levels were more or less the same as seen in **Figure 3.3 B** and **C** respectively.

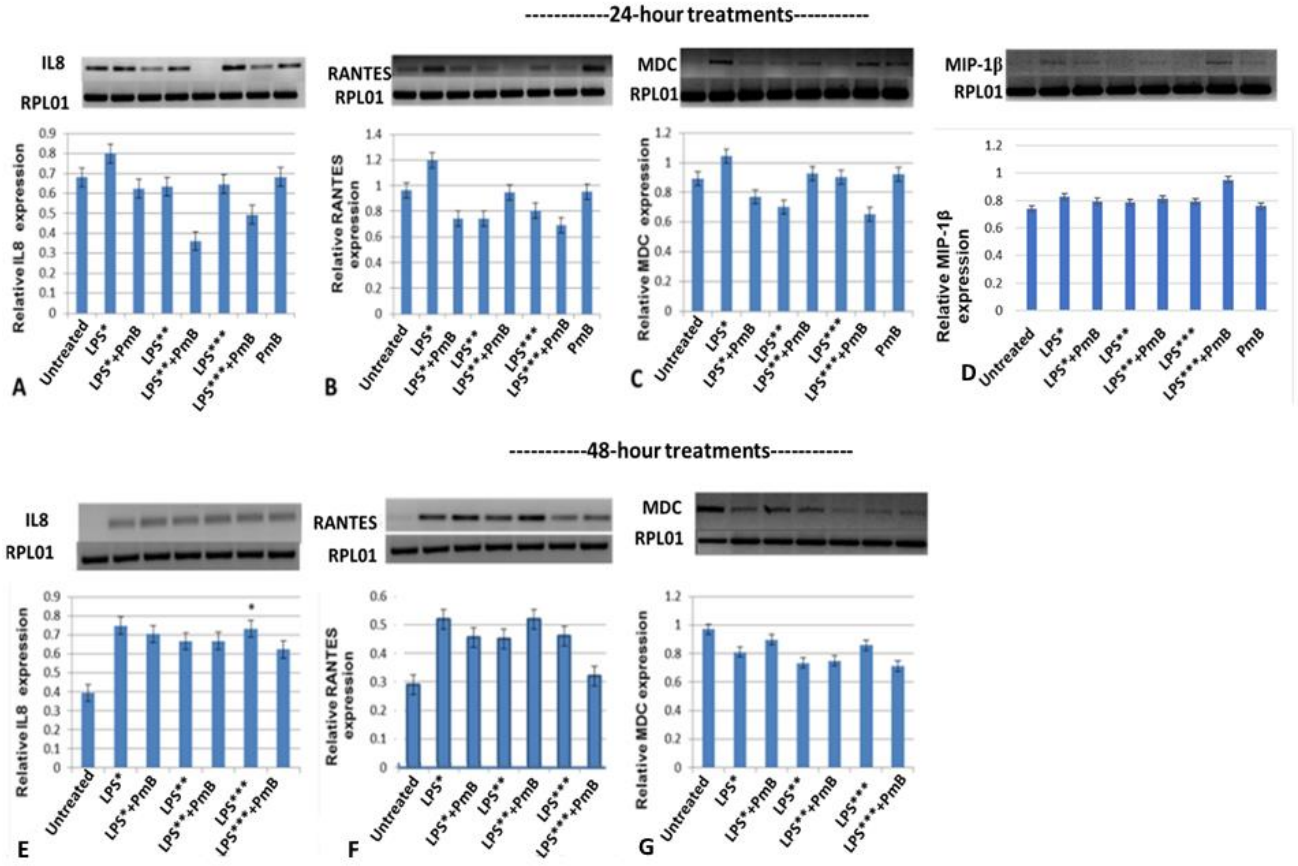

Figure 3.3. LPS-induces transcription of RANTES and IL8, MIP-1β and MDC in THP1: inhibited by polymyxin. RT-PCR illustrating changes in gene expression of IL8, RANTES, MDC, and MIP-1β mRNA. After LPS treatment, 1 µg of extracted total RNA was reverse-transcribed and amplified by PCR. PCR products were run on a 1% agarose gel. The gels were imaged using the ChemiDoc™ MP Imaging machine. Densitometric analyses were performed using MyImageAnalysis™ software. The densitometry results (bar graphs) were normalised with reference gene RPL01. The top panel, **A** to **D** shows 24-hour mRNA expression for IL8, RANTES, MDC, and MIP-1β respectively. The lower panel, **E** to **G** indicates mRNA expression for IL8, RANTES, and MDC respectively. **LPS*** (5 ng/ml LPS), **LPS**** (10 ng/ml LPS), **LPS***** (20 ng/ml LPS). Polymyxin B (PmB) at 10 µg/ml was used as an inhibitor of LPS-induced TLR4 signalling. The data is represented as mean ± SD from 2 independent experiments.

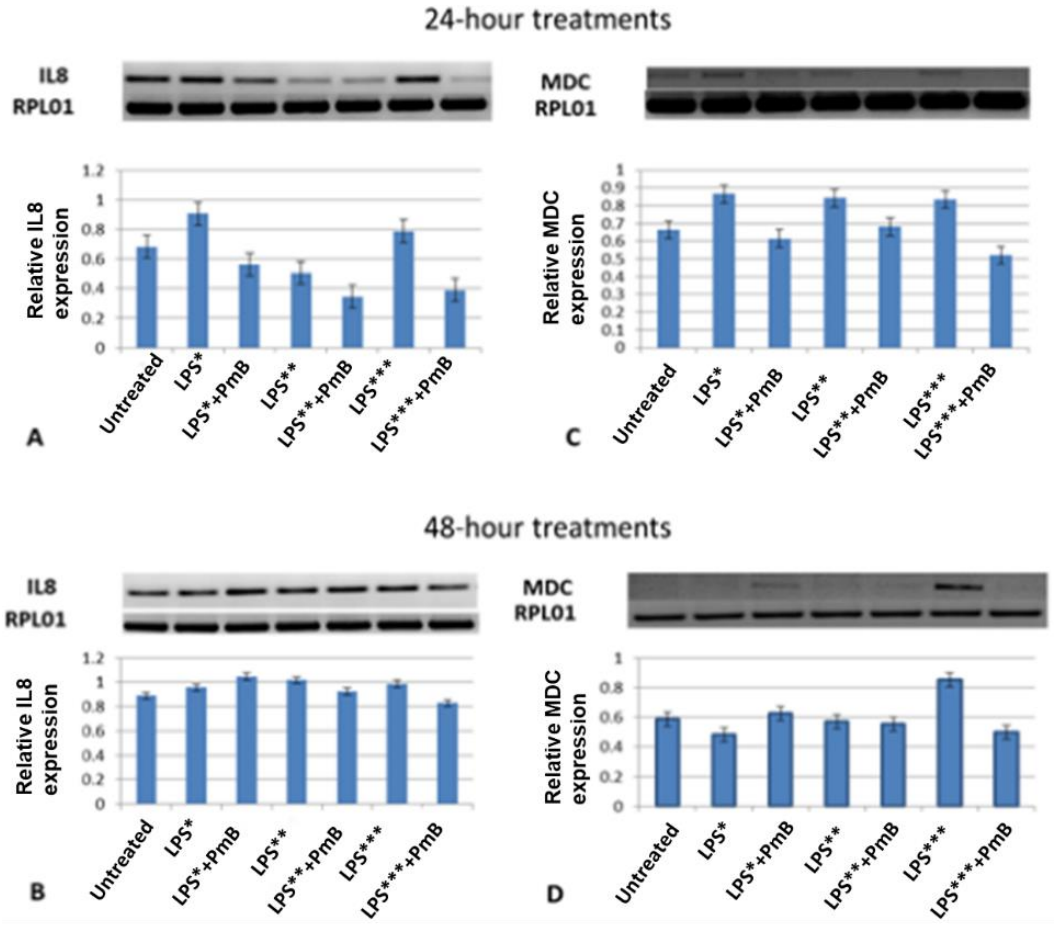

Figure 3.4. LPS-induces transcription IL8, MIP-1β, and MDC in K562: inhibited by polymyxin B. RT-PCR showing changes in gene expression. Cells were treated with LPS, 1 µg of extracted total RNA was reverse-transcribed and amplified by PCR. PCR products were run on a 1% agarose gel. The gels were imaged using the ChemiDoc™ MP Imaging machine. Densitometric analyses were performed using MyImageAnalysis™ software. The densitometry results (bar graphs) were normalised with reference gene RPL01. **A** and **B** show IL8 expression after 24 and 48-hour LPS treatments respectively while **C** and **D** depict MDC expression after 24- and 48 hours respectively. **LPS*** (5 ng/ml LPS), **LPS**** (10 ng/ml LPS), **LPS***** (20 ng/ml LPS). RANTES was not expressed in K562. Polymyxin B (PmB) at 10 µg/ml was used as an inhibitor of LPS-induced TLR4 signalling. The data is represented as mean ± SD from 2 independent experiments.

An overall comparison of THP-1 and K562 mRNA expression (as seen in **Figure 3.3** and **3.4)** shows that although MDC and IL8 were expressed in K562 at mRNA level, RANTES, a potent pro-inflammatory chemokine, was not expressed. However, RANTES was highly expressed in THP-1 cells at both mRNA and protein levels.

3.3 LPS induces glycolytic flux in THP-1 cells which can be inhibited by polymyxin B

The mechanisms that underlie infection-induced carcinogenesis are limited to direct oncogenic transformation by oncogenic viruses; inflammation etc. However, the possibility of microbes aggravating the Warburg effect and causing cell proliferation has not been elucidated. This was investigated by simulating infection in THP-1 and K562 cells using bacterial LPS. To determine the rate of glycolysis, lactate levels, which usually indicate the rate of glycolysis, were measured. It has been reported that lactate, the preferred end product of glycolysis in tumour cells, is primarily the cause of the acidification of the tumour microenvironment (Gottfried et al., 2006; Rogatzki et al., 2015).

An increase in the production of lactate was observed in THP-1 cells following treatment with 5 and 10 ng/ml of LPS (*p* values ± SD: 0.0299±0.03195 and 0.0211 ± 0.0012 respectively) as shown in **Figure 3.5**. There was also a nearly significant secretion of lactate in the sample treated with 20 ng/ml LPS when compared with the untreated sample (*p*-value ±SD: 0.054±0.019). However, there was a slight decline in lactate production when LPS was increased to 20 ng/ml. The fact that LPS-induced glycolytic flux was inhibited by polymyxin B suggested that such a change is likely TLR4-dependent.

There was no significant change in lactate production following treatments with LPS and co-treatments with LPS and polymyxin B in K562 cells (**Figure 3.5**). Even though there was only a slight increase following LPS treatments, a similar scenario was observed when co-treatment with polymyxin B was carried out. Overall, there was no appreciable increase in lactate production following LPS treatments in K562 cells. This implied that LPS did not affect the metabolic program of K562 cells when compared to THP-1 cells. Despite increasing LPS concentration from 5 ng/ml to 20 ng/ml in K562 cells, no significant change in L-lactate production was observed.

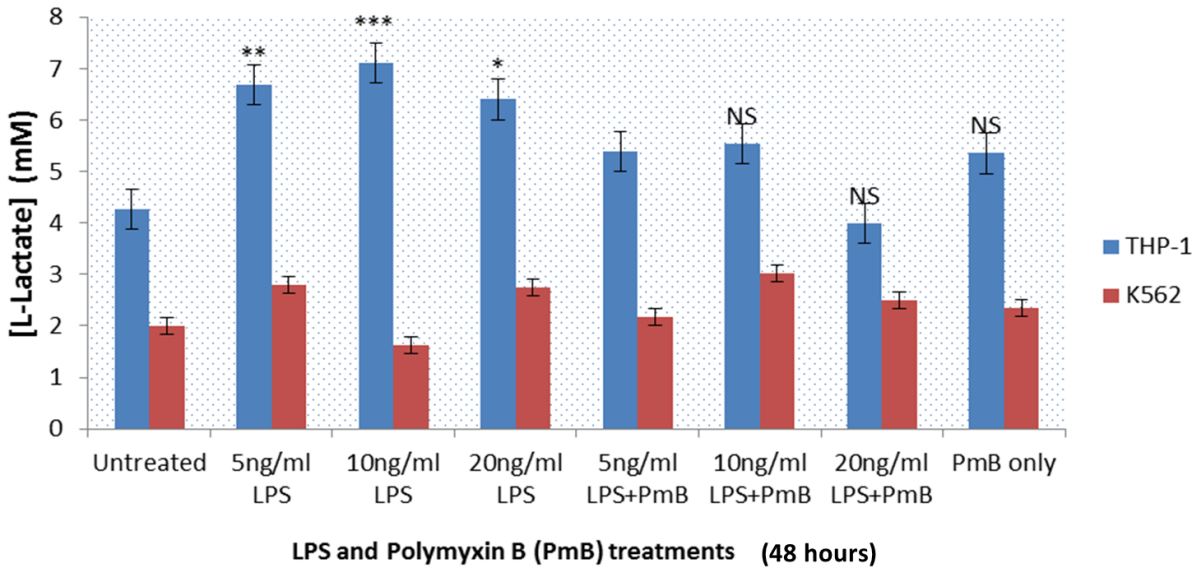

Figure 3.5. LPS induces glycolytic flux in THP-1, but not K562 cells. THP-1 (blue bars) and K562 (red bars) cells were treated for 48 hours. 10 uL of each sample was used to run the lactate assay. Absorbance values were read at 490 nm using a Multiskan™ GO Microplate reader. The data is represented as mean ± SD from 2 independent experiments. * indicates nearly statistically significant (*p*-value ±SD: 0.054±0.019) ** indicates statistically significant (0.0299±0.03195), *** indicates very statistically significant (0.0211 ± 0.0012). GraphPad Quick Calcs software was used to compute all statistics.

3.4 RANTES, IL8, MIP-1β, and MDC show co-expression and other possible interactions with glycolytic proteins

Many proteins function in multi-protein complexes, which are vital in virtually all cellular processes. Proteins rely on the properties and stoichiometry of their interacting partners for proper activity (Kerrigan et al., 2011). This is because the co-expression of interacting protein partners is critical for proper folding and stability which influences the activity of a protein. Hence, the study of protein-protein co-expression is important in elucidating biological systems in health and disease.

Following increased glycolytic flux observed during LPS treatment *in silico* gene interaction analysis was done to investigate possible relationships between cytokines and glycolysis. Hence, possible interactions between the upregulated cytokines in this study and glycolytic proteins were

investigated. A list of input genes comprising of upregulated cytokines in this study and glycolytic proteins (**Table 5, section 2.4.6**) were entered to the IMP web server.

IMP data showed a network of predicted interactions between upregulated cytokines and some glycolytic proteins. For example, CCL4 (MIP-1β) is predicted to interact with HK3. It is also predicted to interact strongly with several cytokines and cytokine receptors as shown in **Figure 3.6**. CCL-5 (RANTES) relates with IL10RA (Interleukin 10 receptor A), which in turn is predicted to interact with HK3. CXCL8 (IL8), in addition to its vast interaction with cytokines and cytokine receptors, also shows a relationship between certain genes which relate to glycolytic enzymes. For example, IL8 relates with BHLHE40 (Basic Helix-Loop-Helix Family Member E40), which shows a relationship with LDHA and ENO1. CCL22 (MDC) relates with IL10RA and CCR5 (a RANTES receptor). Both IL10RA and CCR5 are predicted to interact with HK3. Furthermore, HIF-1α which is known to transcriptionally upregulate several glycolytic genes is also predicted to interact with IL8 which showed marked upregulation in this study. HIF-1α also interacts with PLAUR (Plasminogen Activator, Urokinase Receptor) whose activation influences several cytokines and cytokine receptors as seen in **Figure 3.6.**

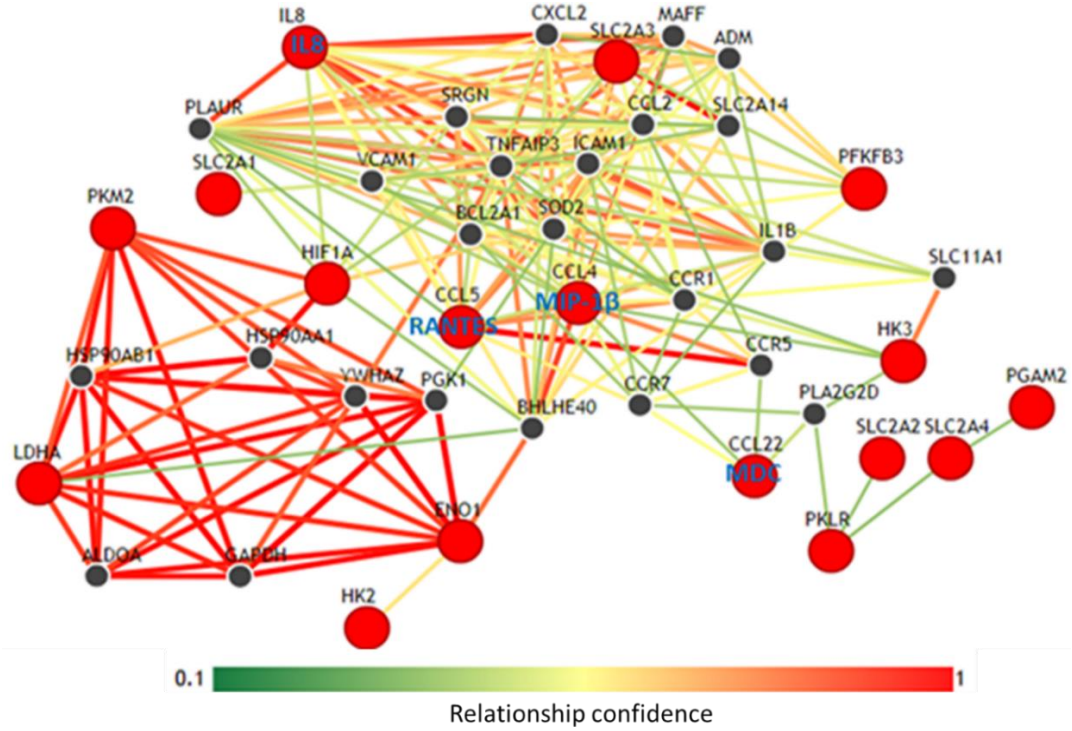

Figure 3.6. Predicted gene interaction network of cytokines and glycolytic genes from IMP webserver. The interaction networks were generated by entering upregulated cytokines and glycolytic

genes into the IMP web server. A **node** represents a gene and an **edge** represents the probability based on high throughput data that a pair of genes participates in a biological process. The relationship confidence bar shown on the figure gives the strength of the interaction based on network weights. Meaning red edges represent stronger interaction confidence while green interactions show weaker confidence. The **red nodes** represent input genes while the **black nodes** represent other interacting genes in the network.

The web of interactions predicted by IMP and depicted in **Figure 3.6** above warranted further investigation of the nature of interactions. It therefore became imperative to use another gene interaction web server. To further validate the predicted interactions made by the IMP webserver and probe the nature of such relationships, GeneMANIA was used. Of all the input genes (as shown in **Table 5**), GeneMANIA (Mostafavi et al., 2008) data showed further multiple interactions between upregulated cytokines in this study and glycolytic proteins as seen in **Figures 3.7 and 3.8.**

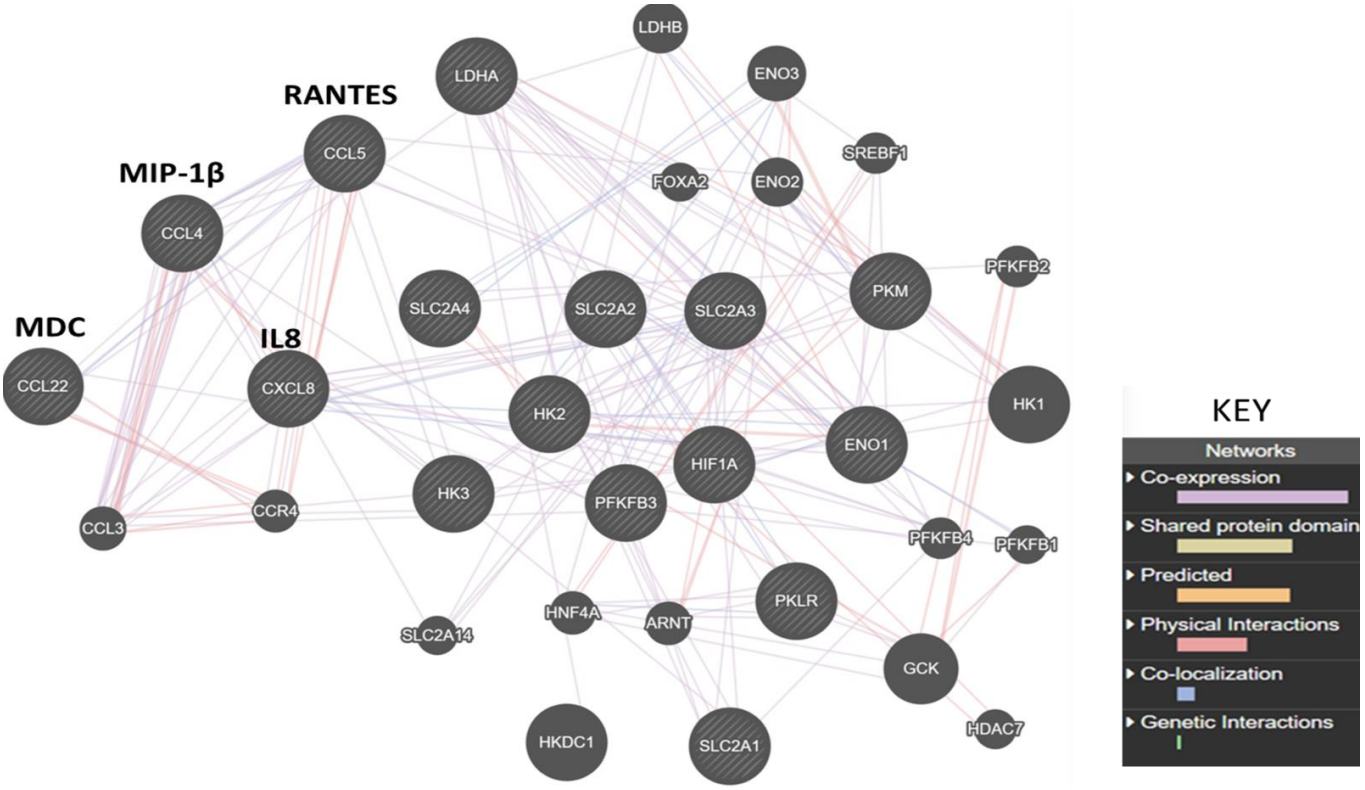

Figure 3.7. Complete GeneMANIA pathways: interaction of cytokines and glycolytic genes. The interaction networks were generated by entering upregulated cytokines and glycolytic genes into the GeneMANIA web server. The striped nodes represent the input genes while the unstriped nodes represent other interacting genes in the network. The edges represent the interactions: The **purple** edges: co-expression, **pink**: physical interactions, yellow: predicted interactions, blue: co-localisation and green: genetic interactions. The key on the left gives a proper colour coding for the interactions shown by the edges. Interactions were considered statistically significant when an FDR (False discovery rate) value is <

0.05. FDR<0.05 represents a 5% chance of getting a false statistically significant result. GeneMANIA computes FDR values using the Benjamini-Hochberg procedure which is in-built to the web server. GeneMANIA network uses weights that indicate the predictive value of each selected data set for the query. Weights are assigned to networks based on how significant they are to the query genes. Non-relevant networks have zero weights and are not shown in the results.

It was observed that, IL8, RANTES, MIP-1β and MDC show co-expression (purple edges) with several glycolytic proteins and co-localisation (blue edges) with a few glycolytic proteins. IL8, RANTES, MIP-1β, and MDC also showed physical interactions (pink edges) among themselves and with other cytokines and cytokine receptors such as "physical interactions" (pink edges). To better analyse each of the interactions between the upregulated cytokines and glycolytic proteins, the cytokines were selected in the GeneMANIA web server, thereby highlighting interactions (**Figure 3.8**).

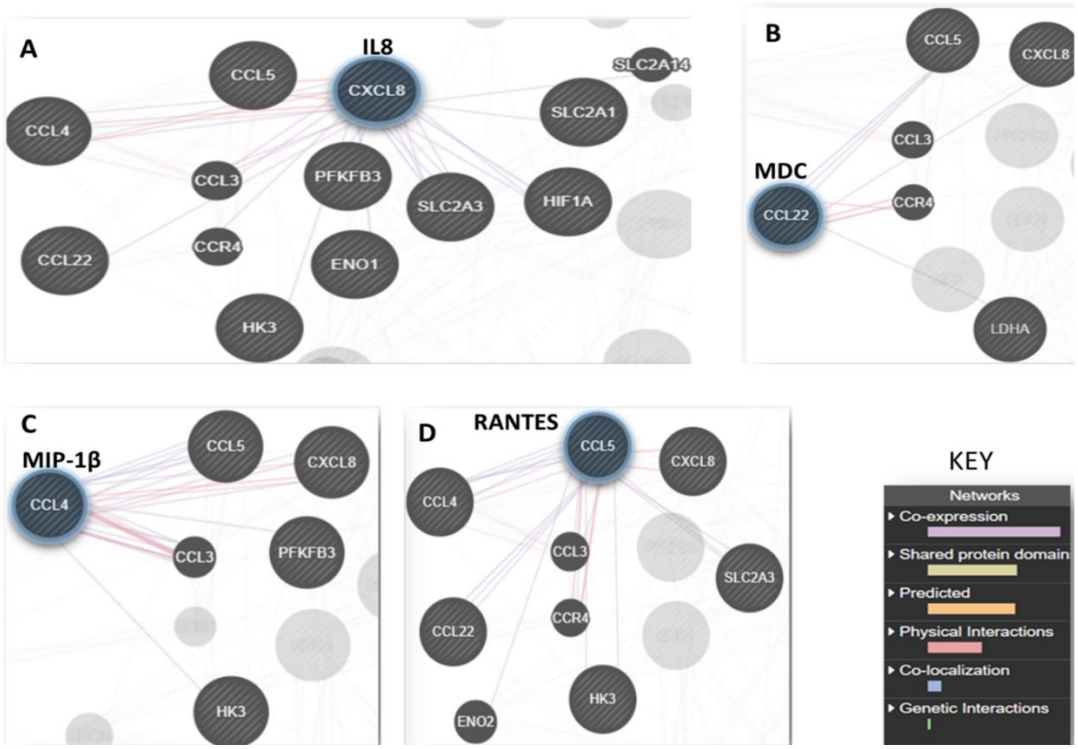

Figure 3.8. Interleukin 8, RANTES, MIP-1β and MDC show co-expression and other potential interactions with glycolytic genes. The interaction networks were generated by entering upregulated cytokines and glycolytic genes into the GeneMANIA web server. **A** shows a focus on IL8 interactions. **B**, **C** and **D** show MDC, MIP-1β and RANTES interactions respectively. The nodes represent genes while the edges represent interactions. All striped nodes show input genes while unstriped nodes represent other interacting genes. Striped nodes with blue outlines represent the focus gene in the interaction network. The edge colour denotes the type of gene interaction: The **purple** edges: co-expression, **pink**: physical

interactions, yellow: predicted interactions, blue: co-localisation and green: genetic interactions. The key on the left gives a proper colour coding for the interactions shown by the edges (see the key inserted). Interactions were considered statistically significant when an FDR (False discovery rate) value is < 0.05. FDR<0.05 represents a 5% chance of getting a false statistically significant result. GeneMANIA computes FDR values using the Benjamini-Hochberg procedure which is in-built to the web server. GeneMANIA network uses weights that indicate the predictive value of each selected data set for the query. Weights are assigned to networks based on how significant they are to the query genes. Non-relevant networks have zero weights and are not shown in the results. **Table 6** shows interactions, corresponding network weights, and references.

IL8, MIP-1β, and RANTES showed co-expression with HK-3, (white blood cell-type isoform 3-which phosphorylates glucose in the first step of glycolysis) IL8, in addition being co-expressed with HK-3, also showed co-expression with GLUT1 (SLC2A1) and PGM, and co-localised with ENO1. MDC showed co-expression with the LDHA which is usually upregulated in several types of cancer. Both IL8 and MIP-1β are co-expressed with PFKFB3. Furthermore, both HIF-1α, GLUT3 (SLC2A3) are co-expressed and co-localised with IL8. **Table 6** summarises the interactions, supported by appropriate references.

Table 6. Cytokines co-express and co-localise with glycolytic proteins and glucose transporters

Cytokine-Glycolytic protein pair	Interaction	Network weights*	References
		IL8 (CXCL8)	
IL8-GLUT1	Co-expression	0.006498751	(Burington et al., 2008)
IL8-GLUT3	Co-expression	0.015069837	(Wang et al., 2006)
	Co-expression	0.010163048	(Ramaswamy et al., 2001)
		0.027028402	(Roth et al., 2006)
		0.019684862	(Boldrick et al., 2002)
		0.012002146	(Innocenti et al., 2011)
	Co-localisation	0.009628404	(Johnson et al., 2003)
IL8-HIF1-α	Co-localisation	0.022712165	(Schadt et al., 2004)
	Co-expression	0.020582383	(Boldrick et al., 2002)
IL8-HK3	Co-expression	0.010228073	(Roth et al., 2006)
IL8- PFKFB3	Co-expression	0.012226868	(Ramaswamy et al., 2001)
		0.013425241	(Noble et al., 2008)
IL8-ENO1	Co-localisation	0.010370574	(Schadt et al., 2004)
		RANTES (CCL5)	
RANTES-GLUT3	Co-expression	0.01901005	(Boldrick et al., 2002)
	Co-expression	0.012890254	(Burington et al., 2008)
	Co-expression	0.019818643	(Wu et al., 2007)
RANTES-ENO2	Co-expression	0.01997907	(Rieger et al., 2004)
RANTES-HK3	Co-expression	0.008441823	(Bild et al., 2006)
		MIP-1β (CCL4)	
MIP-1β-HK3	Co-expression	0.011541992	(Bild et al., 2006)
MIP-1β- PFKFB3	Co-expression	0.018491235	(Ramaswamy et al., 2001)
		MDC (CCL22)	
MDC-LDHA	Co-expression	0.007362005	(Wang et al., 2015)

*GeneMANIA network uses weights that indicate the predictive value of each selected data set for the query. Weights are assigned to networks based on how significant they are to the query genes. Non-relevant networks have zero weights and are not shown in the results. The network weighting algorithms used by GeneMANIA have been validated in previous studies (Mostafavi et al., 2008; Warde-Farley et al., 2010).

RANTES, IL8, MIP-1β, and MDC are involved in similar biological processes as some glycolytic genes

The IMP web server was used to further investigate shared biological processes of each of the upregulated cytokines (IL8, RANTES, MIP-1β, and MDC) with each of the glycolytic proteins previously stated (**Table 5).** It was found that several biological processes are shared by the afore-mentioned cytokines and some glycolytic proteins. Examples include T cell activation, regulation of cellular homeostasis and regulation of cytokine production (**Figure 3.9 A** to **D**, and **Table 7**).

As seen in **Figure 3.9** IL8 is involved with HK3 in regulating CD8+ T cell activation (**A**); is involved with ENO1 in regulating cellular homeostasis (**B**) and participates with the glucose transporter SLC2A3(GLUT3) to regulate the response to nitrogen compounds (**C**). HIF-1α, a master regulator of glycolysis participates with IL8 in several processes such as immune regulation, angiogenesis, and receptor metabolic processes.

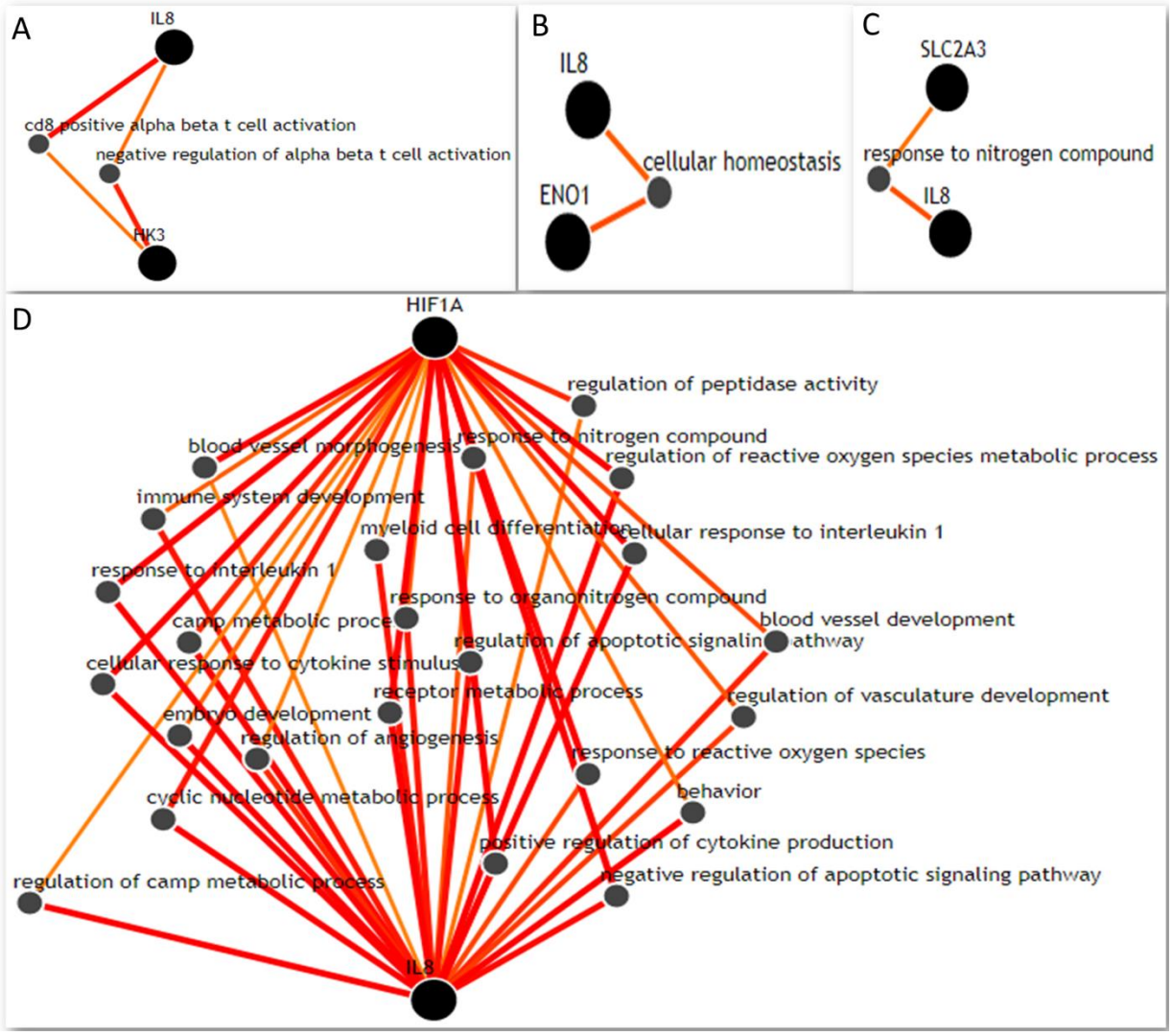

Figure 3.9 Network diagram showing biological processes shared by IL8 and glycolytic genes from IMP web server. Each upregulated cytokine was used as an input gene in the IMP web server alongside the glycolytic proteins previously investigated and "Biological processes" was run. **A** shows processes shared by IL8 and HK3 while **B** shows shared processes between IL8 and ENO1; **C**: IL8 and SLC2A3 (GLUT3); **D**: IL8 and HIF-1α. Big nodes show input genes while smaller nodes represent enriched biological processes. The edges represent links to shared biological processes; with the colour intensity indicating the strength of the interaction.

It was also observed that RANTES participated in several biological processes with HK3, a hexokinase isoform involved in glucose phosphorylation in the first step of glycolysis. These processes included T-cell regulation and cytokine production (**Figure 3.10A**). RANTES was also

involved in several biological processes with HIF-1α (**Figure 3.10B**), which is known to regulate both immune and metabolic processes (Haddad and Harb, 2005).

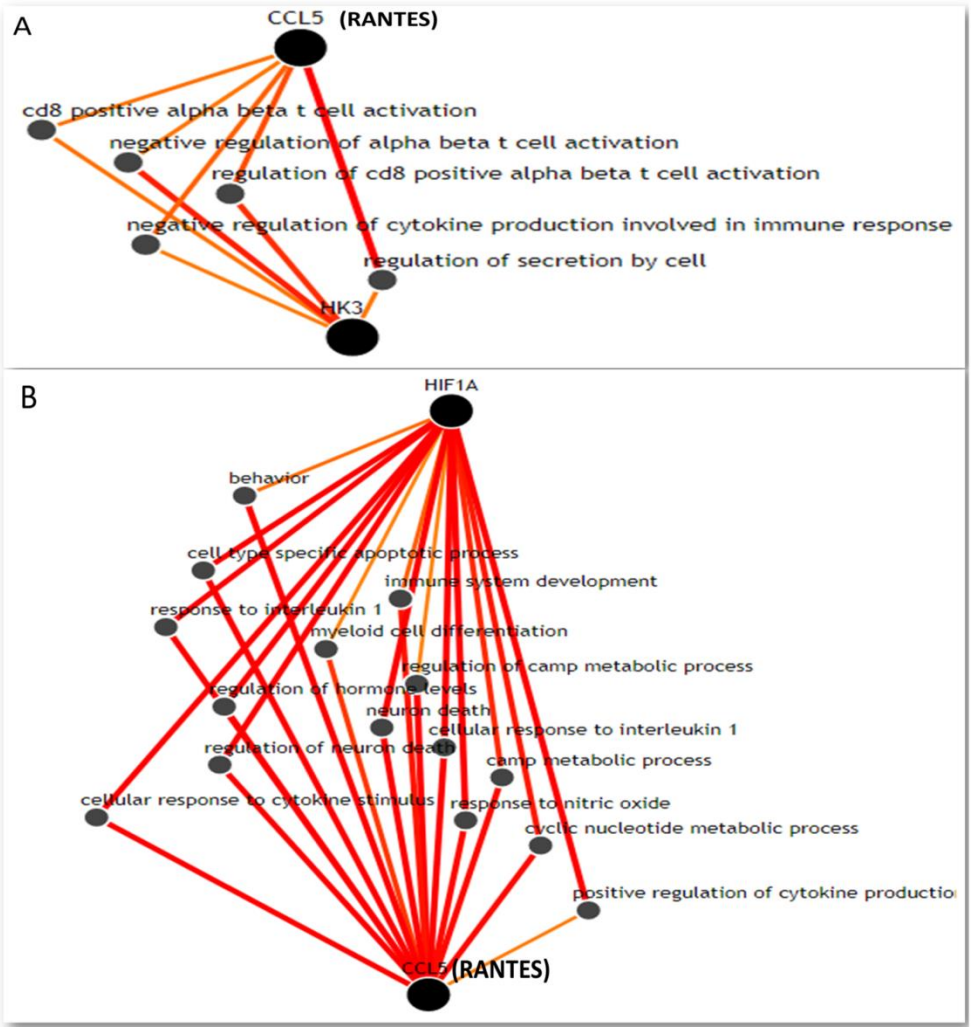

Figure 3.10. Network diagram showing biological processes shared by RANTES from IMP web server. Each upregulated cytokine was used as an input gene in the IMP web server alongside the glycolytic proteins previously investigated and "Biological processes" was run. **A** shows processes shared by RANTES and HK3 while **B** shows shared processes between RANTES and HIF-1α. Big nodes show input genes while smaller nodes represent enriched biological processes.

MIP-1β participates in biological processes with HK3 (**A**), HIF-1α (**B**) and ENO1 (**C**) As shown in **Figure 3.11**. MDC is involved in biological processes with HIF-1α (E) and HK3 (F). An interesting observation was that HK3 was involved in biological processes with all upregulated cytokines: IL8 (**Figure 3.9 A**) RANTES **(3.10 A**), MIP-1β (**3.11 A**) and MDC (**3.11 E**). It should be noted that HK3 was also co-expressed with all the upregulated cytokines (**Table 6**).

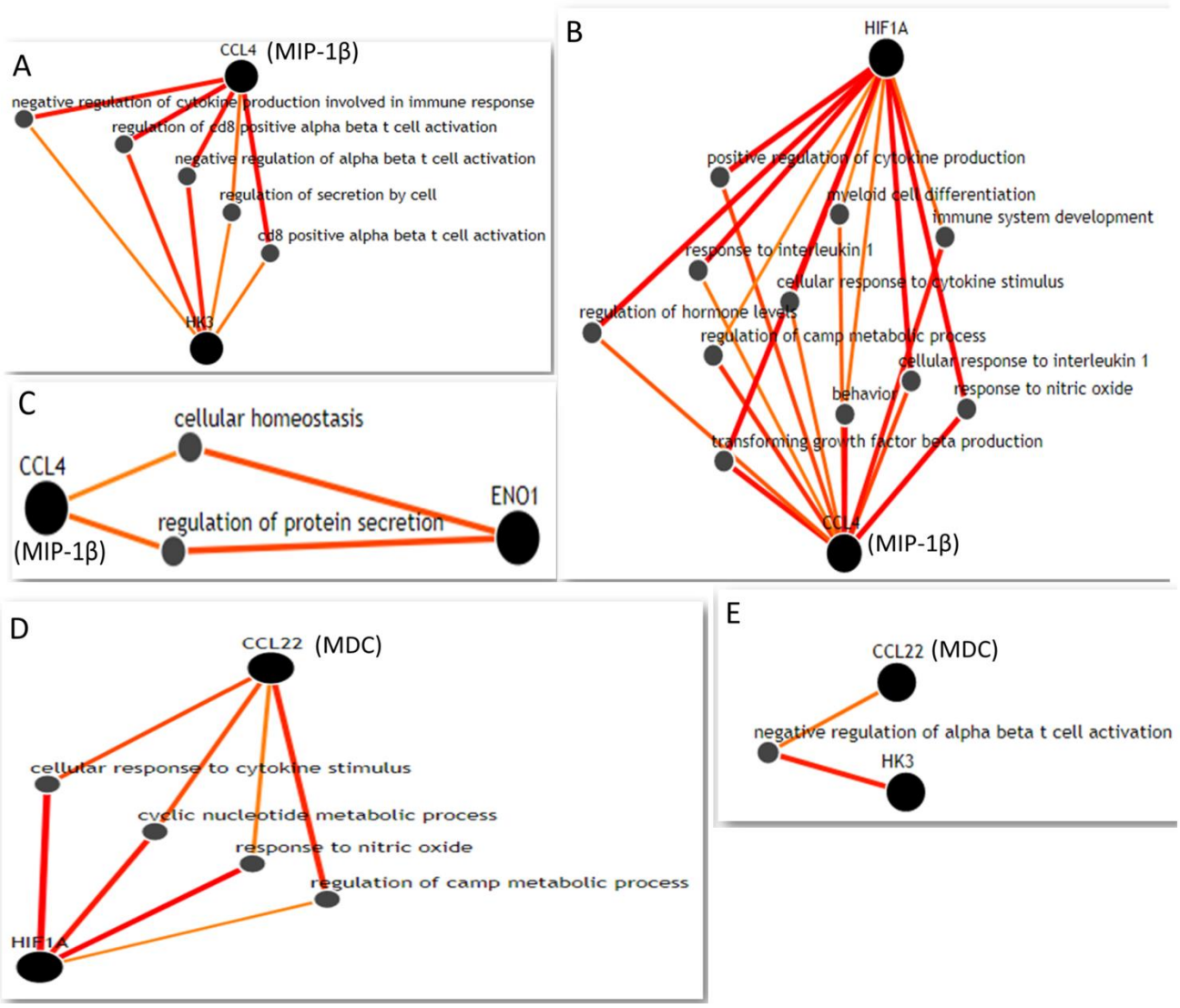

Figure 3.11 Network diagram showing biological processes shared by MDC and MIP-1β from IMP web server. Each upregulated cytokine was used as an input gene in the IMP web server alongside the glycolytic proteins previously investigated and "Biological processes" was run. **A** shows processes shared by MIP-1β and HK3 while **B** shows shared processes between MIP-1β and HIF-1α; **C**: MIP-1β and ENO1; **D**: MDC and HIF-1α; and **E**: MDC and HK3. Big nodes show input genes while smaller nodes represent enriched biological processes. The edges represent links to shared biological processes; with the colour intensity indicating the strength of the interaction.

The shared biological processes between IL8, RANTES, MIP-1β and MDC and glycolytic proteins depicted in **Figures 3.9**, **3.10** and **3.11** above are summarised in **Table 7.**

Table 7. Shared biological processes between cytokines and glycolytic proteins

Cytokine-glycolytic protein pair	Shared biological processes
IL8-HK3	• CD8 positive alpha beta T-cell activation
	• Negative regulation of alpha beta T-cell activation
IL8-GLUT3	• Response to nitrogen compound
IL8-ENO1	• Cellular homeostasis
RANTES-HK3	• CD8 positive alpha beta T-cell activation
	• Negative regulation of CD8 positive alpha beta T-cell activation
	• Regulation of CD8 positive alpha beta T-cell activation
	• Negative regulation of cytokine production involved in immune response
	• Regulation of secretion by cell
MIP-1β-HK3	• CD8 positive alpha beta T-cell activation
	• Negative regulation of cytokine production involved in immune response
	• Regulation of CD8 positive alpha beta T-cell activation
	• Negative regulation of alpha beta T-cell activation
	• Regulation of secretion by cell
MIP-1β-ENO1	• Regulation of protein secretion
	• Cellular homeostasis
MDC-HK-3	• Negative regulation of alpha beta T-cell activation

Some cytokines (IL8, RANTES, MIP-1β, and MDC) are co-expressed with glycolytic proteins (**Table 6**) and these proteins also share important biological processes with glycolytic proteins and glucose transporters (**Table 7**). However, most of the enriched biological processes are found in the innate and adaptive arms of the immune system. Another important finding is that IL8,

RANTES, and MIP-1β are all involved with HK3 in regulating CD8+ T-cell activation. To further understand the significance of such relationships, the role of the afore-mentioned glycolytic enzymes were further probed in normal leukocyte physiology and leukaemia carcinogenesis. The findings are discussed in chapter four.

3.5 LPS downregulates mitochondrial membrane potential (MMP) in both THP-1 and K562 cells

Otto Warburg initially proposed that the reduced oxidative phosphorylation observed in tumours was as a result of dysfunctional mitochondria (Warburg, 1956). However, except for a few tumour types that show deregulated or mutated genes such as succinate dehydrogenase and fumarate hydratase (Alam et al., 2005; Astuti et al., 2001), a majority of tumours show properly functioning mitochondria despite reduced OxPhos. Even though a handful of mechanisms for ATP generation exist, a boost in glycolysis is usually accompanied by a corresponding compensatory decrease in OxPhos (which is highly dependent on MMP) that keeps ATP levels relatively constant. To improve understanding of the metabolic picture, changes in MMP were investigated. MMP can be used as a measure of ATP synthesis (Duchen et al., 1993; Krippeit-Drews et al., 2000). Moreover, MMP is an important determinant of a cells capacity to synthesise ATP by OxPhos (Perry et al., 2011). The assay used the JC-10 dye to probe the percentage of cells with polarized mitochondrial membranes compared with those showing depolarized mitochondrial membranes after LPS treatments. These data indicate that LPS induced a drop (depolarisation) in the MMP suggestive of a decline in the rate of mitochondrial respiration (OxPhos). **Figure 3.12A and 3.12B** show MMP data for K562 and THP-1 cells respectively. The original cytograms for the MMP assay are shown in the appendix section (**Figure A3.6** and **Figure A3.7**).

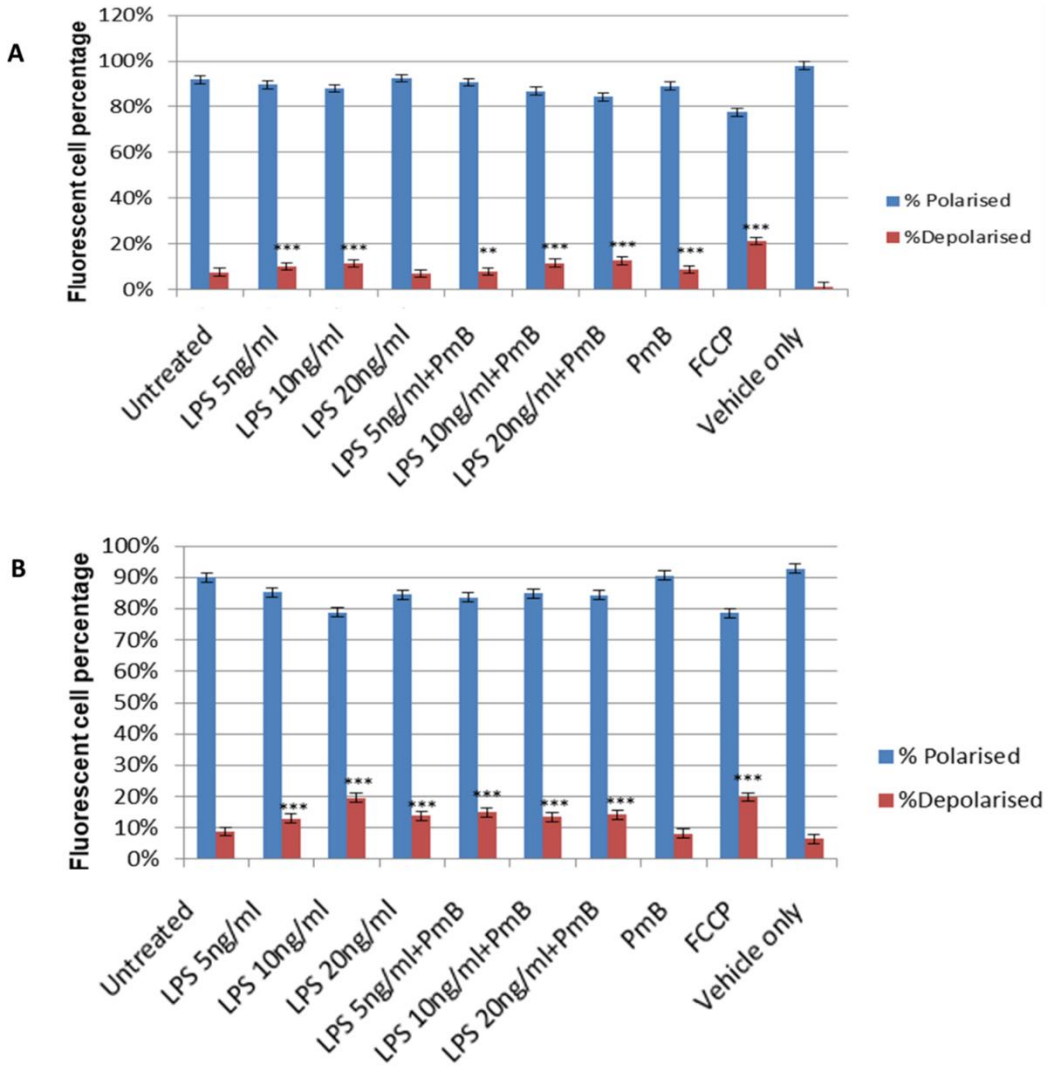

Figure 3.12. LPS depolarises the mitochondrial membrane in both THP-1 and K562 cells. Following treatments for 48 hours, JC-10 assay was performed, and fluorescence intensity was monitored using FL1 (green) and FL2 (orange) fluorescent channels in a BD Acuri C6 flow cytometer. **A** represents THP-1 cells while **B** depicts K562 cells. The **red bars** show the percentage of depolarised cells while **blue bars** indicate polarised cells. FCCP dissolved in 95% ethanol as used as the positive control while those treated with the 95% ethanol-treated cells were used as the negative control. The data represent mean ± SD of 3 independent experiments. (* indicates p <0.05, ** indicates p <0.01, *** indicates p <0.001). GraphPad Quick Calcs software was used to compute all statistics. Polymyxin B (PmB) concentration used was 10 µg/ml.

Both cell lines showed a significant, dose-dependent decrease in MMP, with maximal depolarisation observed at 10 ng/ml LPS. There was a significant increase in membrane depolarisation at 5 ng/ml (p-value ± SD=0.0001 ± 0.01323) and 10 ng/ml (p-value ± SD= 0.0001 ± 0.0144) following treatment of THP-1 with LPS (**B**). In K562 cells (**A**), all changes were

statistically significant (shown with three asterisks) with *p* values less than 0.0001 following LPS treatment. *P*-values±SD: 0.0001±0.0326, 0.0001±0.0419 and 0.0001±0.0255 for 5, 10 and 20 ng/ml LPS treatments respectively. Further details such as gating strategy and various quadrants can be seen in the cytograms in the appendix (**Figures A3.7 (**THP-1**)** and **A3.8 (**K562**)**)

3.6 LPS does not drive cell cycle progression in THP-1 and K562 cells

Following an enhancement of the glycolytic phenotype in THP-1, a progression in the cell cycle was expected because the Warburg effect is one of the hallmarks of cancer (Hanahan and Weinberg, 2011). In addition, after observing the upregulated expression of IL8, RANTES, MIP-1β, and MDC, it was postulated that these may be able to drive cell cycle progression. It has been reported that cytokines/chemokines are able to drive cell cycle progression in several cell types (Grivennikov and Karin, 2011).

Exogenous lactate has been shown to stimulate the progression into the S phase of the cell cycle and also induce proliferation in mouse fibroblasts (Rutz and Little, 1995). Increased glycolytic flux which is characteristic of the Warburg effect is also associated with cell cycle progression (Bao et al., 2013). Furthermore, enhanced glycolysis as seen from increased lactate flux is partly because of increased activity of glycolytic enzymes; many of which have non-glycolytic, survival and proliferative functions (Yu and Li, 2016). After 24 hours of LPS treatments, no cell cycle changes were observed (**Figure 3.13A**). However, after 48 hours, a significant decrease of cells in the G2/M phase of the cell cycle (*p*-value: 0.0392) was observed in cells treated with 5 ng/ml LPS, but no cell cycle progression was seen in all LPS treatments in THP-1 cells. There was also a significant increase in sub-G0/G1 (dead) cells following LPS treatments at 48 hours (5, 10 and 20 ng/ml LPS (*p* values: 0.0302, 0.0072 and 0.0161 respectively), indicating that LPS induces cell death in THP-1 cells. Furthermore, treatment with polymyxin B only showed a significant amount of sub-G0/G1 population of cells, indicating that polymyxin B induces cell death in THP-1 cells (**Figure 3.13B**).

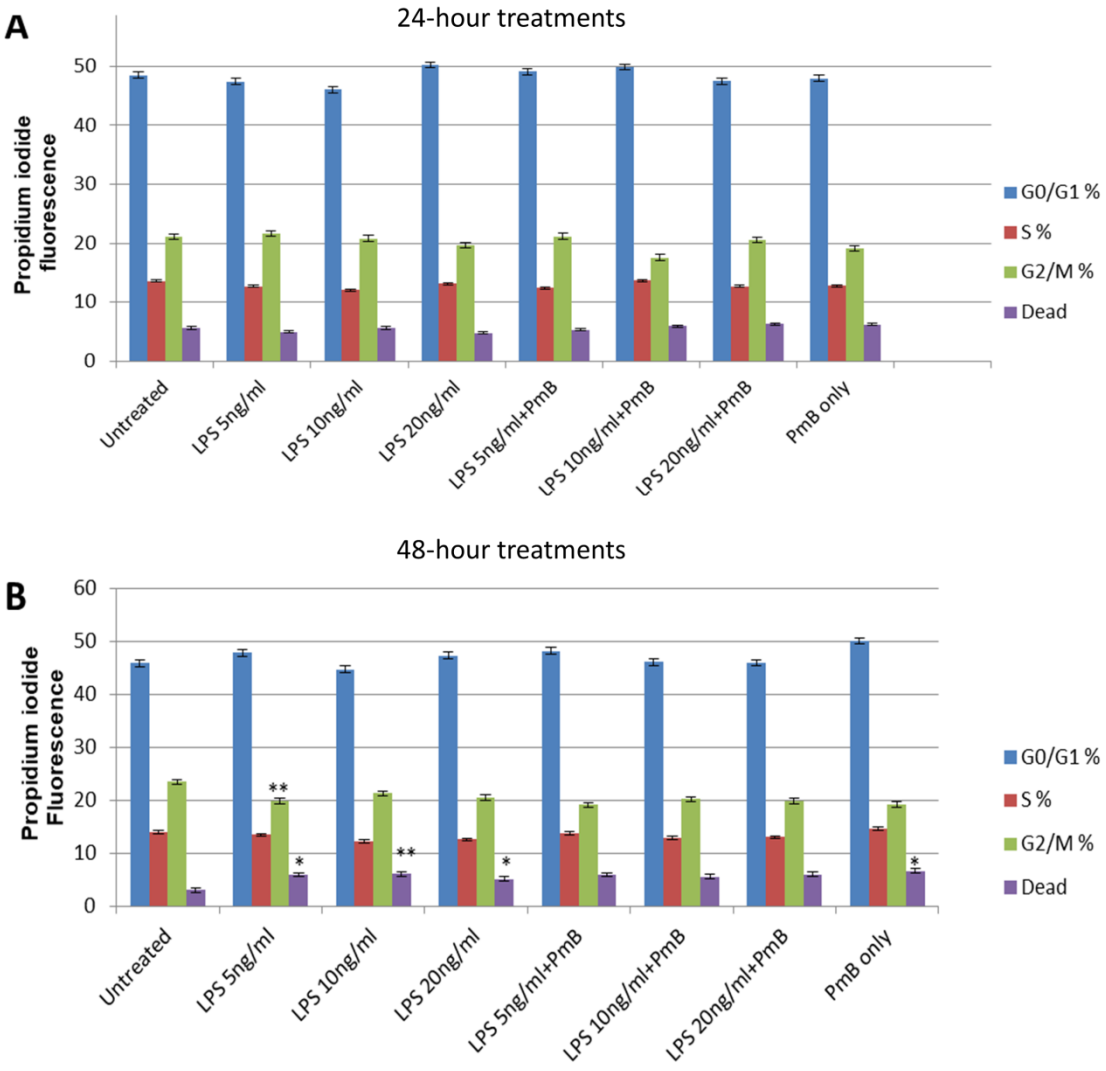

Figure 3.13. Cell cycle analysis in THP-1 cells following dose-dependent LPS treatment. A represents 24-hour treatments while **B** shows 48-hour treatments. The cell cycle analysis data was acquired using the BD FACS Aria III flow cytometer. **G0/G1** phase in **blue**, **S-phase** in **red**, and **G2/M phase** in green and the **Sub G0/G1 phase** is shown in **purple.** Data is represented as mean ± SD from 3 independent experiments and was considered statistically significant when p <0.05 (* indicates p <0.05, ** indicates p <0.01, *** indicates p <0.001). GraphPad Quick Calcs software was used to compute all statistics. Original cell cycle histograms are shown in the appendix (**Figure A3.3** and **A3.4**).

In K562 cells however, after 24 hours, a significant G0/G1 cell cycle arrest was observed (p values: 0.0256, 0.0177 and 0.0073; for 5, 10, and 20 ng/mL of LPS treatment respectively), accompanied by a significant decrease in S-phase populations (p values: 0.0001, 0.0061 and 0.0104) (**Figure 3.14A**). Nevertheless, the

cells seemed to recover from LPS-induced cell cycle changes after 48 hours, as no significant changes in the cell cycle were observed (**Figure 3.14B**).

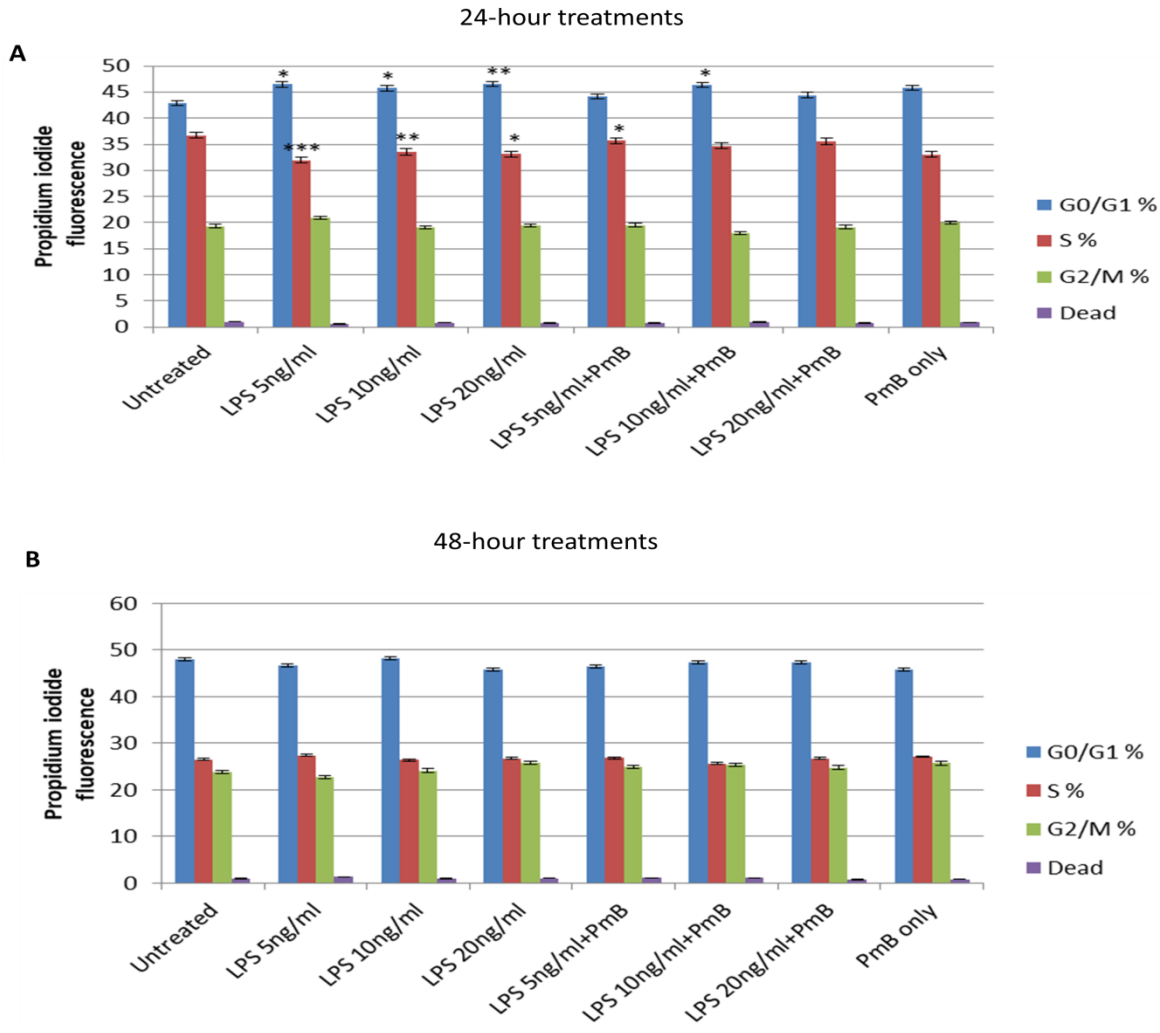

Figure 3.14. Cell cycle analysis in K562 cells following dose-dependent LPS treatment. A represents 24-hour treatments while **B** shows 48-hour treatments. The cell cycle analysis data was acquired using the BD FACS Aria III flow cytometer. **G0/G1** phase in **blue**, **S-phase** in **red**, and **G2/M phase** in green and the **Sub G0/G1 phase** is shown in **purple.** Data is represented as mean ± SD from 3 independent experiments (* indicates p <0.05, ** indicates p <0.01, *** indicates p <0.001). GraphPad Quick Calcs software was used to compute all statistics. Original cell cycle histograms are shown in the appendix (**Figure A3.4** and **A3.5**).

3.7 LPS induces cell death in THP-1 but no changes in K562 cell viability

Cells at the G0/G1 phase of the cell cycle show a diploid number (2n) of chromosomes while those in the S-phase show between 2n and 4n. Cells that are at the G2/M phase of the cell cycle are characterized by a 4n chromosome number. In a cell cycle histogram, some cells sit below the G0/G1 peak. These are characterized by DNA content less than 2n. These cells have fragmented DNA (dead cells). This sub G0/G1 population of cells was analysed to determine the amount of cell death observed following treatments with LPS and PMB. Untreated cells were used as negative control.

THP-1 cells showed a significant amount of sub-G0/G1 cells following LPS treatments at 48 hours, indicating increased cell death (*p*-values ± SD: 0.0302±1.3, 0.0072±0.680 and 0.0161±0.462 for 5, 10 and 20 ng/ml LPS). Co-treatments showed approximately the same amount of cell death compared to LPS treatments. Treatment with polymyxin B only showed a significant amount of cell death in THP-1 cells after 48 hours (*p*-value ± SD 0.037 ± 1.87). This shows that polymyxin B had effects on cell viability (**Figure 3.15A**). However, it was observed that there was no significant difference in cell death following LPS treatments after 24 and 48 hours in K562 cells (**Figure 3.15B**).

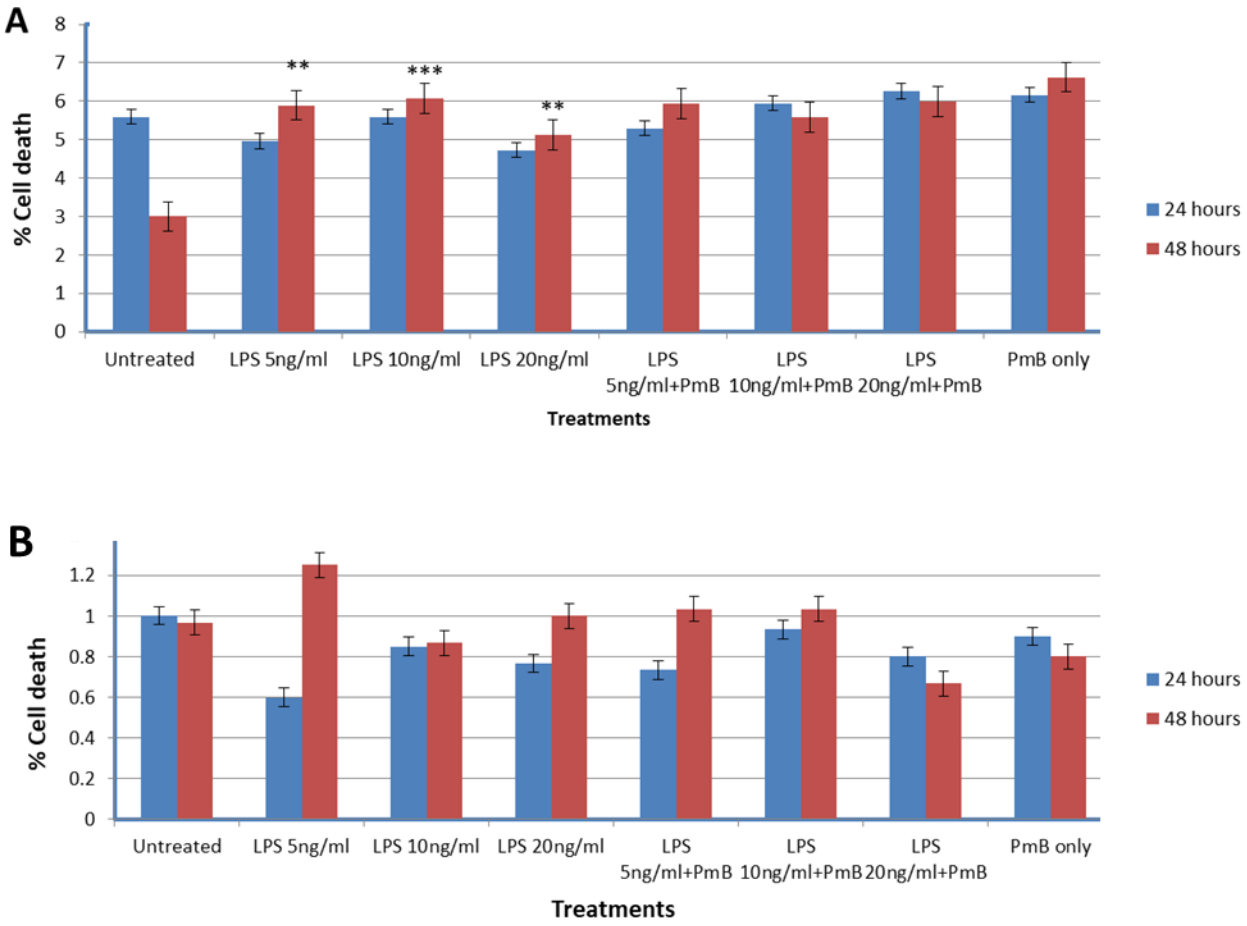

Figure 3.15. LPS induces cell death in THP-1 and not in K562 cells. Sub G0/G1 populations were computed following cell cycle analysis. **A** depicts THP-1 while **B** shows K562 cells. The blue and red bars show 24- and 48-hour treatments respectively. Polymyxin B (PmB) was used at 10 µg/ml. Data is represented as mean ± SD from 3 independent experiments (* indicates p <0.05, ** indicates p <0.01, *** indicates p <0.001). GraphPad Quick Calcs software was used to compute all statistics.

3.8 Cell proliferation is not induced in THP-1 cells following LPS treatment

Exogenous lactate has been shown to stimulate the progression into the S phase of the cell cycle and also induce proliferation in mouse fibroblasts (Rutz and Little, 1995). I used a proliferation index calculation by analysing the percentage of the ratio between S-phase and G2/M phase cells, versus the cells in G0/G1, S, and G2/M phases. Since enhanced glycolysis which is characteristic of the Warburg effect was observed, it was expected that THP-1 cells would proliferate, given that the Warburg effect is a hallmark of cancer. The proliferative index can be used to provide a more comprehensive understanding of how rapidly cancer cells are growing. Proliferation indices were calculated using the formula: **Proliferation index: [(G2M+S)/(G0G1+S+G2M)]X100** (Huang et

al., 2012; Ying et al., 2010; Yu et al., 2009b). However, no significant changes were observed at the different phases of the cell cycle following treatments as shown in **Figure 3.16**.

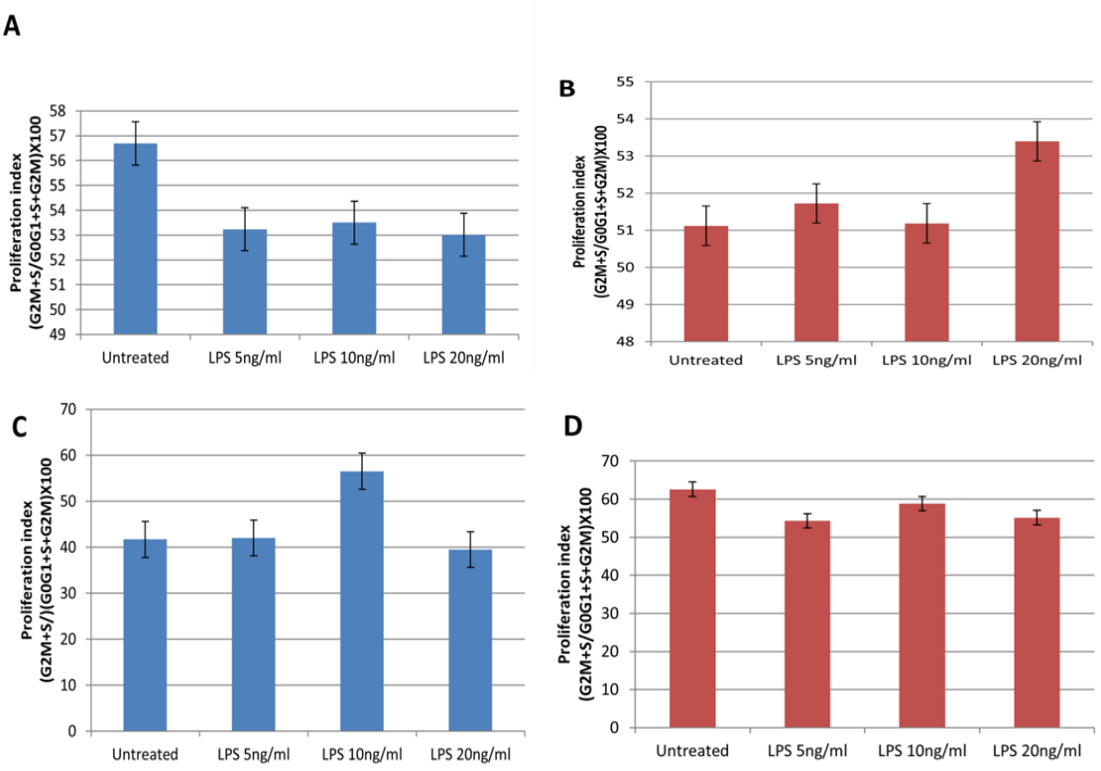

Figure 3.16. LPS treatment does not lead to cell proliferation in both THP-1 and K562 cells. Following cell cycle analysis, the Proliferation Index was computed using the following formula: [(G2M+S)/(G0G1+S+G2M)]X100. **A** and **B** show K562 cells' proliferative index in 24 and 48-hour time points respectively; while **C** and **D** indicate the proliferative indices of THP-1 cells in 24 and 48 hours respectively. The blue bars show 24-hour treatments while the red bars indicate 48-hour treatments.

Even though most proliferating cells, especially cancer cells are associated with enhanced glycolysis characterised by increases lactate production, no proliferation was observed in both cell lines. These data indicate that the increase in glycolysis in THP-1 cells following LPS treatment served a purpose other than for cell proliferation.

3.9 Summarised differences between THP-1 and K562 cells, and in response to LPS

The afore-mentioned results showed several differences between THP-1 and K562 cells in response to LPS which are summarised in **Table 8**.

Table 8. Experimental differences between THP-1 and K562 in this study

	THP-1	**K562**
Cytokine expression	Express IL8, RANTES, MIP1-β and MDC	Express IL8 and MDC (No RANTES expressed)
TLR4 expression	Express TLR4, LPS dose-dependent	Express TLR4, not LPS dose-dependent
Glycolysis	Upregulate glycolysis following LPS treatment	Glycolysis unchanged
Cell cycle	Few cell cycle changes, with increased sub G0/G1 following LPS treatment	No notable cell cycle changes
Cell proliferation	No cell proliferation following infection	Cell proliferation at higher concentrations (20 ng/ml)
Mitochondrial membrane potential	Depolarises mitochondrial membrane	Higher MMP depolarisation

The key observations were that K562, unlike THP-1 did not express RANTES with or without LPS treatment. Furthermore, LPS did not induce an increase in glycolysis in K562 cells. This was evident in THP-1 cells.

Chapter 4 -Discussion

4.1 Summary

Carcinogenesis is characterized by at least 10 hallmarks, which are in turn influenced by complex molecular mechanisms. These mechanisms, which are hardwired in cells, are developed during the multi-stage process of carcinogenesis (Hanahan and Weinberg, 2011). Elucidating molecular mechanisms contributes to basic scientific knowledge and is indispensable to the discovery of novel diagnostic and therapeutic targets and to the overall management of disease.

In the present study, it is demonstrated that, in THP-1 monocytes, LPS can enhance the glycolytic phenotype in a TLR4-dependent manner. Although this has also been demonstrated in macrophages, this is the first time in undifferentiated monocytes. LPS also caused a decline in mitochondrial membrane potential which is characteristic of decreased OxPhos. Furthermore, THP-1 monocytes were shown to upregulate pro-inflammatory chemokines: RANTES, IL8, MIP-1, and MDC at mRNA and protein levels in a TLR4-dependent manner. Interestingly, this study showed that RANTES, which was highly upregulated in THP-1 monocytes was not expressed in another myeloid-derived line – the K562 erythroleukaemia cell line even after LPS stimulation. Furthermore, LPS-mediated glycolytic phenotype in THP-1 monocytes which is reminiscent of the Warburg effect, is not accompanied by increased cell proliferation in this study and instead cell death is noticed upon LPS treatment. Furthermore, this study showed that the upregulated cytokines can be co-expressed and/or co-localised with certain glycolytic proteins and glucose transporters (GLUT1 and GLUT3) suggesting a pathway for the observed enhancement for the glycolytic phenotype. Most importantly, all the upregulated cytokines were co-expressed with HK3, an enzyme that catalyses the first, irreversible step of glycolysis. HK3 has been shown to be instrumental in leukaemia pathogenesis.

4.1.1 LPS stimulates a dose-dependent change in TLR4 expression in THP-1 and not K562 cells

LPS was first discovered as a TLR4 ligand via studies in mice. It was shown that macrophages and B cells from TLR4 deficient mice were unresponsive to LPS and that LPS endotoxin-tolerant mice had mutations of the TLR4 gene (Hoshino et al., 1999; Qureshi et al., 1999). Moreover, it

has been shown that inflammatory signalling by LPS is mediated by TLR4 (Chow et al., 1999; Hoshino et al., 1999; Kalis et al., 2003). Hence, I decided to investigate TLR4 expression prior to and post LPS stimulation in THP-1 and K562 cells. In this study, it was observed that LPS stimulated the expression of TLR4 in THP-1 cells in a dose-dependent manner. The highest expression of TLR4 was observed at the lowest concentration, 5 ng/ml, followed by a downregulation of TLR4 mRNA at higher concentrations of LPS. A previous study also showed that LPS upregulates the expression of TLR4 in human peripheral blood monocytes (Muzio et al., 2000). In K562 cells, there was a weaker stimulation of TLR4 expression observed following LPS treatment when compared with THP-1 cells. Similar to THP-I cells, expression was downregulated at higher concentration of 10 ng/ml but again upregulated at 20 ng/ml. This anomaly might have been an experimental flaw, given that several replicates of the experiment were not carried out. Overall, TLR4 appeared to be constitutively expressed in K562 cells but only weakly stimulated by LPS compared to THP-1 cells.

The reason for the difference in LPS-induced TLR4 expression in THP-1 and K562 cells is not clear. However, K562 cells are highly undifferentiated erythroleukaemic cells previously classified under the granulocytic series while THP-1 cells are acute monocytic cells (Andersson et al., 1979; Klein et al., 1976; Lozzio and Lozzio, 1975). Hence, K562 cells may be less equipped to handle bacterial infection; thereby leading to a weaker response to LPS. Nevertheless, monocytes are equipped to protect the body against invasion by micro-organisms; some of which are Gram-negative pathogens. The expression of co-receptor proteins in THP-1 is different from that of K562, leading to a difference in responsiveness to LPS ─ an important factor in TLR4 expression. It has been reported that CD14, a marker for monocytes is required for LPS- stimulated TLR4 signalling (Tobias et al., 1993). CD14 is not expressed in K562 (Funda et al., 2001; Sullivan et al., 2007). This may explain the weak signal observed. Furthermore, MD-2 expression which is also important for TLR4 expression and function is expressed in THP-1 and not in K562 cells (Shimazu et al., 1999; Zarember and Godowski, 2002). This result would also require to be replicated to determine its significance.

4.1.2 LPS-induced glycolytic flux does not induce cell proliferation in THP-1 cells

Glycolytic flux, as evidenced by high levels of lactate production, is characteristic of the Warburg effect. Following LPS-induced enhancement of glycolysis in THP-1 cells, this study finds that THP-1 cells did not proliferate as expected. In support of the present study, previous studies have shown that dendritic cells and macrophages which are differentiated monocytes, in response to infection, reprogram their metabolism, reminiscent of the Warburg effect; but do not proliferate (Everts et al., 2014; Krawczyk et al., 2010b). The primary difference is that, the present study used transformed monocytes, THP-1 cells, and not normal, differentiated monocytes as shown in the previous study. Therefore, the present study suggests that the LPS-induced enhancement of glycolysis is required primarily for immune activation which demands temporal surges of energy in response to infection rather than cell proliferation.

THP-1 cells, in addition to being innate immune cells are also transformed cells. This gives them the possibility to respond to LPS-induced metabolic reprogramming as innate immune cells or as cancer cells or both: making their response somewhat unpredictable. First, a THP-1 cell may respond as a normal monocyte which gets activated by boosting glycolysis for defence against infection. In this case, monocytes do not proliferate. Second, it may respond as a typical cancer cell which proliferates following a glycolysis-inducing signal, given that glycolytic flux, a signature of the Warburg effect, is often accompanied by cell proliferation. Third, the response could be an entirely new metabolic and/or proliferative phenotype arising from the combination of a normal monocyte and that of a transformed monocyte (cancer cell).

Nevertheless, I hypothesised that LPS-induced glycolytic flux in THP-1 cells would be accompanied by proliferation, given that metabolic reprogramming is a hallmark of cancer. However, even though LPS induced a glycolytic flux consistent with the Warburg phenotype in THP-1 cells, no proliferation was observed when proliferative indices of both cell lines were observed. Furthermore, analysing sub G0/G1 populations, THP-1 cells rather exhibited some cell death following LPS treatment, despite upregulated glycolysis. Hence, this study showed that observing one hallmark of cancer and attempting to predict its significance in cancer progression is misleading. This is because at least 10 hallmarks are known to date as drivers of carcinogenesis; even though the relative influence of each hallmark to cancer progression has not been explored.

Cancer metabolism is rewired primarily to support biosynthesis of growth metabolites which is essential for proliferation, rather than for efficient energy production. Targeting metabolic vulnerabilities in cancer remains a promising avenue for therapy. However, even though it is tempting to generalise that the Warburg effect is a metabolic signature in cancer, several studies show that different tumours show varying degrees of dependence on glycolysis and OxPhos for ATP synthesis (Suganuma et al., 2010; Wolpaw and Dang, 2018). This implies that the Warburg effect may not be as important in the malignancy of one cancer when compared to another. A previous study showed that inhibition of glycolysis in THP-1 cells with 2-deoxyglucose had no significant effect in proliferation, showing no dependence on glycolysis for proliferation. They showed that THP-1 cells predominantly depend on OxPhos for ATP synthesis, based on their sensitivity to mitochondrial beta-oxidation inhibitors (Suganuma et al., 2010). A possible reason for their oxidative nature is that monocytes may function in inflammatory microenvironments with drastically reduced glucose concentrations; forcing them to adapt to mitochondrial respiration for energy requirements. Proliferation was not observed in this study following a boost in glycolysis, a Warburg phenomenon, likely because monocytes do not depend on glycolysis for proliferation.

Recent studies on THP-1 cells in our laboratory showed that exogenous pyruvate can reverse LPS-induced metabolic reprogramming and induce cell cycle arrest at the S-phase. Nevertheless, this reversal of metabolism did not lead to cell death; showing that enhanced glycolysis observed in THP-1 cells is to fulfill other cellular requirements other than induce cell proliferation. Reversing the Warburg effect is emerging as an attractive strategy for combatting cancer. For example, reversing the metabolic program of non-haematopoietic cancer cells such as A549 (lung adenocarcinoma) using exogenous pyruvate induced apoptosis when used with a genotoxic agents or alone but protected a normal lung fibroblast cell line, the MRC5 from genotoxic stress (Monchusi and Ntwasa, 2017). Another study using methylene blue (MB) to reverse the Warburg Effect in glioblastoma cells supports this approach (Poteet et al., 2013). MB inactivates acetyl-CoA-carboxylase which catalyses irreversible carboxylation of acetyl CoA to malonyl-CoA and fatty acid biosynthesis. In the glioblastoma cells, MB induced S-phase arrest and apoptosis, making it a promising strategy for glioblastoma.

To further understand the relationship between the glycolytic profile of a cell and its proliferative state, different cell types and their rate of proliferation were investigated from existing literature as shown in **Table 9**.

Table 9. The glycolytic potential of different cell types and their proliferative abilities

Cell type	Glycolytic rate	Proliferative rate	References
Normal (fully differentiated adult) cells	Low	Low	(Hume et al., 1978; WANG et al., 1976)
Embryonic cells	High	High	(Kondoh et al., 2007; Krisher and Prather 2012)
Activated T-helper cells: Th1, Th2, Th17	High	High	(Fox et al., 2005; Jones and Thompson)
Haematopoietic cells	Very High	High	(Bauer et al., 2004)
Activated macrophages/monocytes (M1)	High	Low	(Newsholme et al., 1987)
Activated macrophages/monocytes (M2)	Low	Low	(Sag et al., 2008; Vats et al., 2006)
Dendritic cells (Resting)	Low	Low	(Krawczyk et al., 2010)
Dendritic cells (Activated)	High	Low	(Krawczyk et al., 2010)
Most cancer cells	High	High	(Heiden et al., 2009)
Murine colon carcinoma cells MC26 (Untreated)	Not investigated	High	(Huang et al., 2005)
Murine colon carcinoma cells MC26 (LPS-treated)	Not investigated	Very high	(Huang et al., 2005)
Transformed acute monocytic cells (THP-1 cells) (Untreated)	Low	High	(Suganuma et al., 2010)
Transformed acute monocytic cells (THP-1 cells) (LPS-treated)	High	Low	Present study

The table above shows that the glycolytic state of a cell may or may not influence its viability or proliferation. Otto Warburg (1956) erroneously assumed that the trigger for carcinogenesis was dysfunctional mitochondria, which led to high glycolytic rates even in the presence of oxygen to compensate for energy production (Warburg, 1956). Nevertheless, several studies have shown that

many cancer cells have fully functional mitochondria, but still prefer increased glycolysis; while others do not display enhanced glycolysis for ATP synthesis but utilise their mitochondria for most ATP synthesised.

This study shows that metabolic processes in carcinogenesis, even though co-occur with cell viability and proliferation in many cancer cell types, can still occur independently in some innate immune cells such as monocytes ─ whether they are cancerous or not. Bauer and colleagues (2015) showed that haematopoietic cells displayed a rate of glycolysis that exceeded what was required for cell proliferation (Bauer et al., 2004). Other studies showed that glycolysis is not a requisite for proliferation as in normal dendritic cells (Everts et al., 2014; Krawczyk et al., 2010b). However, most studies show that proliferation generally requires increased glycolysis as seen in most cancer cells and other proliferating cells (Krisher and Prather, 2012; Heiden et al., 2009).

I suggest that the afore-mentioned observations should guide cancer diagnosis and therapy, given that tumours vary in their mode of energy metabolism. Therapeutic inhibitors of glycolysis may not be effective in specific tumour types because their metabolic profiles have not been fully evaluated.

4.1.3 LPS induces over-expression of largely pro-inflammatory cytokines in THP-1 and K562 cells.

The role of the inflammatory tumour microenvironment has been explored in several manuscripts (Coussens and Werb, 2002; Grivennikov et al., 2010; Landskron et al., 2014; O'Connor et al., 2010); firmly establishing inflammation as a hallmark of cancer (Hanahan and Weinberg, 2011). Inflammatory cytokines are involved in several aspects of cancer progression in both myeloid- and non-myeloid-derived cancers. Examples of such carcinogenic processes include tumour growth, metastasis and angiogenesis (Kupsa et al., 2012; Vicari and Caux, 2002).

In this study, the chemokines, IL8, RANTES, MDC and MIP-1β were upregulated following LPS treatment. In particular, IL8 and RANTES were markedly upregulated and both have been reported to promote carcinogenesis. These are chemokines which are generally intended to attract neutrophils, T-cells and other immune cells to sites of infection. This study showed a marked

TLR4-dependent upregulation of RANTES and IL8 expression. In addition, MIP1-β and MDC were slightly upregulated in THP-1 cells.

Previous studies have focused on cytokine production in macrophage- or dendritic cell-differentiated monocytes and peripheral blood monocytes. Furthermore, none of the studies explored so far showed that LPS-induced expression of such chemokines was dependent on TLR4 expression (Locati et al., 2002). To the best of my knowledge, this is the first study that shows that THP-1 monocytes, when stimulated with LPS, produce IL8, RANTES, MIP-1β and MDC in a TLR4-dependent manner (as they were inhibited by polymyxin B).

Unexpectedly, IL-1β and TNF-α, which are known to be induced by LPS in monocytes and macrophages were not detected in this study. Nevertheless, further analysis of previous reports showed that either the concentration of LPS or the duration of incubation with LPS differed when compared with those in the current study (Segura et al., 2002; Wataha et al., 1996). Such factors are important in the production of cytokines after exposure to PAMPs (Barksby et al., 2009; Hamza et al., 2017).

After observing elevated LPS-induced expression of IL8 and RANTES, it was postulated that there would be increased cell survival or proliferation observed since both cytokines have been implicated in cancer progression. The following paragraphs explore the roles of IL8, RANTES MIP-1β, and MDC in carcinogenesis.

IL8 (CXCL8)

As reviewed by Waugh and Wilson (2008), IL8 has been associated with cancer progression in several reports (Waugh and Wilson, 2008). For example, IL8 signalling stimulates angiogenesis in endothelial cells, survival, and proliferation of endothelial and cancer cells, and enhances the migration adhesion, migration and invasion of gastric cancer cells (Kuai et al., 2012). IL8 also activates the infiltration of neutrophils to the tumor microenvironment. IL8 has been shown to promote the proliferation of prostate cancer cells in an androgen-independent manner. Furthermore, IL8 was also shown to induce chemotherapeutic resistance in cancer cells (Kuai et al., 2012).

IL8 activates two main proliferative kinase pathways: PI3K and mitogen-activated protein kinase (MAPK) signalling. IL8–dependent stimulation of PI3K promotes chemotaxis of neutrophils, as a

result of resulting in increased phosphorylation of Akt, the PI3K substrate (Knall et al., 1997). By stimulating NF-κB transactivation, IL8 is also known to enhance melanoma growth through the MEKK1/p38 MAPK signalling network (Wang and Richmond, 2001).

Cytokines are quite instrumental in modulating myelopoietic activities by either stimulating or inhibiting the proliferation of myeloid progenitor cells. In contrast to its growth-promoting activities, IL8 inhibits the proliferation of myeloid progenitor cells by ligating one of its GPCRs, CXCR2 (Sanchez et al., 1998). Furthermore, expression of IL8 was associated with etoposide or the nitric oxide (NO) donor DETA-NO-induced apoptotic cell death in U937 cells and peripheral blood mononuclear cells (Mühl et al., 1999).

Despite the overwhelming proliferative and pro-survival activities of IL8 discussed in the above paragraphs, no proliferation was observed in this study following LPS-induced IL8 expression. This suggests that the role of anti-proliferative signals was dominant, leading to cell death as observed in THP-1 cells. Furthermore, the role of the tumour microenvironment is important in carcinogenesis. Many tumours occur in environments with high microflora which also possess cytokine-secreting immune cells. IL8, for example, is involved in promoting carcinogenesis via its action on the tumour microenvironment (Waugh and Wilson, 2008). Since THP-1 and K562 cells used in this study were cultured in isolation *in vitro*, the role of the IL8 in the tumour microenvironment could not be evaluated.

RANTES (CCL5)

RANTES promotes invasion and migration of pancreatic cancer cells (Singh et al., 2018). Inhibition of RANTES retards growth in both colorectal and triple negative breast cancer cells (Cambien et al., 2011; Lv et al., 2013). Furthermore, RANTES is expressed in ovarian cancer stem cells and induces invasion and migration (Long Haixia et al., 2012; Tsukishiro et al., 2006). Along with CCL3 and CCL4, RANTES was also shown to be upregulated in ascetic fluids of ovarian cancer patients; with high expression correlating with increased T-cell infiltration. RANTES increases lung cancer migration through PI3K/Akt and NF-κB signalling pathways (Huang et al., 2009).

It is not surprising that both RANTES and IL8, which were upregulated in this study, promote migration in carcinogenesis; given that these are potent chemokines responsible for attracting innate immune cells to inflammatory sites. Still, it has been shown that glycolysis is the main source of ATP required for migrating neutrophils and T-cells to sites of inflammation (Bao et al., 2014; Chan et al., 2012). This could explain, at least in part the upregulated glycolysis observed in this study. Incidentally, RANTES upregulates the same pathway (PI3K/Akt) involved in both in proliferation/migration and glycolysis. Besides, glycolysis has been shown to be the primary ATP-generating pathway for tumour migration in prostate, breast and other cancers (Beckner et al., 1990; Shiraishi et al., 2015).

MIP-1β

Macrophage inflammatory protein-1β (MIP-1β), also known as CCL4 is a CC chemokine which acts via CCR5and CCR8 receptors. MIP-1β is expressed by B cells, T cells, monocytes, endothelial cells, fibroblasts, and epithelial cells and it induces chemotaxis in monocytes, natural killer cells, and other immune cells. MIP-1β, as well as RANTES and MIP-1α, is a major HIV-suppressive factor produced by CD8+ T cells (Cocchi et al., 1995). Serum levels of MIP-1β, MIP-1α and IL8 are significantly high in breast cancer patients (Li et al., 2017). Macrophages and hypoxia stimulate cell invasion in glioblastoma via the CCL4/CCR5 axis, upregulating their expression (Wang et al., 2016)

In contrast, a clinical study suggested that CCL4 polymorphisms have a role to play in oral carcinogenesis: associating increased risk in oral squamous cell carcinoma cancer to mutations in the CCL4 gene (Lien et al., 2017), thereby suggesting a protective role for fully functional CCL4 in cancer.

MDC (CCL22)

MDC (CCL22) is a constitutively expressed CC chemokine which can be upregulated by pro-inflammatory stimuli such as microbial products and other cytokines such as IL-4, IL-13 and type I interferons (Andrew et al., 1998). As seen in this study, MDC was constitutively expressed in both THP-1 and K562. MDC expressed mainly by macrophages and dendritic cells and exerts its action by binding to GPCR chemokine receptors, especially CCR4 on the cell surfaces of its target cells. It is a potent chemoattractant of T-cells, dendritic cells and natural killer cells (Guo et al.,

2002). MDC expression shows an inverse correlation in cancer progression. After profiling the expression of MDC in 40 patients, Nakanishi and colleagues (2006) found that upregulated MDC mRNA expression in lung cancer patients was significantly correlated with longer survival and reduced risk of relapse after tumour resection. MDC gene transfer to mice also showed anti-tumour activity in by inducing anti-tumour immunity in lung carcinoma (Guo et al., 2002). Furthermore, a large clinical study involving 1,208 glioma cases and 976 controls showed that reduced serum levels of MDC correlate with lowered CD4 counts, and decreased survival in glioma patients. MDC expression was further proposed as a prognostic marker in glioma and in tumour-related suppression of immune function (Zhou et al., 2015).

The expression of MDC and MIP-1β has been studied in macrophage-differentiated THP-1 monocytes (Harrison et al., 2005). Nevertheless, no study has shown TLR4-dependent LPS-induced THP-1 expression in undifferentiated monocytes. Both MDC and MIP-1β appear to induce anti-tumour effects by suppression of immune function. This effect can only be appreciated in an *in vivo* setting given that several immune regulatory cells and a cocktail of cytokines are involved in immunosuppression as seen in cancer.

Moreover, many tumours occur in a microenvironment which is also dominated by microorganisms which could constitute normal flora or pathogenic micro-organisms. Examples are gut microbiota which co-occur with colorectal and gastric tumours. It is well known that monocytes are attracted to sites of infection or inflammation; meaning that several tumours exist in a microenvironment having immune cells which are secreting cytokines. Monocytes leave the blood and enter tissues via leukocyte extravasation before subsequently differentiating to tissue macrophages. Since both immune and non-immune cells also express cytokine receptors, it is plausible that the generation of cytokines by monocytes to the tumour microenvironment may not only influence other immune cells but also neighbouring tumour cells. In other words, the paracrine activity of chemokines produced by monocytes stimulated by infectious pathogens could aggravate tumour progression. It is possible that presence of IL8 and RANTES in a tumour microenvironment could lead to cell proliferation. However, this possibility was not tested since this study was not performed *in vivo*.

4.1.4 LPS-mediated TLR4 signalling induces cell death in THP-1 cells

There is increased evidence, that TLR signalling in innate immune and cancer cells may act as a double-edged sword (Huang et al., 2008; O'Neill et al., 2009). While inducing TLR signalling with specific agonists may alleviate symptoms in certain inflammatory disorders or promote apoptosis in specific tumour types, the reverse may be true in other scenarios (O'Neill et al., 2009; Shi et al., 2016). Following a boost in the Warburg effect upon LPS treatment, it was expected that THP-1 cells would proliferate. However, this study shows that LPS stimulation induces some limited cell death in THP-1 cells after 48 hours. In K562 cells however, no cell death was observed.

The mechanisms of LPS-induced cell death are quite diverse and seem dependent on cell type, cellular context, and concentration. These mechanisms include apoptosis and necrosis. For example, LPS induces apoptosis in alveolar macrophages through CD14 and P2X7 receptors. LPS-induced ROS release through NAD(P)H oxidase enzymes (Nox2 and Nox4) causes necrosis in endothelial cells of the human umbilical vein (Simon and Fernández, 2009). LPS binding to TLR4 also induces TNF-α-independent, receptor-interacting kinase-3 (RIK3)-dependent programmed necrosis in mouse macrophages (He et al., 2011). In contrast, another study showed that LPS induced apoptosis in human macrophages via autocrine TNF-α release and iNOS-mediated NO release (Xaus et al., 2000). These studies show that LPS may induce TNF-α-dependent and –independent apoptosis in macrophages. Another study using a higher concentration of LPS (500 ng/ml) on THP-1 monocyte cells showed that LPS could not induce apoptosis based on sub G0/G1 populations (Li et al., 2005).

A study conducted in our laboratory showed that most of the cell death induced by LPS on THP-1 cells was via the necrotic pathway. Surprisingly, TNF-α which is a key mediator of necrosis was not detected following LPS stimulation for 24 hours. Further studies need to be performed to ascertain the mechanism LPS-induced cell death in THP-1 cells.

Several factors influence the fate of a cell following treatment with LPS. LPS concentration, treatment exposure time, cell line, cytokine and cytokine receptor, and co-stimulatory molecule expression, p53 status and other oncogenes or tumour suppressor gene expression may regulate the fine balance between survival and death.

LPS-mediated cell death is cell type-dependent. LPS treatment for 48 hours led to cell death in THP-1 cell but not K562 cells**.** This has profound implications given that several mechanisms are involved in LPS signalling in different cell types, leading to different effects on viability (Suzuki et al., 2004). For example, LPS-mediated activation of extracellular regulated kinase (ERK) promotes survival in neutrophils (Klein et al., 2001). LPS also prevents apoptosis in human peripheral blood monocytes (Mangan et al., 1991). Contrarily, LPS induces apoptosis in thymocytes, lymphoid organs (Kato et al., 1997) and B cells (Yokochi et al., 1996) and necrotic cell death in alveolar macrophages (Dagvadorj et al., 2015). This further complicates our comprehension infection-cancer relationship due to the variety of LPS-containing Gram-negative bacteria that are associated with cancer. Noteworthily, several types of LPS molecules have been found in different bacterial species. The LPS molecule is made up of three main components: the highly variable O antigen region, core oligosaccharide and a highly conserved Lipid A region (endotoxic region) (Tzeng et al., 2002). Although the Lipid A component which considered to be is highly conserved, structural differences still occur between species and strains of different bacteria, which may affect their toxicity (Khan et al., 2018; Matsuura, 2013). It is therefore probable that a different repertoire of effector molecules could result from LPS from different species of micro-organisms.

Both cell lines (THP-1 and K562) expressed TLR4 as shown in this study. However, the repertoire of cytokines synthesized, and cytokine receptors expressed may be responsible for the differences in cell viability upon LPS treatments observed in both cell lines. For example, prior to and post LPS treatment, THP-1 cells in this study expressed RANTES while K562 cells did not. Although RANTES has been shown to be involved in tumour progression (Cambien et al., 2011; Huang et al., 2009; Zhou et al., 2015), other studies show that it may also stimulate apoptosis in certain cell types such as T-cells (Chang et al., 2012; Murooka et al., 2006).

4.1.5 Polymyxin B, alone or in complex with LPS induces cell death in THP-1 cells, not in K562

In this study, it was observed that even though PmB effectively inhibited LPS-induced lactate production, it did not enhance or inhibit any stages of the cell cycle, which may be dependent on glycolysis. There was a significant amount of cell death at 48 hours in THP-1 cells following

treatment with increasing concentrations of LPS as seen in Sub G0/G1 populations. However, polymyxin B co-treatment with LPS was unable to promote or prevent cell death. This study shows that PmB has death inducing properties in THP-1 cells independent of the LPS-TLR4 signalling pathway. PmB has been implicated in several reports as being responsible for cell death via diverse mechanisms. For example, PmB induces apoptosis in rat kidney tubule cells via induction of Fas ligand, caspase 3, 8 and 9 and altering mitochondrial morphology to the fragmented, stressed state (Azad et al., 2013, 2015). PmB also induces cell death in regulatory T cells via its interaction with purinoceptor 7 ($P2X_7$) (Cappelli et al., 2012). $P2X_7$ is known to act as a PRR for extracellular ATP-induced apoptosis (Kawano et al., 2012). DNA damage is a typical biochemical hallmark of apoptosis; and PmB induces DNA damage in mice and HK-2 (human kidney cells (Yun et al., 2018).

However, the viability of K562 cells was unaffected by PmB; suggesting that other unknown mechanisms could be preventing PmB-mediated induction of cell death in K562 cells. Subjecting TLR4 to siRNA-mediated ablation could further give insights into the impact of inhibiting LPS-mediated signalling on the viability of THP-1 and K562 cells.

4.1.6 THP-1 and K562 lineages may explain their differences in terms of TLR4 expression, cytokine profile, glycolytic profile, and viability

To understand cell-type specific differences between THP-1 cells and K562 cells, it was important to trace their lineages and differentiation status in context with haematopoiesis (**Figure 4.1**). This is important because the function of a cell is highly dependent on its differentiation or specialisation. Besides, the differentiation of haematopoietic cells requires the synergistic and concerted effort of distinct groups of cytokines acting in a temporal fashion.

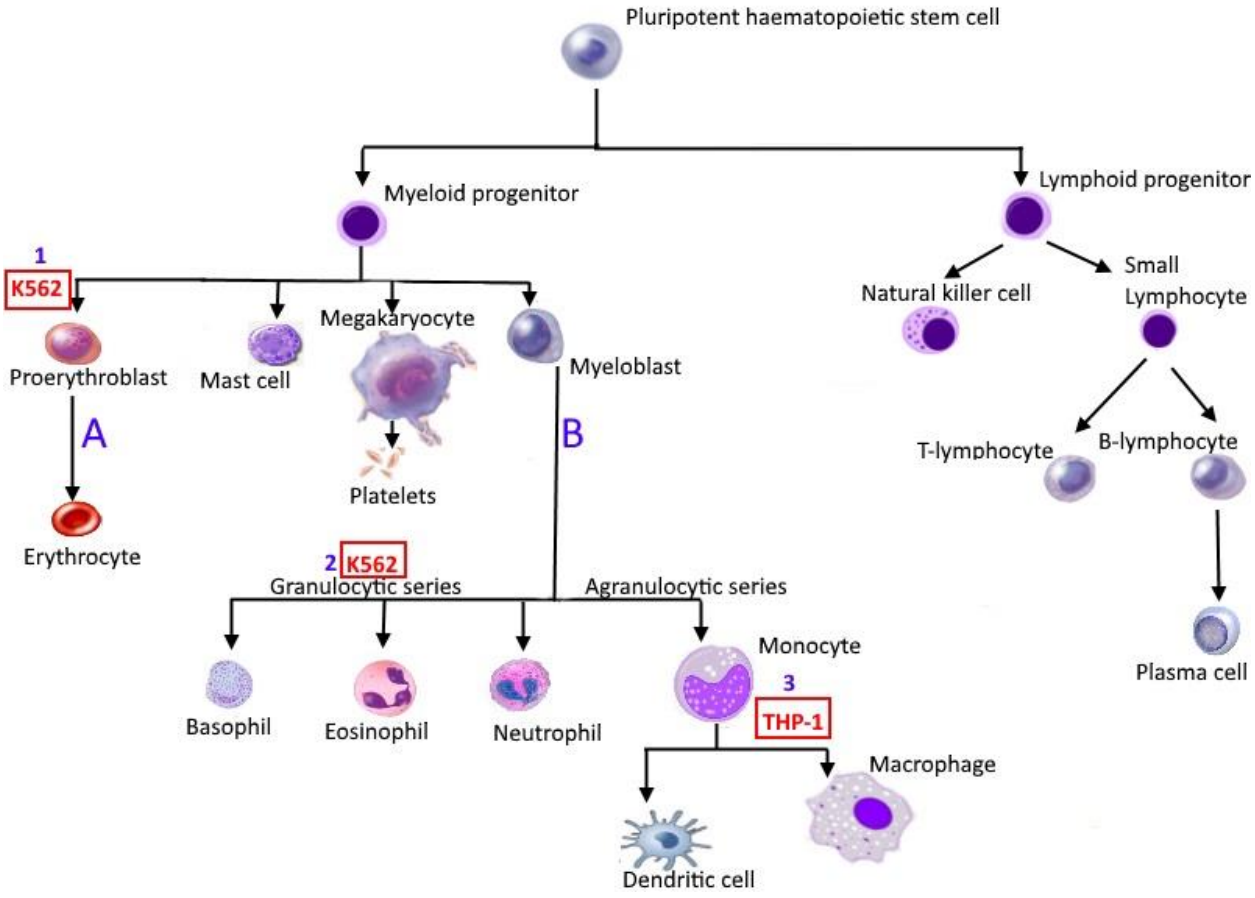

Figure 4.1. THP-1 and K562 cell lines in the context of haematopoiesis. The pluripotent haematopoietic stem cell branches off myeloid and lymphoid progenitor cells. Both THP-1 and K562 cell lines belong to the myeloid progenitor lineage. **1.** Shows the lineage of K562 described as being an erythroleukaemia cell line. **2.** Represents the first description of K562 cells as being in the granulocytic series. **3.** Shows THP-1 cells in the monocytic series, better differentiated than K562 cells. **A**. indicates the erythroid series which is a non-immune lineage while **B.** shows the myeloblast series which is an immune cell lineage.

K562 cells were characterised as chronic myelogenous cell line positive for the Philadelphia chromosome (Lozzio and Lozzio, 1975). They were reported as highly undifferentiated cells in the granulocytic series (Klein et al., 1976; Lozzio and Lozzio, 1975). However, further investigation by immunofluorescence and immunoprecipitation showed that they expressed a major red blood cell sialoglycoprotein, known as glycophorin, displaying a striking semblance to erythrocytes. Furthermore, K562 cells can synthesize embryonic and foetal haemoglobin. This led to their classification as an erythroleukemic cell line (Andersson et al., 1979). Being an erythroleukaemia

cell line with high undifferentiated status makes K562 cells less able to respond to infection (LPS). As seen in **Figure 4.1** above, cells in the erythroid series of the myeloid arm are in the process of differentiation to mature erythrocytes. Erythrocytes are specialised in haemoglobin-aided oxygen transport to tissues and transport of carbon-dioxide from tissues to the lungs. This means that cells in the erythroid lineage may not be involved in defence against infection. It is therefore not surprising that K562 cells showed a poorer cellular response to LPS stimulation as compared to THP-1. K562 cells were shown in this study to stimulate TLR4 expression. Nevertheless, the LPS stimulation of TLR4 expression in K562 cells was quite weak.

THP-1 cells, on the other hand, are acute monocytic leukaemia cells classified under acute myeloid leukaemia (Tsuchiya et al., 1980). These are already committed monocytes which are well able to carry out their immune functions of responding to infection which include phagocytosis, antigen presentation, and cytokine production. Furthermore, a key characteristic of monocytes is their expression of CD14, which has been shown to be important in LPS-mediated TLR4 signalling. By contrast, K562 cells are CD14 negative; suggesting one of the reasons for their poor response to LPS (**Table 10**). This study also showed that RANTES was highly upregulated in THP-1 cells and virtually absent in both unstimulated and LPS-stimulated K562 cells. **Table 10** summarises several differences between THP-1 and K562 (Bosshart and Heinzelmann, 2016; Klein et al., 1976; Lozzio and Lozzio, 1975; Tsuchiya et al., 1980).

Table 10. Differences between THP-1 and K562

	THP-1	K562
Progenitor	Myeloid, monocytic series	Myeloid, granulocytic series
Karyotype	Diploid	Triploid
Disease	Acute monocytic leukaemia	Chronic myeloid leukaemia
Mutations	Bcrb-abl negative	Bcrb-abl gene positive
Origin	Peripheral blood of a 1-year old male human with acute monocytic leukaemia	53-year old female with chronic myelogenous leukaemia in blast crisis
Adherence	Non-adherent	Non-adherent
Morphology	Large, Rounded, single celled-monocytic	Rounded
	Phagocytic	Non-phagocytic
Receptors	Fc and 3cb receptors, lack immunoglobulin receptors	Express MHC class I, A2 and A3
Antigen expression	HLA A2, A9, B5, DRw1, DRw2[58053]	I and l-antigens
Differentiation agents	phorbol 12-myristate 13-acetate to macrophages	Deacetylases
Polarisation	Can be polarised to M1 macrophages using LPS and IFN gamma or to M2 macrophages by IL-4	None
P53 status	Mutant	Mutant
CD14 status	CD14+	CD14-

It was also shown in this study that LPS induces a TLR4-dependent upregulation of glycolysis in THP-1 cells which was abrogated by polymyxin B. Nevertheless, no increase in glycolysis was seen in K562 cells. LPS-induced upregulation of glycolysis has been reported in macrophages and dendritic cells previously, however, this is the first study that shows that THP-1 monocytes can also enhance their glycolysis in a TLR4-dependent fashion to cope with infection.

4.1.7 Chemokine interaction with glycolytic proteins may constitute one of the mechanisms involved in LPS-induced glycolytic flux and may be important for leukaemia carcinogenesis

A question raised in this study is whether the upregulated cytokines could interact with glycolytic enzymes and boost glycolysis. This is because some cytokines are known to boost glycolysis, or proliferation (which usually co-occurs with increased glycolysis). For example, interleukin 6 is known to boost glycolysis through expressing glycolytic enzymes hexokinase 2 and 6-phosphofructo-2-kinase/fructose-2,6-bisphosphatase-3 through the transcription factor STAT3 (Ando et al., 2010) and also induces aerobic glycolysis by activating PFKFB3 at the primary stage of colorectal cancer (Han et al., 2016). IL-1β also increases glucose consumption and stimulates aerobic glycolysis in cultured murine ovarian cells (Ben-Shlomo et al., 1997) while RANTES boosts glucose uptake to facilitate chemotaxis in activated T-cells (Chan et al., 2012). Interleukin 22 stimulates aerobic glycolysis, via targeting hexokinase 2, correlating with increased proliferation in colon cancer cells (Liu et al., 2017). Chemokines are associated with chemotaxis; which utilises glycolysis as the main source of ATP production (Borregaard and Herlin, 1982), further justifying why it was speculated that the upregulated chemokines in this study could be partly responsible in the boost of glycolysis observed following LPS treatment.

Analysis of gene interaction networks and shared biological processes using IMP and GeneMANIA webservers showed several relationships (co-expression, co-localisation and shared biological processes) between upregulated cytokines in this study and glycolytic proteins. These postulated interactions have profound implications. For example, it can be suggested that, following an infection, monocytes temporally produce cytokines which may interact with glycolytic genes to boost glycolysis which is necessary for immune activation.

It is pertinent to understand the role played by each glycolytic gene that appears to be associated with the upregulated cytokines and elucidate their potential role in boosting glycolysis and in acute myeloid leukaemia carcinogenesis. The observations from this exercise led to the elucidation of the role of key transcription factors that regulate both cytokines and glycolytic genes in leukaemia carcinogenesis. The result is a proposed pathway map that conceptually predicts the mechanisms of AML carcinogenesis and the potential roles of RANTES, IL8, MDC, and MIP-1β glycolytic genes and glucose transporters in context. Furthermore, the potential role of infection, as simulated by LPS in this study in AML carcinogenesis is proposed.

This study showed that GLUT1 and GLUT3 were co-expressed with both IL8 and RANTES and GLUT3 further co-localised with IL8. GLUT3 is further involved with IL8 in a biological process known as "response to nitrogen compound". LPS is known to trigger nitric oxide via inducible nitric oxide synthase gene (iNOS), which is involved in the activation of immune cells. Furthermore, the glycolytic phenotype is necessary for immune activation in normal monocytes and dendritic cells (Kelly and O'Neill, 2015; Krawczyk et al., 2010b) and it was shown that monocytes (THP-1 cells) express GLUTs; mainly GLUT1, GLUT3. However, while GLUT1 expression was markedly increased following LPS treatment, GLUT3 expression declined (Fu et al., 2004). GLUT1 has further been shown to be the primary rate-limiting GLUT in pro-inflammatory macrophages; strongly mediating metabolic reprogramming (Freemerman et al., 2014) Nevertheless, GLUT3 has been shown to induce metabolic reprogramming in xenograft mice harbouring glioblastoma, which correlated with resistance to antiangiogenic therapy (Kuang et al., 2016). This further highlights the specialised role of GLUTs in facilitating glucose transport in different tissue types.

Glucose phosphorylation by hexokinases (HKs) is necessary to maintain the glucose concentration gradient required for facilitated glucose import to the cell. It has been shown that HK3, a 100 kD isoform is upregulated in several tumours and may promote cell survival by boosting ATP production, mitigating antioxidant stress, maintaining mitochondrial membrane potential and promoting mitochondrial biogenesis (Wyatt et al., 2010). HK3 is commonly expressed in myeloid cells and represents 70-80% of HK activity in granulocytic cells (Federzoni et al., 2012; Rijksen et al., 1982).

As can be seen in **Table 6** and **7**, HK3 showed co-expression and shared biological processes with all the upregulated cytokines in this study. This observation warranted further investigation. A literature search from PubMed for transcription factors regulating HK3 showed that haematopoietic differentiation factors regulate its expression. Both PU-box-binding protein 1 (PU.1) and Acute Promyelocytic Leukaemia-retinoic Acid Receptor alpha fusion gene (PML/RARα) showed *in vivo* binding to HK3 promoter (Federzoni et al., 2012). It was found that HK3 is transcriptionally activated by PU.1 and repressed by PML-RARα (Federzoni et al., 2012), both master regulators of haematopoietic myeloid and B-cell cell differentiation (McKercher et al., 1996). PML/RARα, which is frequently mutated in several AML cell lines represses the

expression of PU.1 (Wang et al., 2010). These findings suggest that HK3 is involved in the mechanisms that control AML differentiation and hence carcinogenesis. Furthermore, HK3 which showed increased expression in the myeloid lineage was upregulated during the differentiation of neutrophils and showed lower expression in most AML cell lines (Federzoni et al., 2012). Hence, HK3 expression is critical for differentiation, whose deregulation is common in AML carcinogenesis.

The disruption of the normal process of haematopoiesis is critical in leukaemia carcinogenesis, since most AML leukaemias occur because of aberrant haematopoietic differentiation of myeloid progenitor cells (Lindner et al., 2003; Olsson Inge et al., 1996). HK3 was further found to be regulated by the transcription factor CCAAT/enhancer binding protein α (CEBPA), which codes for a protein that is involved in myeloid cell priming and neutrophil differentiation (Avellino et al., 2016). CEBPA activates HK3 and mutations of CEBPA are important in haematological malignancies (Wouters et al., 2009). CEBPA, which is known to be frequently mutated in AML, is known to be important in myeloid cell differentiation (Avellino et al., 2016). Importantly, HK3 which was co-expressed with all upregulated chemokines in this study and co-localised with IL8 further showed a close association with key regulators of myeloid differentiation: PU.1, PLM-RARα, and CEBPA, which are important factors for leukaemia carcinogenesis.

Another glycolytic protein that showed an association with some of the upregulated cytokines in this study is PFKFB3. PFKFB3 is highly expressed in several cancers (Atsumi et al., 2002) and thought to contribute to metabolic reprogramming macrophages and dendritic cells (Kelly and O'Neill, 2015). In this study, PFKFB3 showed co-expression with IL8 and MIP-1β following GeneMANIA gene network analysis (**Table 6**). It has been shown that overexpression of PKFKB3 boosts lactate production which activates TLR4 signalling, producing IL6 and IL8 which promotes cell proliferation in MCF-7 breast cancer cells and is thought to contribute to paclitaxel resistance (Ge et al., 2016). mTOR-mediated upregulation of PFKFB3 promotes myeloid leukaemia cell survival (Feng and Wu, 2017). Nevertheless, no cell cycle progression or cell proliferation was observed in THP-1 cells.

Enolase 1 (ENO1) is another glycolytic protein that showed co-expression with IL8 as well as shared biological processes with IL8 and MIP-1β in this study. ENO1 is an HIF-1α target gene that participates in glycolysis and gluconeogenesis. It catalyses the reversible dehydration of 2-

phosphoglycerate to phosphoenolpyruvate. ECM degradation is known to be important in carcinogenesis. Furthermore, ENO1 is expressed on the cell surface of several tumour types and is therefore considered a potential therapeutic target (Capello Michela et al., 2011; Principe et al., 2015). Moreover, it has been shown that *H. pylori* CagA protein upregulates ENO1 through stimulating the Src and MEK/ERK signalling pathways (Chen et al., 2014). Since CagA is important in *H. pylori*-induced carcinogenesis, upregulating ENO1 shows a new mechanism in microbial carcinogenesis.

Interestingly, soluble ENO1 showed similar cytokine stimulatory profile like LPS by activating TLR4 in a CD14-dependent manner on monocytes in rheumatoid arthritis (Guillou et al., 2016). It seems plausible to suggest that LPS-induced activation of ENO1, in a bid to boost glycolysis following infection, may also inadvertently promote ENO1-mediated cytokine release. These seemingly unrelated roles of ENO1 makes it important in innate immunity and carcinogenesis.

4.1.8 Proposed mechanisms based on *in vitro* and *in silico* studies

An analysis of predicted gene network interactions from IMP (**Figure 3.6**) showed that the basic helix-loop-helix protein Family Member E40 (BHLHE40) interacts with glycolytic genes ENO1 and LDHA, a glycolytic gene regulator (HIF-1α) and cytokines shown to be upregulated in this study (IL8 and MIP-1β), and other proinflammatory cytokines such as IL-1β. Further probing of the possibility of BHLHE40 in AML carcinogenesis in literature showed a possible involvement through circadian rhythm genes Clock and Bmal1 (Puram et al., 2016). BHLHE40 is a transcriptional repressor which is thought to be involved in the regulation of circadian rhythms, cell growth and differentiation (Honma et al., 2002; Sato et al., 2016). It is also known to regulate the production of several cytokines in T cells (Lin et al., 2014). BHLHE40 and BHLHE41 have been shown to control tumour progression and circadian rhythms. They regulate apoptosis, cell proliferation, hypoxia response, and epithelial-to-mesenchymal transition of tumour cells (Sato et al., 2016).

It has been shown recently that circadian control transcription factors (TFs) such as PU.1, BHLHE40, and CEBPA have a role to play in leukaemia carcinogenesis (Puram et al., 2016; Sato et al., 2016). Remarkably, these circadian transcription factors (TFs) which typically downregulate

circadian rhythm-related genes are also critical in myeloid cell differentiation which is a key controlling factor in myeloid leukaemia carcinogenesis (Puram et al., 2016; Rahman et al., 2017). My study further suggests an association between each of the proposed transcription factors that control the circadian rhythm and differentiation into a proposed gene regulatory network in myeloid leukaemia. Furthermore, this study embraces the potential role of certain beta chemokines, their connection with glycolytic genes and overall potential association with the afore-mentioned TFs. The proposed role of simulated infection with LPS also puts microbial carcinogenesis in context with the overall proposed mechanism **(Figure 4.2)**. The overall proposal is that key genes regulating the circadian rhythm may additionally utilise glycolytic genes in regulating leukaemia carcinogenesis.

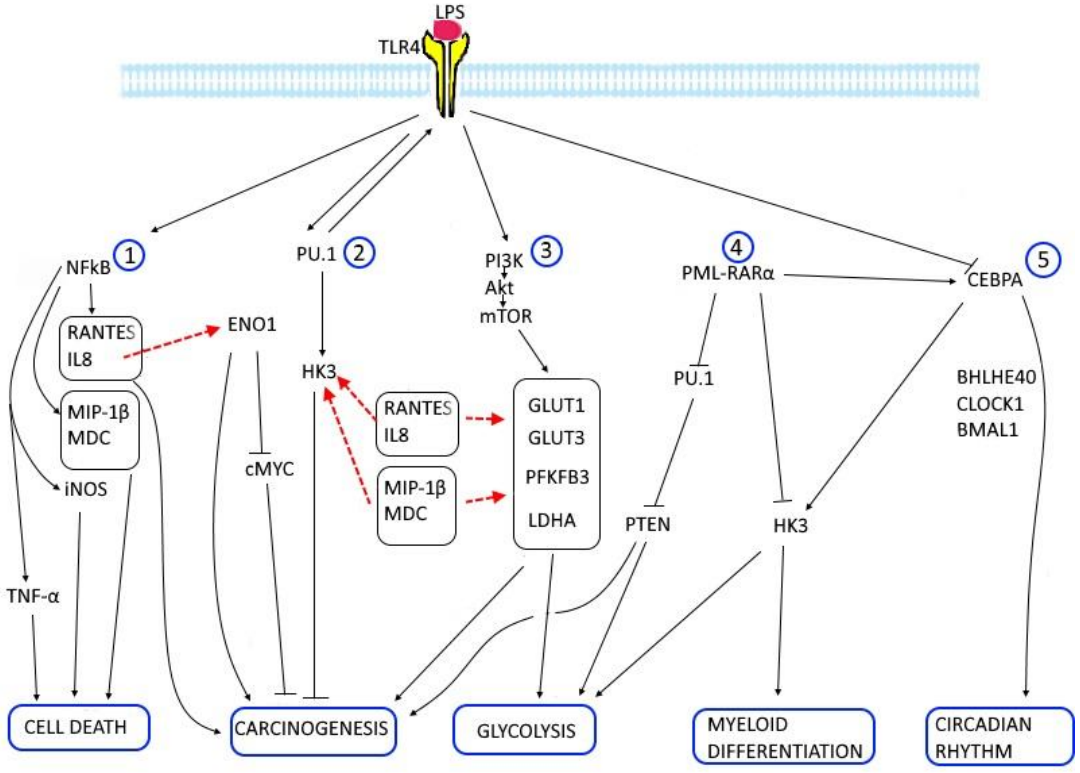

Figure 4.2 Proposed role of chemokines and glycolytic genes in acute myeloid leukaemia progression. The red broken arrows indicate proposed associations as observed in this study, while black solid arrows show established associations from literature. **1.** Binding of LPS to TLR4 activates transcription factors such as NF-κB which transactivates proinflammatory chemokines RANTES, IL8, MDC, and MIP-1β. While RANTES and IL8 are frequently associated with tumour progression, MDC and MIP-1β are rather associated with cell death. ENO1 which showed co-expression and co-localisation with IL8 is known to be involved in myeloid and pancreatic cancer progression. By contrast, nuclear ENO1 can inhibit cMYC, thereby inhibiting tumour progression. iNOS is also important in LPS-mediated cell death, through the

production of nitric oxide or TNF-α. **2.** Transcription factor PU.1 is activated by LPS, and PU.1, in turn, induces TLR4 expression. PU.1 activates HK3 which is known to stimulate myeloid differentiation, inhibiting carcinogenesis. **3.** LPS upregulates glycolysis through PI3K/Akt/mTOR-mediated activation of glycolytic genes. Additionally, PKFKB3, GUT1/3, and LDHA are promoters of carcinogenesis. Upregulated cytokines showed co-expression with the glycolytic genes shown by red broken arrows. HK3 is co-expressed with RANTES, IL8, MIP-1β, and MDC. **4.** and **5**. PML-RARα and CEBPA are both regulators of the circadian rhythm by activating CLOCK1, BMAL1, and BHLHE40 genes. Interestingly, both genes are critical in myeloid cell differentiation by interacting with HK3: PML-RARα represses HK3 while CEBPA activates HK3 expression **5.** Further shows that CEBPA is negatively regulated by LPS.

Finally, HIF-1α, a key transcriptional activator of glycolytic genes showed co-expression co-localisation with IL8 and shared biological processes with all the upregulated cytokines in this study (IL8, RANTES, MIP-1β, and MDC). The expression of HIF-1α is regarded as a general occurrence in infection and the inflammatory microenvironment (Werth et al., 2010; Zinkernagel et al., 2007). However, further probing of its expression and function in innate immune cells following infection showed that it was dependent on the differentiation status of the cells. For example, HIF-1α has been shown to be upregulated following LPS stimulation of monocyte-derived dendritic cells in normoxic conditions (Spirig et al., 2010). Furthermore, LPS induces HIF-1α in macrophage-differentiated THP-1 cells in a TLR4-dependent manner (Frede et al., 2006; Nishi et al., 2008), but not in THP-1 monocytes (Nishi et al., 2008). HIF-1α also increases the expression of several glycolysis-related genes such as GLUT1, PFKFB3, ENO1 and LDHA (Chen et al., 2001; Cui et al., 2017; Obach et al., 2004; Semenza et al., 1996) and is involved in metabolic reprogramming in carcinogenesis in lung cancer, glioma and hepatoma (Lu et al., 2002; Zhao et al., 2014). However, it appears that LPS-induced metabolic reprogramming in THP-1 cells used in this study may be HIF-1α -independent; even though HIF-1α is a key transcriptional activator of glycolytic gene expression and metabolic reprogramming. This is because previous reports have shown that LPS-mediated activation of HIF-1α only occurs in differentiated macrophages and dendritic cells, and not undifferentiated ones (Frede et al., 2006; Spirig et al., 2010).

4.2 Model proposal

It can be suggested that, if every hallmark that controls the malignancy of a tumour can be adequately defined, and the relative effect it has on proliferation quantified, more effective diagnostic and targeted combination therapies can be developed.

Why did a boost in the Warburg effect in this study not promote cell viability or proliferation? It is likely because other hallmarks of cancer may have been more critical in determining the malignancy of THP-1 cells. Nevertheless, it is beyond the scope of this work to individually assess possible changes in the other cancer hallmarks which could answer our question.

By designing a model that incorporates strategies to individually evaluate the influence of various hallmarks on proliferation, we could contribute to cancer diagnosis and likely propose more effective therapeutic strategies. This study proposes a model for the assessment of the hallmarks of cancer, using distinctive features and molecular markers. It can be suggested that cancers could be classified based on an assessment of all known cancer hallmarks which they exhibit. Such evaluations could be performed using cellular, molecular and biochemical methods in cell lines, 3D cultures, organoids and genetically engineered animal models such as xenograft mice. Thereafter, the relative influence of each of the hallmarks on the severity of a cancer could be assessed. By differentially inhibiting/enhancing each hallmark and evaluating tumour malignancy, the dominant hallmarks for each tumour type can be deciphered. This model may provide insight into the mechanisms which are critical in carcinogenesis for different cancers, based on the most critical hallmarks observed. This may open a new vista of diagnostic and therapeutic significance.

The malignancy of a tumour is dependent on specific hallmarks: these hallmarks have varying degrees of influence on the overall malignancy of a tumour. In the case of THP-1 cells, boosting glycolysis, a signature of the Warburg phenotype which is a hallmark of cancer, could not induce cell proliferation; indicating that the Warburg effect may not be critical in the malignancy of THP-1 cells. It is likely that other hallmarks may be have been more important for cell proliferation.

4.3 Prospects

In this study, polymyxin B was used to inhibit LPS-mediated TLR4 signalling. Even though its effects were potent enough to block LPS induced glycolysis, it did not show any significant

differences in the cell cycle when administered alone or in combination with LPS. Polymyxin B effectively inhibited glycolysis in a TLR4-dependent manner. However, the cell cycle profile differed from the untreated cells. This is not surprising given that polymyxin B has been shown to have cytotoxic effects and is only used as an antibiotic in resistant Gram-negative bacterial infections (Duwe et al., 1986; Vattimo et al., 2016; Viljanen and Vaara, 1984). Subjecting TLR4 to siRNA ablation could provide better clues than using inhibitors which also have the potential to interact through other pathways.

LPS is one of several pathogen-associated molecular patterns (PAMPs): molecular signatures on/in infectious agents (bacteria, viruses, fungi, and protozoa) that can be recognised by pattern-recognition receptors (PRRs). **Figure 1** in the introductory section showed nine TLRs responding to different PAMPs. It would be interesting to investigate the metabolic profiles and proliferative states of THP-1, K562 and other cell types following treatment with other PAMPs such as dsRNA (TLR3 ligand), bacterial lipopeptides (TLR1, 2 and 6 ligands) and others. This is because their signalling mechanisms and effector molecules could have different effects on the metabolism and viability of various cells.

Moreover, the inflammatory microenvironment is quite complex: teeming with inflammatory cells (such as infiltrating leukocytes, neutrophils), cytokines and co-stimulatory molecules with one agenda: to neutralise the infection via innate, and subsequently adaptive immune mechanisms. This complexity which is typical of an *in vivo* environment is impossible to replicate *in vitro*. This necessitates the use of an *in vivo* environment. For example, infecting xenograft mouse models with bacterial LPS and investigating the metabolic profile and proliferative state of the tumour cells would give a better inference.

Finally, TP53, dubbed ‘the guardian of the genome” (Lane, 1992) and “cellular gatekeeper” (Levine, 1997) because of its potent tumour-suppressive effects may also employ metabolic control strategies for tumour suppression (Puzio-Kuter, 2011; Vousden and Ryan, 2009). p53 is mutated in about 50% of all cancers. It is tempting to propose that, at least part of the metabolic reprogramming observed in several tumours is mutant-p53-dependent. Previous findings about the response of innate immune cells to PAMPs in the context of metabolism and proliferation have been focused on normal macrophages and dendritic cells with wild type p53. It would be pertinent to investigate the effect of PAMP-mediated metabolic reprogramming on malignant innate

immune cells with wild-type p53; since both cell lines used in this study (THP-1 and K562) had mutant p53 status.

An interesting finding in breast cancer cells was that TLR4 modulated cell proliferation in a manner dependent on the presence of wild type p53. Activation of TLR4 in wild type p53 cells impeded cell proliferation but enhanced proliferation in p53-mutant cells (Haricharan and Brown, 2015). This further accentuates the importance of unravelling the mechanisms involved in controlling carcinogenesis in the context of p53 status and TLR4 activity.

4.4 Conclusion

This study has shown that LPS enhances the Warburg Effect in the monocytic cancer cell line, THP-1, but induces cell death. In other words, a glycolytic phenotype that is characteristic of cancer cells is not required for cell proliferation in the immune-related cancer cell line. Furthermore, simulating infection in THP-1 monocytes using bacterial LPS upregulates the expression of IL8, RANTES, MDC, and MIP-1β in a TLR4-dependent manner. Importantly, this study further showed that RANTES was not expressed in the erythroleukaemia cell line K562 derived from the same lineage as THP-1 but less differentiated. Bioinformatic analyses show that IL8, RANTES, MDC, and MIP-1β may interact with glycolytic enzymes which may explain, at least in part, the observed boost in glycolysis in THP-1 monocytes. Moreover, enhanced glucose uptake which is characteristic of glycolytic flux is carried out by glucose transporters. This study showed that GLUT1 and GLUT3 co-express with IL8 while GLUT3 is co-expressed with RANTES. Furthermore, biological processes such as the regulation of CD8+ T-cell activation, is shared by IL8, RANTES, MIP-1β and glycolytic genes.

These results show that innate immune cells have an important temporal expression of chemokines of important functional significance. The study further suggests that these chemokines influence the metabolic programme in THP-1 monocytes probably through mechanisms that involve the glucose transporters (GLUT1 and GLUT3), HK3 and other glycolytic proteins.

Appendix

Table A2.1. Kits, manufacturers and catalogue numbers

Kit	Manufacturer and Catalogue number
Revert Aid first strand cDNA synthesis kit	Thermofischer Scientific, K1622
FxCycle™PI/RNAse	Molecular Probes, F10797
The Human, bacterial Multi analyte ELISA array kit	Qiagen, MEH-008A
JC-10 Mitochondrial Membrane Potential Kit	Sigma Aldrich, MAK160-1KT

Table A2.2. Instruments, manufactures and product catalogue numbers

Instrument	Manufacturer and Catalogue number
Nanodrop spectrophotometer	ND-1000 UV
Electrophoresis tank	Scieplus VG Sys 30020529
Power supply	Sigma techware PS250-2
Chemi-Doc imaging	Bio-Rad Gel Doc XR^+
BD Acuri C6 Flow cytometer	BD Biosciences
BD FACSAria™ III Flow cytometer	BD Biosciences
Microcentrifuge, Sigma 1-15	Sigma
Multiskan™ GO Microplate Spectrophotometer	Thermofischer Scientific,
Varioskan Flash Multimode microplate reader	Thermofischer Scientific, 5250030
PCR thermal cycler	Geneamp PCR system 2400

Table A2.3 Chemicals/reagents, manufactures and catalogue numbers where appropriate

Reagent/Chemical	Manufacturer and Catalogue number
Agarose	Lonza 50004
Oligonucleotide primers	Inqaba Biotec
Bacterial lipopolysaccharides (LPS) from *Escherichia coli*	Sigma, O111:B4
polymyxin B	Sigma-81334
Carbonyl cyanide-p-trifluoromethoxyphenylhydrazone (FCCP)	Sigma-C2920
Phosphate-buffered saline (PBS)	Sigma, P4417
Trizma base	Sigma T1503-500G
Foetal Bovine Serum (FBS)	Biowest S1815-500
Penicillin-Streptomycin	Sigma P433-20ml
DMEM	Sigma D5796-500ml
Hams F12	Biowest, L0136-500
RPMI 1640	Sigma, 51536C
RNase-free water	Qiagen, 129317
Ethidium bromide	Sigma, E1510
DNA Molecular weight marker	Thermofischer scientific, SM1333
6X DNA loading dye	Thermofischer scientific, R0611
2X PCR Mastermix	New England Biolabs, M0270
Glycolysis assay substrate	Cayman Chemicals, 600451
Glycolysis assay co-factor	Cayman Chemicals, 600454
L-lactate standards 10mM stock solution	Cayman Chemicals, 600455

Table A2.4 Bioinformatics and other websites and software used

Software used	Purpose	Website
NCBI	PCR Primer design	https://www.ncbi.nlm.nih.gov/pubmed
GeneMANIA	Pathway analysis	https://genemania.org/
IMP	Pathway analysis	http://imp.princeton.edu/
MyImageAnalysis™ software	Densitometry	https://www.thermofisher.com/order/catalog/product/62237
GraphPad Quick Calcs Prism	Statistical significance test	https://www.graphpad.com/quickcalcs/ttest1/?Format=SD

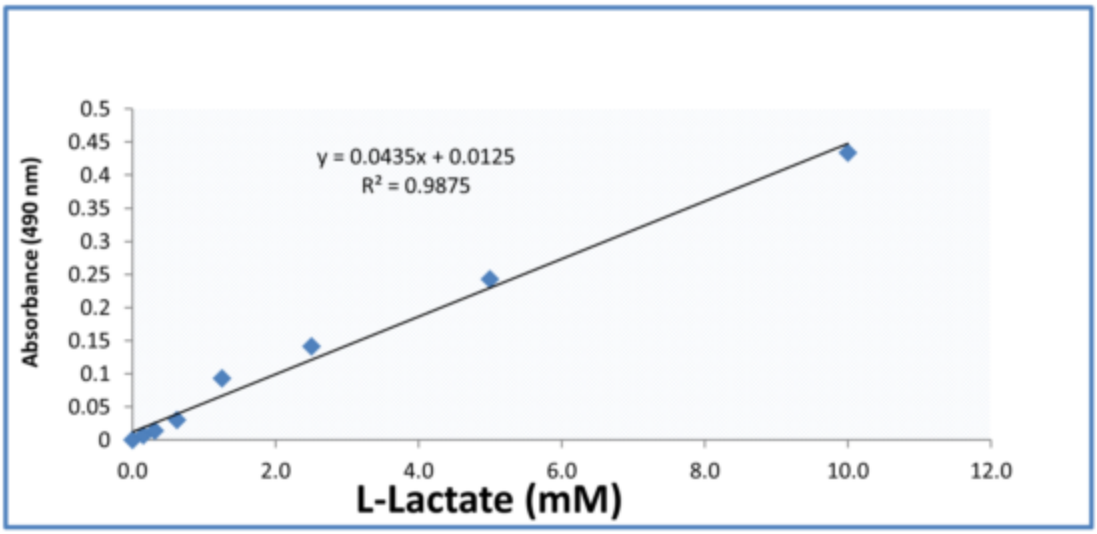

Figure A3.1. L-Lactate standard curve. L-lactate standards (10, 5, 2.5, 1.25, 0.625, 0.313, 0.156 and 0 mM) were prepared from the 10 mM stock solution.10 uL of each sample was used to run the lactate assay. Absorbance values were read at 490 nm using a Multiskan™ GO Microplate reader. The average absorbance values were computed, and the blank absorbance was subtracted from all values to obtain the corrected absorbance values. The corrected absorbance values for each of the standards were plotted against their corresponding concentration values to obtain a standard curve.

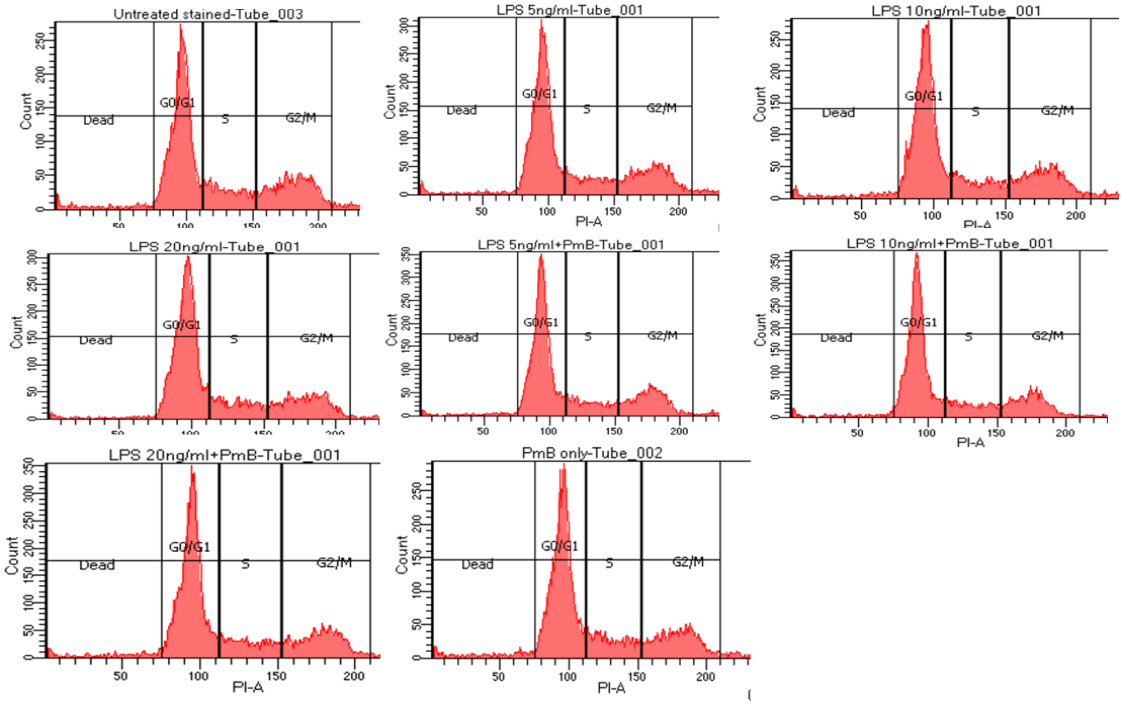

Figure A3.2. THP1-Cell cycle histograms, 24-hour treatments. THP-1 cells were treated for 24 hours and stained with propidium iodide (PI)/RNAse. Cell cycle data was acquired using the BD FACS Aria III flow cytometer. The sample flow rate was set to 'slow', and 10,000 events were acquired. Sample populations were gated by identifying singlet populations on the forward scatter versus side scatter plot. PI intensity was read on an FL3 channel at a wavelength of 488 nm. Results are representative of three biological replicates.

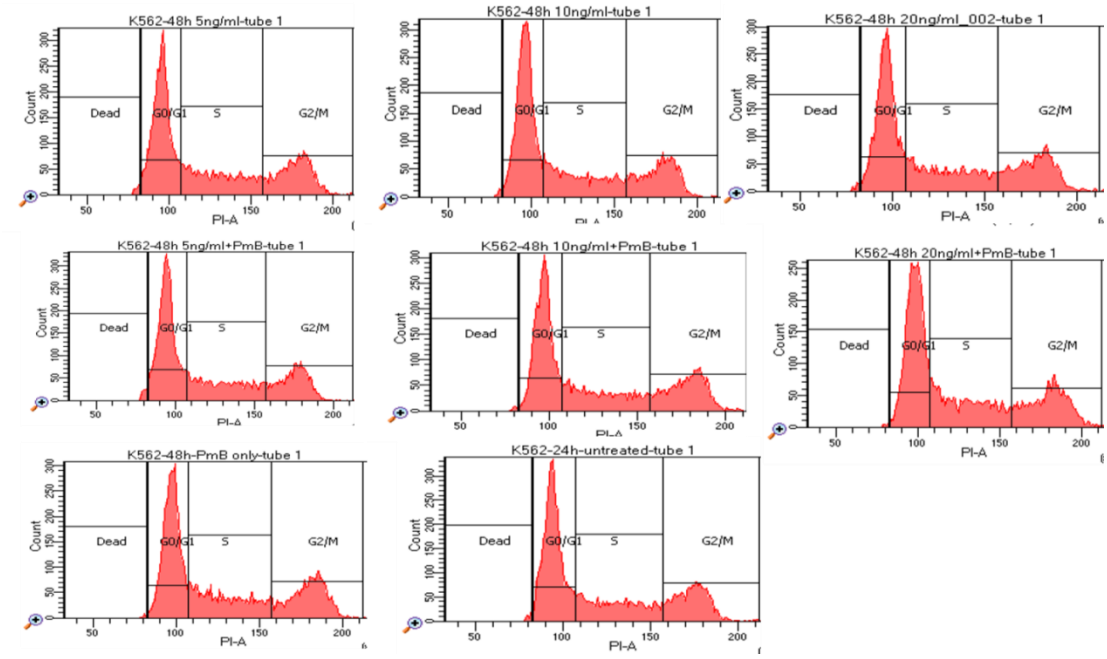

Figure A3.3. THP1-Cell cycle histograms, 48-hour treatments. THP-1 cells were treated for 48 hours and stained with propidium iodide/RNase. Cell cycle data was acquired using the BD FACS Aria III flow cytometer. The sample flow rate was set to 'slow', and 10,000 events were acquired. Sample populations were gated by identifying singlet populations on the forward scatter versus side scatter plot. PI intensity was read on an FL3 channel at a wavelength of 488 nm. Results are representative of three biological replicates.

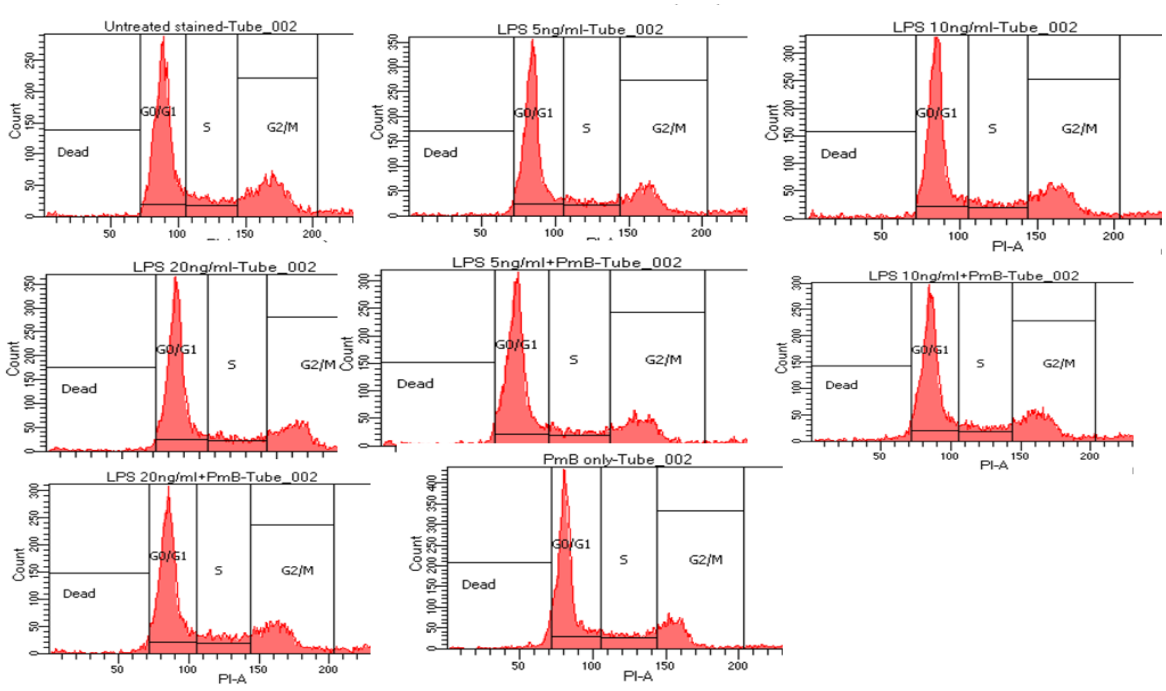

Figure A3.4. K562-Cell cycle histograms, 24-hour treatments. K562 cells were treated for 24 hours and stained with propidium iodide/RNase. Cell cycle data was acquired using the BD FACS Aria III flow cytometer. The sample flow rate was set to 'slow', and 10,000 events were acquired. Sample populations were gated by identifying singlet populations on the forward scatter versus side scatter plot. PI intensity was read on an FL3 channel at a wavelength of 488 nm. Results are representative of three biological replicates.

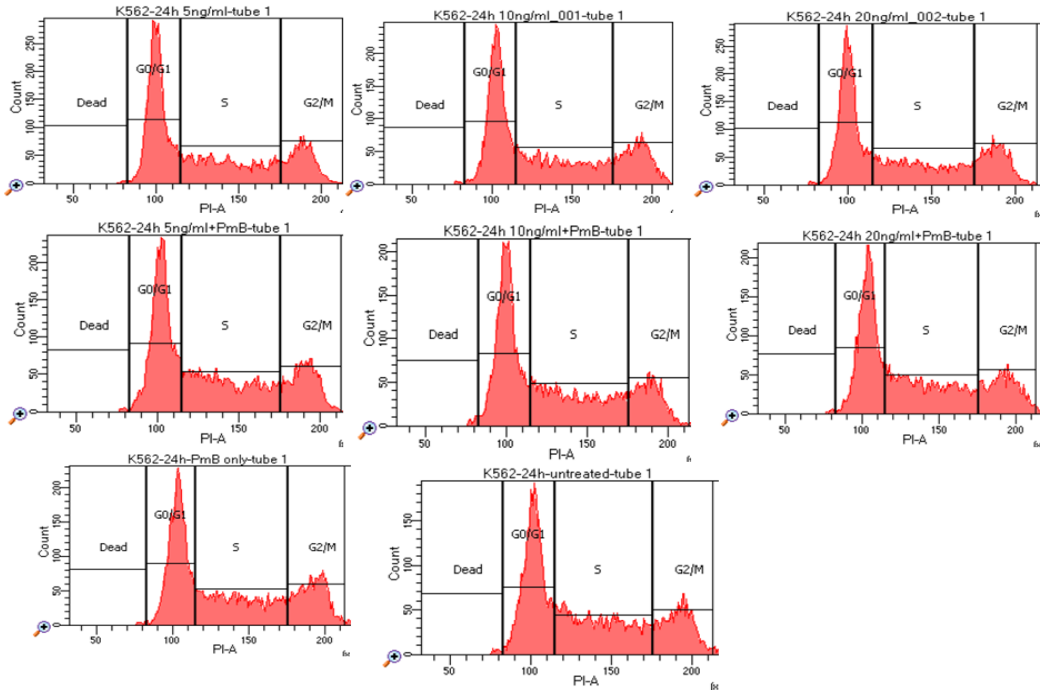

Figure A3.5. K562 Cell cycle histograms, 48-hour treatments. K562 cells were treated for 24 hours and stained with propidium iodide/RNase. Cell cycle data was acquired using the BD FACS Aria III flow cytometer. The sample flow rate was set to 'slow', and 10,000 events were acquired. Sample populations were gated by identifying singlet populations on the forward scatter versus side scatter plot. PI intensity was read on an FL3 channel at a wavelength of 488 nm. Results are representative of three biological replicates.

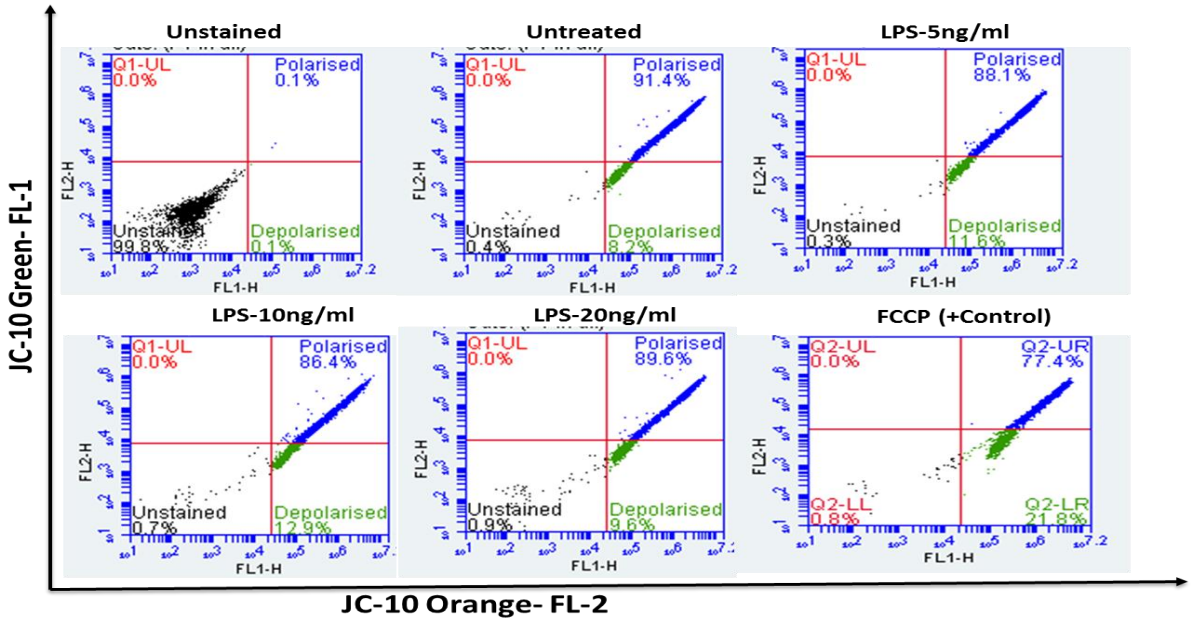

Figure A3.6. Mitochondrial membrane potential assay, THP-1 cells. Cytograms show mitochondrial membrane depolarisation following LPS treatment. Following LPS and combination treatments with polymyxin B for 48 hours, the mitochondrial membrane potential assay was performed, and fluorescence intensity was monitored using FL1 (green) and FL2 (orange) fluorescent channels in a BD Acuri C6 flow cytometer. Quadrants showing green fluorescence (lower right) indicate depolarised cells while blue (upper right) shows polarised cells. Black dots indicate unstained cells as seen in the lower left quadrants. FCCP was used as a positive control. Data are representative of 3 independent experiments.

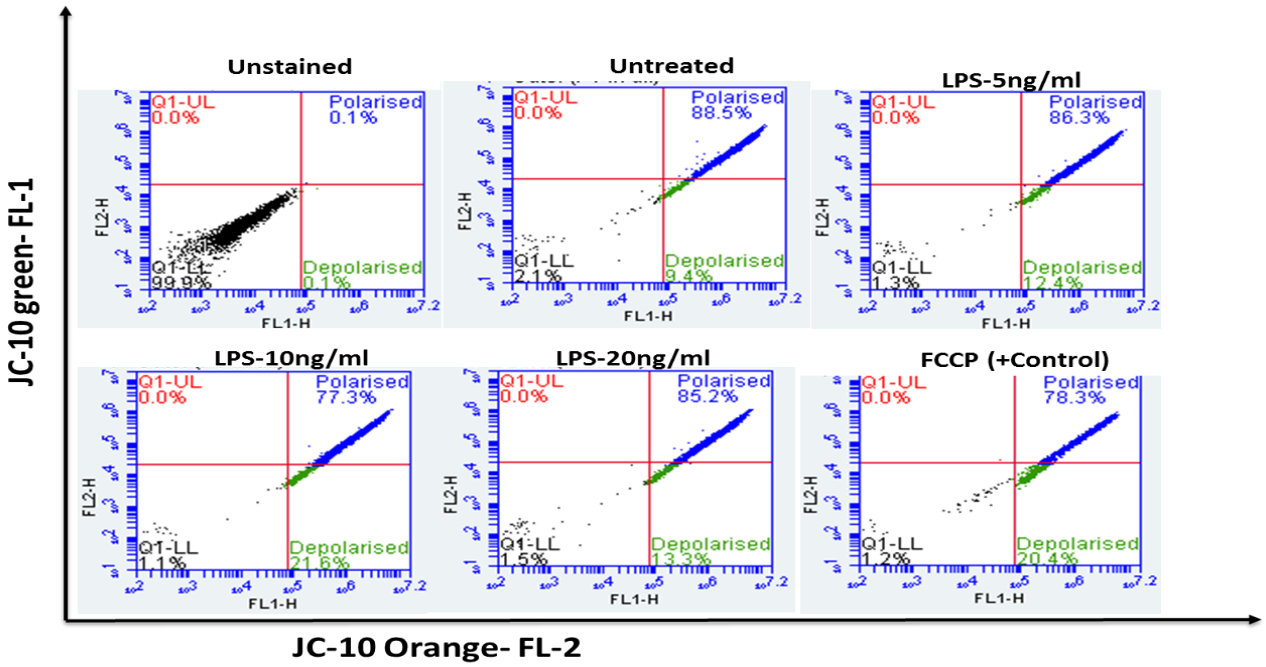

Figure A3.7. Mitochondrial membrane potential assay, K562 cells. Cytograms show mitochondrial membrane depolarisation following LPS treatment. Following LPS and combination treatments with polymyxin B for 48 hours, the mitochondrial membrane potential assay was performed, and fluorescence intensity was monitored using FL1 (green) and FL2 (orange) fluorescent channels in a BD Acuri C6 flow cytometer. Quadrants showing green fluorescence (lower right) indicate depolarised cells while blue (upper right) shows polarised cells. Black dots indicate unstained cells as seen in the lower left quadrants. FCCP was used as a positive control. The data are representative of 3 independent experiments.

References

Achtman, A.H., Khan, M., MacLennan, I.C.M., and Langhorne, J. (2003). *Plasmodium chabaudi chabaudi* Infection in Mice Induces Strong B Cell Responses and Striking But Temporary Changes in Splenic Cell Distribution. J. Immunol. *171*, 317.

Akira, S., Nishio, Y., Inoue, M., Wang, X.-J., We, S., Matsusaka, T., Yoshida, K., Sudo, T., Naruto, M., and Kishimoto, T. (1994). Molecular cloning of APRF, a novel IFN-stimulated gene factor 3 p91-related transcription factor involved in the gp130-mediated signaling pathway. Cell *77*, 63–71.

Alam, N.A., Olpin, S., and Leigh, I.M. (2005). Fumarate hydratase mutations and predisposition to cutaneous leiomyomas, uterine leiomyomas and renal cancer. Br. J. Dermatol. *153*, 11–17.

Alenzi, F.Q.B. (2004). Links between apoptosis, proliferation and the cell cycle. Br. J. Biomed. Sci. *61*, 99–102.

Alexopoulou, L., Holt, A.C., Medzhitov, R., and Flavell, R.A. (2001). Recognition of double-stranded RNA and activation of NF-κB by Toll-like receptor 3. Nature *413*, 732–738.

Almuhaideb, A., Papathanasiou, N., and Bomanji, J. (2011). (18)F-FDG PET/CT Imaging In Oncology. Ann. Saudi Med. *31*, 3–13.

Altenberg, B., and Greulich, K.O. (2004). Genes of glycolysis are ubiquitously overexpressed in 24 cancer classes. Genomics *84*, 1014–1020.

Andersen, A.P., Flinck, M., Oernbo, E.K., Pedersen, N.B., Viuff, B.M., and Pedersen, S.F. (2016). Roles of acid-extruding ion transporters in regulation of breast cancer cell growth in a 3-dimensional microenvironment. Mol. Cancer *15*, 45.

Andersson, L.C., Nilsson, K., and Gahmberg, C.G. (1979). K562—A human erythroleukemic cell line. Int. J. Cancer *23*, 143–147.

Ando, M., Uehara, I., Kogure, K., Asano, Y., Nakajima, W., Abe, Y., Kawauchi, K., and Tanaka, N. (2010). Interleukin 6 enhances glycolysis through expression of the glycolytic enzymes hexokinase 2 and 6-phosphofructo-2-kinase/fructose-2,6-bisphosphatase-3. J. Nippon Med. Sch. Nippon Ika Daigaku Zasshi *77*, 97–105.

Andrew, D.P., Chang, M., McNinch, J., Wathen, S.T., Rihanek, M., Tseng, J., Spellberg, J.P., and Elias, C.G. (1998). STCP-1 (MDC) CC Chemokine Acts Specifically on Chronically Activated Th2 Lymphocytes and Is Produced by Monocytes on Stimulation with Th2 Cytokines IL-4 and IL-13. J. Immunol. *161*, 5027.

Ashburner, M., Ball, C.A., Blake, J.A., Botstein, D., Butler, H., Cherry, J.M., Davis, A.P., Dolinski, K., Dwight, S.S., Eppig, J.T., et al. (2000). Gene Ontology: tool for the unification of biology. Nat. Genet. *25*, 25.

Astuti, D., Latif, F., Dallol, A., Dahia, P.L.M., Douglas, F., George, E., Sköldberg, F., Husebye, E.S., Eng, C., and Maher, E.R. (2001). Gene Mutations in the Succinate Dehydrogenase Subunit

SDHB Cause Susceptibility to Familial Pheochromocytoma and to Familial Paraganglioma. Am. J. Hum. Genet. *69*, 49–54.

Atsumi, T., Chesney, J., Metz, C., Leng, L., Donnelly, S., Makita, Z., Mitchell, R., and Bucala, R. (2002). High Expression of Inducible 6-Phosphofructo-2-Kinase/Fructose-2,6-Bisphosphatase (iPFK-2; PFKFB3) in Human Cancers. Cancer Res. *62*, 5881.

Avellino, R., Havermans, M., Erpelinck, C., Sanders, M.A., Hoogenboezem, R., van de Werken, H.J.G., Rombouts, E., van Lom, K., van Strien, P.M.H., Gebhard, C., et al. (2016). An autonomous CEBPA enhancer specific for myeloid-lineage priming and neutrophilic differentiation. Blood *127*, 2991–3003.

Azad, M.A.K., Finnin, B.A., Poudyal, A., Davis, K., Li, J., Hill, P.A., Nation, R.L., Velkov, T., and Li, J. (2013). Polymyxin B Induces Apoptosis in Kidney Proximal Tubular Cells. Antimicrob. Agents Chemother. *57*, 4329–4335.

Azad, M.A.K., Akter, J., Rogers, K.L., Nation, R.L., Velkov, T., and Li, J. (2015). Major Pathways of Polymyxin-Induced Apoptosis in Rat Kidney Proximal Tubular Cells. Antimicrob. Agents Chemother. *59*, 2136–2143.

Backert, S., and Blaser, M.J. (2016). The Role of CagA in the Gastric Biology of *Helicobacter pylori*. Cancer Res. *76*, 4028.

Bao, Y., Mukai, K., Hishiki, T., Kubo, A., Ohmura, M., Sugiura, Y., Matsuura, T., Nagahata, Y., Hayakawa, N., Yamamoto, T., et al. (2013). Energy Management by Enhanced Glycolysis in G_1-phase in Human Colon Cancer Cells *In Vitro* and *In Vivo*. Mol. Cancer Res. *11*, 973.

Bao, Y., Ledderose, C., Seier, T., Graf, A.F., Brix, B., Chong, E., and Junger, W.G. (2014). Mitochondria Regulate Neutrophil Activation by Generating ATP for Autocrine Purinergic Signaling. J. Biol. Chem. *289*, 26794–26803.

Barksby, H.E., Nile, C.J., Jaedicke, K.M., Taylor, J.J., and Preshaw, P.M. (2009). Differential expression of immunoregulatory genes in monocytes in response to Porphyromonas gingivalis and Escherichia coli lipopolysaccharide. Clin. Exp. Immunol. *156*, 479–487.

Barron, C., Tsiani, E., and Tsakiridis, T. (2012). Expression of the glucose transporters GLUT1, GLUT3, GLUT4 and GLUT12 in human cancer cells. BMC Proc. *6*, P4–P4.

Bartels, K., Grenz, A., and Eltzschig, H.K. (2013). Hypoxia and inflammation are two sides of the same coin. Proc. Natl. Acad. Sci. *110*, 18351–18352.

Basu, P., Banerjee, D., Singh, P., Bhattacharya, C., and Biswas, J. (2013). Efficacy and safety of human papillomavirus vaccine for primary prevention of cervical cancer: A review of evidence from phase III trials and national programs. South Asian J. Cancer *2*, 187–192.

Bauer, D.E., Harris, M.H., Plas, D.R., Lum, J.J., Hammerman, P.S., Rathmell, J.C., Riley, J.L., and Thompson, C.B. (2004). Cytokine stimulation of aerobic glycolysis in hematopoietic cells exceeds proliferative demand. FASEB J. *18*, 1303–1305.

Baysal, B.E., Ferrell, R.E., Willett-Brozick, J.E., Lawrence, E.C., Myssiorek, D., Bosch, A., van der Mey, A., Taschner, P.E., Rubinstein, W.S., Myers, E.N., et al. (2000). Mutations in SDHD, a mitochondrial complex II gene, in hereditary paraganglioma. Science *287*, 848–851.

Beckner, M.E., Stracke, M.L., Liotta, L.A., and Schiffmann, E. (1990). Glycolysis as primary energy source in tumor cell chemotaxis. J. Natl. Cancer Inst. *82*, 1836–1840.

Belinda, L.W.-C., Wei, W.X., Hanh, B.T.H., Lei, L.X., Bow, H., and Ling, D.J. (2008). SARM: a novel Toll-like receptor adaptor, is functionally conserved from arthropod to human. Mol. Immunol. *45*, 1732–1742.

Bender, C.M., Pao, M.M., and Jones, P.A. (1998). Inhibition of DNA Methylation by 5-Aza-2′-deoxycytidine Suppresses the Growth of Human Tumor Cell Lines. Cancer Res. *58*, 95.

Bensaad, K., Tsuruta, A., Selak, M.A., Vidal, M.N.C., Nakano, K., Bartrons, R., Gottlieb, E., and Vousden, K.H. (2006). TIGAR, a p53-Inducible Regulator of Glycolysis and Apoptosis. Cell *126*, 107–120.

Ben-Shlomo, I., Kol, S., Roeder, L.M., Resnick, C.E., Hurwitz, A., Payne, D.W., and Adashi, E.Y. (1997). Interleukin (IL)-1beta increases glucose uptake and induces glycolysis in aerobically cultured rat ovarian cells: evidence that IL-1beta may mediate the gonadotropin-induced midcycle metabolic shift. Endocrinology *138*, 2680–2688.

Berridge, M.V., Herst, P.M., and Tan, A.S. (2010). Metabolic flexibility and cell hierarchy in metastatic cancer. Mitochondrion *10*, 584–588.

Bild, A.H., Yao, G., Chang, J.T., Wang, Q., Potti, A., Chasse, D., Joshi, M.-B., Harpole, D., Lancaster, J.M., Berchuck, A., et al. (2006). Oncogenic pathway signatures in human cancers as a guide to targeted therapies. Nature *439*, 353–357.

Blaser, M.J., Perez-Perez, G.I., Kleanthous, H., Cover, T.L., Peek, R.M., Chyou, P.H., Stemmermann, G.N., and Nomura, A. (1995). Infection with *Helicobacter pylori* Strains Possessing *cagA* Is Associated with an Increased Risk of Developing Adenocarcinoma of the Stomach. Cancer Res. *55*, 2111.

Boguski, M.S., Lowe, T.M.J., and Tolstoshev, C.M. (1993). dbEST [mdash] database for [ldquo]expressed sequence tags[rdquo]. Nat Genet *4*, 332–333.

Boldrick, J.C., Alizadeh, A.A., Diehn, M., Dudoit, S., Liu, C.L., Belcher, C.E., Botstein, D., Staudt, L.M., Brown, P.O., and Relman, D.A. (2002). Stereotyped and specific gene expression programs in human innate immune responses to bacteria. Proc. Natl. Acad. Sci. U. S. A. *99*, 972–977.

Borregaard, N., and Herlin, T. (1982). Energy Metabolism of Human Neutrophils during Phagocytosis. J. Clin. Invest. *70*, 550–557.

Boss, O., Hagen, T., and Lowell, B.B. (2000). Uncoupling proteins 2 and 3: potential regulators of mitochondrial energy metabolism. Diabetes *49*, 143.

Bosshart, H., and Heinzelmann, M. (2016). THP-1 cells as a model for human monocytes. Ann. Transl. Med. *4*, 438–438.

Braaten, K.P., and Laufer, M.R. (2008). Human Papillomavirus (HPV), HPV-Related Disease, and the HPV Vaccine. Rev. Obstet. Gynecol. *1*, 2–10.

Brady, G., MacArthur, G.J., and Farrell, P.J. (2007). Epstein–Barr virus and Burkitt lymphoma. J. Clin. Pathol. *60*, 1397–1402.

Brown, J.M. (2007). Tumor Hypoxia in Cancer Therapy. In Methods in Enzymology, (Academic Press), pp. 295–321.

Burington, B., Barlogie, B., Zhan, F., Crowley, J., and Shaughnessy, J.D. (2008). Tumor cell gene expression changes following short-term in vivo exposure to single agent chemotherapeutics are related to survival in multiple myeloma. Clin. Cancer Res. Off. J. Am. Assoc. Cancer Res. *14*, 4821–4829.

Calcinotto, A., Filipazzi, P., Grioni, M., Iero, M., De Milito, A., Ricupito, A., Cova, A., Canese, R., Jachetti, E., Rossetti, M., et al. (2012). Modulation of microenvironment acidity reverses anergy in human and murine tumor-infiltrating T lymphocytes. Cancer Res. *72*, 2746–2756.

Cambien, B., Richard-Fiardo, P., Karimdjee, B.F., Martini, V., Ferrua, B., Pitard, B., Schmid-Antomarchi, H., and Schmid-Alliana, A. (2011). CCL5 Neutralization Restricts Cancer Growth and Potentiates the Targeting of PDGFRβ in Colorectal Carcinoma. PLoS ONE *6*, e28842.

Capello Michela, Ferri-Borgogno Sammy, Cappello Paola, and Novelli Francesco (2011). α-enolase: a promising therapeutic and diagnostic tumor target. FEBS J. *278*, 1064–1074.

Cappelli, C., López, X., Labra, Y., Montoya, M., Fernández, R., Imarai, M., Rojas, J.L., Miranda, D., Escobar, A., and Acuña-Castillo, C. (2012). Polymyxin B increases the depletion of T regulatory cell induced by purinergic agonist. Immunobiology *217*, 307–315.

Chan, O., Burke, J.D., Gao, D.F., and Fish, E.N. (2012). The Chemokine CCL5 Regulates Glucose Uptake and AMP Kinase Signaling in Activated T Cells to Facilitate Chemotaxis. J. Biol. Chem. *287*, 29406–29416.

Chang, L.-Y., Lin, Y.-C., Mahalingam, J., Huang, C.-T., Chen, T.-W., Kang, C.-W., Peng, H.-M., Chu, Y.-Y., Chiang, J.-M., Dutta, A., et al. (2012). Tumor-Derived Chemokine CCL5 Enhances TGF-β–Mediated Killing of $CD8^+$ T Cells in Colon Cancer by T-Regulatory Cells. Cancer Res. *72*, 1092.

Chang, M.H., Shau, W.Y., Chen, C.J., Wu, T.C., Kong, M.S., Liang, D.C., Hsu, H.M., Chen, H.L., Hsu, H.Y., and Chen, D.S. (2000). Hepatitis B vaccination and hepatocellular carcinoma rates in boys and girls. JAMA *284*, 3040–3042.

Chao, T.-K., Huang, T.-S., Liao, Y.-P., Huang, R.-L., Su, P.-H., Shen, H.-Y., Lai, H.-C., and Wang, Y.-C. (2017). Pyruvate kinase M2 is a poor prognostic marker of and a therapeutic target in ovarian cancer. PLOS ONE *12*, e0182166.

Charles A Janeway, J., Travers, P., Walport, M., and Shlomchik, M.J. (2001). Principles of innate and adaptive immunity. Immunobiol. Immune Syst. Health Dis. 5th Ed.

Chellappan, S., Kraus, V.B., Kroger, B., Munger, K., Howley, P.M., Phelps, W.C., and Nevins, J.R. (1992). Adenovirus E1A, simian virus 40 tumor antigen, and human papillomavirus E7 protein share the capacity to disrupt the interaction between transcription factor E2F and the retinoblastoma gene product. Proc. Natl. Acad. Sci. *89*, 4549.

Chen, C., Pore, N., Behrooz, A., Ismail-Beigi, F., and Maity, A. (2001). Regulation of glut1 mRNA by Hypoxia-inducible Factor-1: Interaction between H-ras and hypoxia. J. Biol. Chem. *276*, 9519–9525.

Chen, K., Huang, J., Gong, W., Iribarren, P., Dunlop, N.M., and Wang, J.M. (2007). Toll-like receptors in inflammation, infection and cancer. Int. Immunopharmacol. *7*, 1271–1285.

Chen, S., Duan, G., Zhang, R., and Fan, Q. (2014). Helicobacter pylori cytotoxin-associated gene a protein upregulates α-enolase expression via Src/MEK/ERK pathway: Implication for progression of gastric cancer. Int. J. Oncol. *45*, 764–770.

Cho, L.Y., Yang, J.J., Ko, K.-P., Park, B., Shin, A., Lim, M.K., Oh, J.-K., Park, S., Kim, Y.J., Shin, H.-R., et al. (2011). Coinfection of hepatitis B and C viruses and risk of hepatocellular carcinoma: systematic review and meta-analysis. Int. J. Cancer J. Int. Cancer *128*, 176–184.

Chow, J.C., Young, D.W., Golenbock, D.T., Christ, W.J., and Gusovsky, F. (1999). Toll-like Receptor-4 Mediates Lipopolysaccharide-induced Signal Transduction. J. Biol. Chem. *274*, 10689–10692.

Christofk, H.R., Vander Heiden, M.G., Harris, M.H., Ramanathan, A., Gerszten, R.E., Wei, R., Fleming, M.D., Schreiber, S.L., and Cantley, L.C. (2008). The M2 splice isoform of pyruvate kinase is important for cancer metabolism and tumour growth. Nature *452*, 230–233.

Cloherty, E.K., Sultzman, L.A., Zottola, R.J., and Carruthers, A. (1995). Net sugar transport is a multistep process. Evidence for cytosolic sugar binding sites in erythrocytes. Biochemistry *34*, 15395–15406.

Cloherty, E.K., Diamond, D.L., Heard, K.S., and Carruthers, A. (1996). Regulation of GLUT1-Mediated Sugar Transport by an Antiport/Uniport Switch Mechanism. Biochemistry *35*, 13231–13239.

Cocchi, F., DeVico, A.L., Garzino-Demo, A., Arya, S.K., Gallo, R.C., and Lusso, P. (1995). Identification of RANTES, MIP-1α, and MIP-1β as the Major HIV-Suppressive Factors Produced by $CD8^+$ T Cells. Science *270*, 1811.

Colotta, F., Allavena, P., Sica, A., Garlanda, C., and Mantovani, A. (2009). Cancer-related inflammation, the seventh hallmark of cancer: links to genetic instability. Carcinogenesis *30*, 1073–1081.

Coussens, L.M., and Werb, Z. (2002). Inflammation and cancer. Nature *420*, 860–867.

Crook, T., Vousden, K.H., and Tidy, J.A. (1991). Degradation of p53 can be targeted by HPV E6 sequences distinct from those required for p53 binding and trans-activation. Cell *67*, 547–556.

Cui, X., Han, Z., He, S., Wu, X., Chen, T., Shao, C., Chen, D., Su, N., Chen, Y., Wang, T., et al. (2017). HIF1/2α mediates hypoxia-induced LDHA expression in human pancreatic cancer cells. Oncotarget *8*, 24840–24852.

Dagvadorj, J., Shimada, K., Chen, S., Jones, H.D., Tumurkhuu, G., Zhang, W., Wawrowsky, K.A., Crother, T.R., and Arditi, M. (2015). Lipopolysaccharide induces alveolar macrophage necrosis via CD14 and the P2x7 receptor leading to Interleukin-1α release. Immunity *42*, 640–653.

Dang, C.V. (2010). Rethinking the Warburg Effect with Myc Micromanaging Glutamine Metabolism. Cancer Res. *70*, 859–862.

Dang, C.V. (2012). MYC on the Path to Cancer. Cell *149*, 22–35.

Dang, C.V., Kim, J., Gao, P., and Yustein, J. (2008). The interplay between MYC and HIF in cancer. Nat. Rev. Cancer *8*, 51–56.

De Francesco, E.M., Bonuccelli, G., Maggiolini, M., Sotgia, F., and Lisanti, M.P. (2017). Vitamin C and Doxycycline: A synthetic lethal combination therapy targeting metabolic flexibility in cancer stem cells (CSCs). Oncotarget *8*, 67269–67286.

DeBerardinis, R.J., Lum, J.J., Hatzivassiliou, G., and Thompson, C.B. (2008). The Biology of Cancer: Metabolic Reprogramming Fuels Cell Growth and Proliferation. Cell Metab. *7*, 11–20.

Delgado, T., Carroll, P.A., Punjabi, A.S., Margineantu, D., Hockenbery, D.M., and Lagunoff, M. (2010). Induction of the Warburg effect by Kaposi's sarcoma herpesvirus is required for the maintenance of latently infected endothelial cells. Proc. Natl. Acad. Sci. U. S. A. *107*, 10696–10701.

Diebold, S.S., Kaisho, T., Hemmi, H., Akira, S., and Reis e Sousa, C. (2004). Innate antiviral responses by means of TLR7-mediated recognition of single-stranded RNA. Science *303*, 1529–1531.

Ding, S.-Z., Goldberg, J.B., and Hatakeyama, M. (2010). Helicobacter pylori infection, oncogenic pathways and epigenetic mechanisms in gastric carcinogenesis. Future Oncol. Lond. Engl. *6*, 851–862.

Duchen, M.R., Smith, P.A., and Ashcroft, F.M. (1993). Substrate-dependent changes in mitochondrial function, intracellular free calcium concentration and membrane channels in pancreatic beta-cells. Biochem. J. *294*, 35–42.

Duwe, A.K., Rupar, C.A., Horsman, G.B., and Vas, S.I. (1986). In vitro cytotoxicity and antibiotic activity of polymyxin B nonapeptide. Antimicrob. Agents Chemother. *30*, 340–341.

El-Kenawi, A.E., and El-Remessy, A.B. (2013). Angiogenesis inhibitors in cancer therapy: mechanistic perspective on classification and treatment rationales. Br. J. Pharmacol. *170*, 712–729.

Elstrom, R.L., Bauer, D.E., Buzzai, M., Karnauskas, R., Harris, M.H., Plas, D.R., Zhuang, H., Cinalli, R.M., Alavi, A., Rudin, C.M., et al. (2004). Akt stimulates aerobic glycolysis in cancer cells. Cancer Res. *64*, 3892–3899.

Evan, G.I., and Vousden, K.H. (2001). Proliferation, cell cycle and apoptosis in cancer.

Everts, B., Amiel, E., Huang, S.C.-C., Smith, A.M., Chang, C.-H., Lam, W.Y., Redmann, V., Freitas, T.C., Blagih, J., van der Windt, G.J.W., et al. (2014). TLR-driven early glycolytic reprogramming via the kinases TBK1-IKKε supports the anabolic demands of dendritic cell activation. Nature Immunology *15*, 323–332.

Fantin, V.R., St-Pierre, J., and Leder, P. (2006). Attenuation of LDH-A expression uncovers a link between glycolysis, mitochondrial physiology, and tumor maintenance. Cancer Cell *9*, 425–434.

Federzoni, E.A., Valk, P.J.M., Torbett, B.E., Haferlach, T., Löwenberg, B., Fey, M.F., and Tschan, M.P. (2012). PU.1 is linking the glycolytic enzyme HK3 in neutrophil differentiation and survival of APL cells. Blood *119*, 4963–4970.

Feng, Y., and Wu, L. (2017). mTOR up-regulation of PFKFB3 is essential for acute myeloid leukemia cell survival. Biochem. Biophys. Res. Commun. *483*, 897–903.

Foss, H.-D., Herbst, H., Oelmann, E., Samol, J., Grebe, M., Blankenstein, T., Matthes, J., Qin, Z.-H., Falini, B., Pileri, S., et al. (1993). Lymphotoxin, tumour necrosis factor and interleukin-6 gene transcripts are present in Hodgkin and Reed-Sternberg cells of most Hodgkin's disease cases. Br. J. Haematol. *84*, 627–635.

Foss, H.D., Hummel, M., Gottstein, S., Ziemann, K., Falini, B., Herbst, H., and Stein, H. (1995). Frequent expression of IL-7 gene transcripts in tumor cells of classical Hodgkin's disease. Am. J. Pathol. *146*, 33–39.

Fox, C.J., Hammerman, P.S., and Thompson, C.B. (2005). Fuel feeds function: energy metabolism and the T-cell response. Nat. Rev. Immunol. *5*, 844.

Franceschi, S., Dal Maso, L., Arniani, S., Crosignani, P., Vercelli, M., Simonato, L., Falcini, F., Zanetti, R., Barchielli, A., Serraino, D., et al. (1998). Risk of cancer other than Kaposi's sarcoma and non-Hodgkin's lymphoma in persons with AIDS in Italy. Br. J. Cancer *78*, 966.

Frede, S., Stockmann, C., Freitag, P., and Fandrey, J. (2006). Bacterial lipopolysaccharide induces HIF-1 activation in human monocytes via p44/42 MAPK and NF-κB. Biochem. J. *396*, 517–527.

Freemerman, A.J., Johnson, A.R., Sacks, G.N., Milner, J.J., Kirk, E.L., Troester, M.A., Macintyre, A.N., Goraksha-Hicks, P., Rathmell, J.C., and Makowski, L. (2014). Metabolic Reprogramming of Macrophages: Glucose transporter 1(GLUT1)-mediated glucose metabolism drives a proinflammatory phenotype. J. Biol. Chem. *289*, 7884–7896.

Fu, Y., Maianu, L., Melbert, B.R., and Garvey, W.T. (2004). Facilitative glucose transporter gene expression in human lymphocytes, monocytes, and macrophages: a role for GLUT isoforms 1, 3, and 5 in the immune response and foam cell formation. Stem Cell Plast. *32*, 182–190.

Funda, D.P., Tučková, L., Farré, M.A., Iwase, T., Moro, I., and Tlaskalová-Hogenová, H. (2001). CD14 Is Expressed and Released as Soluble CD14 by Human Intestinal Epithelial Cells In Vitro: Lipopolysaccharide Activation of Epithelial Cells Revisited. Infect. Immun. *69*, 3772–3781.

Gabay, M., Li, Y., and Felsher, D.W. (2014). MYC Activation Is a Hallmark of Cancer Initiation and Maintenance. Cold Spring Harb. Perspect. Med. *4*, a014241.

Ge, X., Cao, Z., Gu, Y., Wang, F., Li, J., Han, M., Xia, W., Yu, Z., and Lyu, P. (2016). PFKFB3 potentially contributes to paclitaxel resistance in breast cancer cells through TLR4 activation by stimulating lactate production. Cell. Mol. Biol. *62*, 119–125.

Girgis, H., Masui, O., White, N.M., Scorilas, A., Rotondo, F., Seivwright, A., Gabril, M., Filter, E.R., Girgis, A.H., Bjarnason, G.A., et al. (2014). Lactate Dehydrogenase A is a potential prognostic marker in clear cell renal cell carcinoma. Mol. Cancer *13*, 1–10.

Goedert, J.J., Coté, T.R., Virgo, P., Scoppa, S.M., Kingma, D.W., Gail, M.H., Jaffe, E.S., and Biggar, R.J. (1998). Spectrum of AIDS-associated malignant disorders. The Lancet *351*, 1833–1839.

Gordan, J.D., Thompson, C.B., and Simon, M.C. (2007). HIF and c-Myc: sibling rivals for control of cancer cell metabolism and proliferation. Cancer Cell *12*, 108–113.

Gottfried, E., Kunz-Schughart, L.A., Ebner, S., Mueller-Klieser, W., Hoves, S., Andreesen, R., Mackensen, A., and Kreutz, M. (2006). Tumor-derived lactic acid modulates dendritic cell activation and antigen expression. Blood *107*, 2013.

Gottlob, K., Majewski, N., Kennedy, S., Kandel, E., Robey, R.B., and Hay, N. (2001). Inhibition of early apoptotic events by Akt/PKB is dependent on the first committed step of glycolysis and mitochondrial hexokinase. Genes Dev. *15*, 1406–1418.

Grivennikov, S.I., and Karin, M. (2011). Inflammatory cytokines in cancer: tumour necrosis factor and interleukin 6 take the stage. Ann. Rheum. Dis. *70*, i104.

Grivennikov, S.I., Greten, F.R., and Karin, M. (2010). Immunity, Inflammation, and Cancer. Cell *140*, 883–899.

Guillou, C., Fréret, M., Fondard, E., Derambure, C., Avenel, G., Golinski, M.-L., Verdet, M., Boyer, O., Caillot, F., Musette, P., et al. (2016). Soluble alpha-enolase activates monocytes by CD14-dependent TLR4 signalling pathway and exhibits a dual function. Sci. Rep. *6*, 23796.

Guo, J., Wang, B., Zhang, M., Chen, T., Yu, Y., Regulier, E., Homann, H., Qin, Z., Ju, D., and Cao, X. (2002). Macrophage-derived chemokine gene transfer results in tumor regression in murine lung carcinoma model through efficient induction of antitumor immunity. Gene Ther. *9*, 793.

Gupta, S.C., Hevia, D., Patchva, S., Park, B., Koh, W., and Aggarwal, B.B. (2012). Upsides and Downsides of Reactive Oxygen Species for Cancer: The Roles of Reactive Oxygen Species in Tumorigenesis, Prevention, and Therapy. Antioxid. Redox Signal. *16*, 1295–1322.

Haddad, J.J., and Harb, H.L. (2005). Cytokines and the regulation of hypoxia-inducible factor (HIF)-1α. Int. Immunopharmacol. *5*, 461–483.

Hamza, E., Kittl, S., and Kuhnert, P. (2017). Temporal induction of pro-inflammatory and regulatory cytokines in human peripheral blood mononuclear cells by Campylobacter jejuni and Campylobacter coli. PloS One *12*, e0171350–e0171350.

Han, J., Meng, Q., Xi, Q., Zhang, Y., Zhuang, Q., Han, Y., Jiang, Y., Ding, Q., and Wu, G. (2016). Interleukin-6 stimulates aerobic glycolysis by regulating PFKFB3 at early stage of colorectal cancer. Int. J. Oncol. *48*, 215–224.

Hanahan, D., and Weinberg, R.A. (2000). The Hallmarks of Cancer. Cell *100*, 57–70.

Hanahan, D., and Weinberg, R.A. (2011). Hallmarks of Cancer: The Next Generation. Cell *144*, 646–674.

Haricharan, S., and Brown, P. (2015). TLR4 has a TP53-dependent dual role in regulating breast cancer cell growth. Proc. Natl. Acad. Sci. U. S. A. *112*, E3216-3225.

Harrison, L.M., van den Hoogen, C., van Haaften, W.C.E., and Tesh, V.L. (2005). Chemokine Expression in the Monocytic Cell Line THP-1 in Response to Purified Shiga Toxin 1 and/or Lipopolysaccharides. Infect. Immun. *73*, 403–412.

Hayashi, F., Smith, K.D., Ozinsky, A., Hawn, T.R., Yi, E.C., Goodlett, D.R., Eng, J.K., Akira, S., Underhill, D.M., and Aderem, A. (2001). The innate immune response to bacterial flagellin is mediated by Toll-like receptor 5. Nature *410*, 1099–1103.

Hayashi, T., Gray, C.S., Chan, M., Tawatao, R.I., Ronacher, L., McGargill, M.A., Datta, S.K., Carson, D.A., and Corr, M. (2009). Prevention of autoimmune disease by induction of tolerance to Toll-like receptor 7. Proc. Natl. Acad. Sci. *106*, 2764.

He, S., Liang, Y., Shao, F., and Wang, X. (2011). Toll-like receptors activate programmed necrosis in macrophages through a receptor-interacting kinase-3–mediated pathway. Proc. Natl. Acad. Sci. *108*, 20054–20059.

He, T.-L., Zhang, Y.-J., Jiang, H., Li, X., Zhu, H., and Zheng, K.-L. (2015). The c-Myc–LDHA axis positively regulates aerobic glycolysis and promotes tumor progression in pancreatic cancer. Med. Oncol. Northwood Lond. Engl. *32*, 187.

Heiden, M.G.V., Cantley, L.C., and Thompson, C.B. (2009). Understanding the Warburg Effect: The Metabolic Requirements of Cell Proliferation. Science *324*, 1029–1033.

Hemmi, H., Takeuchi, O., Kawai, T., Kaisho, T., Sato, S., Sanjo, H., Matsumoto, M., Hoshino, K., Wagner, H., Takeda, K., et al. (2000). A Toll-like receptor recognizes bacterial DNA. Nature *408*, 740–745.

Hestbech, M.S., Lynge, E., Kragstrup, J., Siersma, V., Vazquez-Prada Baillet, M., and Brodersen, J. (2015). The impact of HPV vaccination on future cervical screening: a simulation study of two birth cohorts in Denmark. BMJ Open *5*.

Heytler, P.G., and Prichard, W.W. (1962). A new class of uncoupling agents — Carbonyl cyanide phenylhydrazones. Biochem. Biophys. Res. Commun. *7*, 272–275.

Higuchi, M., Honda, T., Proske, R.J., and Yeh, E.T. (1998). Regulation of reactive oxygen species-induced apoptosis and necrosis by caspase 3-like proteases. Oncogene *17*, 2753.

Ho, N., and Coomber, B.L. (2016). Hexokinase II expression is correlated with colorectal cancer prognosis. Cancer Treat. Commun. *6*, 11–16.

Holzerlandt, R., Orengo, C., Kellam, P., and Albà, M.M. (2002). Identification of New Herpesvirus Gene Homologs in the Human Genome. Genome Res. *12*, 1739–1748.

Honma, S., Kawamoto, T., Takagi, Y., Fujimoto, K., Sato, F., Noshiro, M., Kato, Y., and Honma, K. (2002). Dec1 and Dec2 are regulators of the mammalian molecular clock. Nature *419*, 841.

Hoshino, K., Takeuchi, O., Kawai, T., Sanjo, H., Ogawa, T., Takeda, Y., Takeda, K., and Akira, S. (1999). Cutting Edge: Toll-Like Receptor 4 (TLR4)-Deficient Mice Are Hyporesponsive to Lipopolysaccharide: Evidence for TLR4 as the Lps Gene Product. J. Immunol. *162*, 3749–3752.

Huang, B., Zhao, J., Li, H., He, K.-L., Chen, Y., Chen, S.-H., Mayer, L., Unkeless, J.C., and Xiong, H. (2005). Toll-like receptors on tumor cells facilitate evasion of immune surveillance. Cancer Res. *65*, 5009–5014.

Huang, B., Zhao, J., Unkeless, J.C., Feng, Z.H., and Xiong, H. (2008). TLR signaling by tumor and immune cells: a double-edged sword. Oncogene *27*, 218.

Huang, C.-Y., Fong, Y.-C., Lee, C.-Y., Chen, M.-Y., Tsai, H.-C., Hsu, H.-C., and Tang, C.-H. (2009). CCL5 increases lung cancer migration via PI3K, Akt and NF-κB pathways. Biochem. Pharmacol. *77*, 794–803.

Huang, F., Zhang, Q., Ma, H., Lv, Q., and Zhang, T. (2014). Expression of glutaminase is upregulated in colorectal cancer and of clinical significance. Int. J. Clin. Exp. Pathol. *7*, 1093–1100.

Huang, J., Shen, L., Lu, Y., Li, H., Zhang, X., Hu, D., Feng, T., and Song, F. (2012). Parallel induction of cell proliferation and inhibition of cell differentiation in hepatic progenitor cells by hepatitis B virus X gene. Int. J. Mol. Med. *30*, 842–848.

Hume, D.A., Radik, J.L., Ferber, E., and Weidemann, M.J. (1978). Aerobic glycolysis and lymphocyte transformation. Biochem. J. *174*, 703.

Innocenti, F., Cooper, G.M., Stanaway, I.B., Gamazon, E.R., Smith, J.D., Mirkov, S., Ramirez, J., Liu, W., Lin, Y.S., Moloney, C., et al. (2011). Identification, replication, and functional fine-mapping of expression quantitative trait loci in primary human liver tissue. PLoS Genet. *7*, e1002078.

Ishiji, T. (2000). Molecular Mechanism of Carcinogenesis by Human Papillomavirus-16. J. Dermatol. *27*, 73–86.

James, D.E., Brown, R., Navarro, J., and Pilch, P.F. (1988). Insulin-regulatable tissues express a unique insulin-sensitive glucose transport protein. Nature *333*, 183.

Janeway, C.A., and Medzhitov, R. (2002). Innate Immune Recognition. Annu. Rev. Immunol. *20*, 197–216.

Johnson, J.M., Castle, J., Garrett-Engele, P., Kan, Z., Loerch, P.M., Armour, C.D., Santos, R., Schadt, E.E., Stoughton, R., and Shoemaker, D.D. (2003). Genome-wide survey of human alternative pre-mRNA splicing with exon junction microarrays. Science *302*, 2141–2144.

Jones, R.G., and Thompson, C.B. Revving the Engine: Signal Transduction Fuels T Cell Activation. Immunity *27*, 173–178.

Jurk, M., Heil, F., Vollmer, J., Schetter, C., Krieg, A.M., Wagner, H., Lipford, G., and Bauer, S. (2002). Human TLR7 or TLR8 independently confer responsiveness to the antiviral compound R-848. Nat. Immunol. *3*, 499.

Kalis, C., Kanzler, B., Lembo, A., Poltorak, A., Galanos, C., and Freudenberg, M.A. (2003). Toll-like receptor 4 expression levels determine the degree of LPS-susceptibility in mice. Eur. J. Immunol. *33*, 798–805.

Kang, G.H., Lee, S., Kim, W.H., Lee, H.W., Kim, J.C., Rhyu, M.-G., and Ro, J.Y. (2002). Epstein-Barr Virus-Positive Gastric Carcinoma Demonstrates Frequent Aberrant Methylation of Multiple Genes and Constitutes CpG Island Methylator Phenotype-Positive Gastric Carcinoma. Am. J. Pathol. *160*, 787–794.

Kang, G.H., Lee, H.J., Hwang, K.S., Lee, S., Kim, J.-H., and Kim, J.-S. (2003). Aberrant CpG Island Hypermethylation of Chronic Gastritis, in Relation to Aging, Gender, Intestinal Metaplasia, and Chronic Inflammation. Am. J. Pathol. *163*, 1551–1556.

Kato, Y., Morikawa, A., Sugiyama, T., Koide, N., Jiang, G.-Z., Lwin, T., Yoshida, T., and Yokochi, T. (1997). Augmentation of Lipopolysaccharide-Induced Thymocyte Apoptosis by Interferon-γ. Cell. Immunol. *177*, 103–108.

Kaufmann, S.H., and Earnshaw, W.C. (2000). Induction of Apoptosis by Cancer Chemotherapy. Exp. Cell Res. *256*, 42–49.

Kawano, A., Tsukimoto, M., Noguchi, T., Hotta, N., Harada, H., Takenouchi, T., Kitani, H., and Kojima, S. (2012). Involvement of P2X4 receptor in P2X7 receptor-dependent cell death of mouse macrophages. Biochem. Biophys. Res. Commun. *419*, 374–380.

Kelly, B., and O'Neill, L.A. (2015). Metabolic reprogramming in macrophages and dendritic cells in innate immunity. Cell Res. *25*, 771–784.

Kerrigan, J.J., Xie, Q., Ames, R.S., and Lu, Q. (2011). Production of protein complexes via co-expression. Protein Expr. Purif. *75*, 1–14.

Khan, M.M., Ernst, O., Sun, J., Fraser, I.D.C., Ernst, R.K., Goodlett, D.R., and Nita-Lazar, A. (2018). Mass Spectrometry-based Structural Analysis and Systems Immunoproteomics Strategies for Deciphering the Host Response to Endotoxin. J. Mol. Biol. 430, 2641–2660.

Kim, B., Jung, J.W., Jung, J., Han, Y., Suh, D.H., Kim, H.S., Dhanasekaran, D.N., and Song, Y.S. (2017). PGC1α induced by reactive oxygen species contributes to chemoresistance of ovarian cancer cells. Oncotarget *8*, 60299–60311.

Kim, D.-I., Lim, S.-K., Park, M.-J., Han, H.-J., Kim, G.-Y., and Park, S.H. (2007). The involvement of phosphatidylinositol 3-kinase /Akt signaling in high glucose-induced downregulation of GLUT-1 expression in ARPE cells. Life Sci. *80*, 626–632.

Kisseleva, T., Bhattacharya, S., Braunstein, J., and Schindler, C. (2002). Signaling through the JAK/STAT pathway, recent advances and future challenges. Gene *285*, 1–24.

Klein, E., Ben-Bassat, H., Neumann, H., Ralph, P., Zeuthen, J., Polliack, A., and Vánky, F. (1976). Properties of the K562 cell line, derived from a patient with chronic myeloid leukemia. Int. J. Cancer *18*, 421–431.

Klein, J.B., Buridi, A., Coxon, P.Y., Rane, M.J., Manning, T., Kettritz, R., and McLeish, K.R. (2001). Role of extracellular signal-regulated kinase and phosphatidylinositol-3 kinase in chemoattractant and LPS delay of constitutive neutrophil apoptosis. Cell. Signal. *13*, 335–343.

Knall, C., Worthen, G.S., and Johnson, G.L. (1997). Interleukin 8-stimulated phosphatidylinositol-3-kinase activity regulates the migration of human neutrophils independent of extracellular signal-regulated kinase and p38 mitogen-activated protein kinases. Proc. Natl. Acad. Sci. *94*, 3052.

Kondoh, H., Lleonart, M.E., Nakashima, Y., Yokode, M., Tanaka, M., Bernard, D., Gil, J., and Beach, D. (2007). A High Glycolytic Flux Supports the Proliferative Potential of Murine Embryonic Stem Cells. Antioxid. Redox Signal. *9*, 293–299.

Koppenol, W.H., Bounds, P.L., and Dang, C.V. (2011). Otto Warburg's contributions to current concepts of cancer metabolism. Nat. Rev. Cancer *11*, 325.

Krasnov, G.S., Dmitriev, A.A., Lakunina, V.A., Kirpiy, A.A., and Kudryavtseva, A.V. (2013). Targeting VDAC-bound hexokinase II: a promising approach for concomitant anti-cancer therapy. Expert Opin. Ther. Targets *17*, 1221–1233.

Krawczyk, C.M., Holowka, T., Sun, J., Blagih, J., Amiel, E., DeBerardinis, R.J., Cross, J.R., Jung, E., Thompson, C.B., Jones, R.G., et al. (2010). Toll-like receptor-induced changes in glycolytic metabolism regulate dendritic cell activation. Blood *115*, 4742–4749.

Krippeit-Drews, P., Düfer, M., and Drews, G. (2000). Parallel Oscillations of Intracellular Calcium Activity and Mitochondrial Membrane Potential in Mouse Pancreatic B-Cells. Biochem. Biophys. Res. Commun. *267*, 179–183.

Krisher Rebecca L., and Prather Randall S. (2012). A role for the Warburg effect in preimplantation embryo development: Metabolic modification to support rapid cell proliferation. Mol. Reprod. Dev. *79*, 311–320.

Kuai, W.-X., Wang, Q., Yang, X.-Z., Zhao, Y., Yu, R., and Tang, X.-J. (2012). Interleukin-8 associates with adhesion, migration, invasion and chemosensitivity of human gastric cancer cells. World J. Gastroenterol. WJG *18*, 979–985.

Kuang, R., Jahangiri, A., Mascharak, S., Nguyen, A., Chandra, A., Flanigan, P.M., Yagnik, G., Wagner, J.R., De Lay, M., Carrera, D., et al. (2016). GLUT3 upregulation promotes metabolic reprogramming associated with antiangiogenic therapy resistance. JCI Insight *2*, e88815.

Kupsa, T., Milos Horacek, J., and Jebavy, L. (2012). The role of cytokines in acute myeloid leukemia: A systematic review. Biomed. Pap. *156*, 291–301.

Lamb, R., Ozsvari, B., Lisanti, C.L., Tanowitz, H.B., Howell, A., Martinez-Outschoorn, U.E., Sotgia, F., and Lisanti, M.P. (2015). Antibiotics that target mitochondria effectively eradicate cancer stem cells, across multiple tumor types: Treating cancer like an infectious disease. Oncotarget *6*, 4569–4584.

Landskron, G., De la Fuente, M., Thuwajit, P., Thuwajit, C., and Hermoso, M.A. (2014). Chronic Inflammation and Cytokines in the Tumor Microenvironment. J. Immunol. Res. *2014*, e149185.

Lane, D.P. (1992). Cancer. p53, guardian of the genome. Nature *358*, 15–16.

Lardner, A. (2001). The effects of extracellular pH on immune function. J. Leukoc. Biol. *69*, 522–530.

Le, A., Cooper, C.R., Gouw, A.M., Dinavahi, R., Maitra, A., Deck, L.M., Royer, R.E., Vander Jagt, D.L., Semenza, G.L., and Dang, C.V. (2010). Inhibition of lactate dehydrogenase A induces oxidative stress and inhibits tumor progression. Proc. Natl. Acad. Sci. U. S. A. *107*, 2037–2042.

Lee, S.M.Y., Kok, K.-H., Jaume, M., Cheung, T.K.W., Yip, T.-F., Lai, J.C.C., Guan, Y., Webster, R.G., Jin, D.-Y., and Peiris, J.S.M. (2014). Toll-like receptor 10 is involved in induction of innate immune responses to influenza virus infection. Proc. Natl. Acad. Sci. U. S. A. *111*, 3793–3798.

Lemaitre, B. (2004). The road to Toll. *4*, 521.

Lemaitre, B., Nicolas, E., Michaut, L., Reichhart, J.-M., and Hoffmann, J.A. (1996). The Dorsoventral Regulatory Gene Cassette spätzle/Toll/cactus Controls the Potent Antifungal Response in Drosophila Adults. Cell *86*, 973–983.

Levine, A.J. (1997). p53, the cellular gatekeeper for growth and division. Cell *88*, 323–331.

Levine, A.J., and Puzio-Kuter, A.M. (2010). The Control of the Metabolic Switch in Cancers by Oncogenes and Tumor Suppressor Genes. Science *330*, 1340–1344.

Li, L., Chen, L., Zhang, W., Liao, Y., Chen, J., Shi, Y., and Luo, S. (2017). Serum cytokine profile in patients with breast cancer. Cytokine Signal. Cancer *89*, 173–178.

Li, T., Hu, J., Thomas, J.A., and Li, L. (2005). Differential induction of apoptosis by LPS and taxol in monocytic cells. Mol. Immunol. *42*, 1049–1055.

Li, T., Kon, N., Jiang, L., Tan, M., Ludwig, T., Zhao, Y., Baer, R., and Gu, W. (2012). Tumor Suppression in the Absence of p53-Mediated Cell-Cycle Arrest, Apoptosis, and Senescence. Cell *149*, 1269–1283.

Liao, J.B. (2006). Viruses and Human Cancer. Yale J. Biol. Med. *79*, 115–122.

Lien, M.-Y., Lin, C.-W., Tsai, H.-C., Chen, Y.-T., Tsai, M.-H., Hua, C.-H., Yang, S.-F., and Tang, C.-H. (2017). Impact of CCL4 gene polymorphisms and environmental factors on oral cancer development and clinical characteristics. Oncotarget *8*, 31424–31434.

Lin, C.-C., Bradstreet, T.R., Schwarzkopf, E.A., Sim, J., Carrero, J.A., Chou, C., Cook, L.E., Egawa, T., Taneja, R., Murphy, T.L., et al. (2014). Bhlhe40 controls cytokine production by T cells and is essential for pathogenicity in autoimmune neuroinflammation. Nat. Commun. *5*, 3551.

Lindner, I., Kharfan-Dabaja, M.A., Ayala, E., Kolonias, D., Carlson, L.M., Beazer-Barclay, Y., Scherf, U., Hnatyszyn, J.H., and Lee, K.P. (2003). Induced Dendritic Cell Differentiation of Chronic Myeloid Leukemia Blasts Is Associated with Down-Regulation of BCR-ABL. J. Immunol. *171*, 1780.

Liu, J., Zhang, C., Lin, M., Zhu, W., Liang, Y., Hong, X., Zhao, Y., Young, K.H., Hu, W., and Feng, Z. (2014). Glutaminase 2 negatively regulates the PI3K/AKT signaling and shows tumor suppression activity in human hepatocellular carcinoma. Oncotarget *5*, 2635–2647.

Liu, Y., Xiang, F., Huang, Y., Shi, L., Hu, C., Yang, Y., Wang, D., He, N., Tao, K., Wu, K., et al. (2017). Interleukin-22 promotes aerobic glycolysis associated with tumor progression via targeting hexokinase-2 in human colon cancer cells. Oncotarget *8*, 25372–25383.

Locati, M., Deuschle, U., Massardi, M.L., Martinez, F.O., Sironi, M., Sozzani, S., Bartfai, T., and Mantovani, A. (2002). Analysis of the Gene Expression Profile Activated by the CC Chemokine Ligand 5/RANTES and by Lipopolysaccharide in Human Monocytes. J. Immunol. *168*, 3557.

Lodish, H., Berk, A., Zipursky, S.L., Matsudaira, P., Baltimore, D., and Darnell, J. (2000). Oxidation of Glucose and Fatty Acids to CO2.

Loiarro, M., Capolunghi, F., Fantò, N., Gallo, G., Campo, S., Arseni, B., Carsetti, R., Carminati, P., De Santis, R., Ruggiero, V., et al. (2007). Pivotal Advance: Inhibition of MyD88 dimerization and recruitment of IRAK1 and IRAK4 by a novel peptidomimetic compound. J. Leukoc. Biol. *82*, 801–810.

Long Haixia, Xie Rongkai, Xiang Tong, Zhao Zhongquan, Lin Sheng, Liang Zhiqing, Chen Zhengtang, and Zhu Bo (2012). Autocrine CCL5 Signaling Promotes Invasion and Migration of CD133+ Ovarian Cancer Stem-Like Cells via NF-κB-Mediated MMP-9 Upregulation. STEM CELLS *30*, 2309–2319.

Lozzio, C.B., and Lozzio, B.B. (1975). Human chronic myelogenous leukemia cell-line with positive Philadelphia chromosome. Blood *45*, 321–334.

Lu, H., Forbes, R.A., and Verma, A. (2002). Hypoxia-inducible Factor 1 Activation by Aerobic Glycolysis Implicates the Warburg Effect in Carcinogenesis. J. Biol. Chem. *277*, 23111–23115.

Lv, D., Zhang, Y., Kim, H.-J., Zhang, L., and Ma, X. (2013). CCL5 as a potential immunotherapeutic target in triple-negative breast cancer. Cell. Mol. Immunol. *10*, 303–310.

Mangan, D.F., Welch, G.R., and Wahl, S.M. (1991). Lipopolysaccharide, tumor necrosis factor-alpha, and IL-1 beta prevent programmed cell death (apoptosis) in human peripheral blood monocytes. J. Immunol. *146*, 1541.

Mathupala, S.P., Heese, C., and Pedersen, P.L. (1997). Glucose catabolism in cancer cells. The type II hexokinase promoter contains functionally active response elements for the tumor suppressor p53. J. Biol. Chem. *272*, 22776–22780.

Matoba, S., Kang, J.-G., Patino, W.D., Wragg, A., Boehm, M., Gavrilova, O., Hurley, P.J., Bunz, F., and Hwang, P.M. (2006). p53 regulates mitochondrial respiration. Science *312*, 1650–1653.

Matsuura, M. (2013). Structural Modifications of Bacterial Lipopolysaccharide that Facilitate Gram-Negative Bacteria Evasion of Host Innate Immunity. Front. Immunol. *4*, 109–109.

McKercher, S.R., Torbett, B.E., Anderson, K.L., Henkel, G.W., Vestal, D.J., Baribault, H., Klemsz, M., Feeney, A.J., Wu, G.E., Paige, C.J., et al. (1996). Targeted disruption of the PU.1 gene results in multiple hematopoietic abnormalities. EMBO J. *15*, 5647–5658.

McLaughlin-Drubin, M.E., and Munger, K. (2008). Viruses associated with human cancer. Biochim. Biophys. Acta BBA - Mol. Basis Dis. *1782*, 127–150.

Medzhitov, R. (2001). Toll-like receptors and innate immunity. *1*, 135.

Mesri, E.A., Cesarman, E., and Boshoff, C. (2010). Kaposi's sarcoma and its associated herpesvirus. Nat. Rev. Cancer *10*, 707.

Miao Ping, Sheng Shile, Sun Xiaoguang, Liu Jianjun, and Huang Gang (2013). Lactate dehydrogenase a in cancer: A promising target for diagnosis and therapy. IUBMB Life *65*, 904–910.

Mitchell, P. (1974). A chemiosmotic molecular mechanism for proton-translocating adenosine triphosphatases. FEBS Lett. *43*, 189–194.

Mitchell, P. (2011). Chemiosmotic coupling in oxidative and photosynthetic phosphorylation. Spec. Sect. Peter Mitchell - 50th Anniv. Chemiosmotic Theory *1807*, 1507–1538.

Mitchell, P., and Moyle, J. (1967). Chemiosmotic Hypothesis of Oxidative Phosphorylation. Nature *213*, 137.

Mittal, M., Siddiqui, M.R., Tran, K., Reddy, S.P., and Malik, A.B. (2014). Reactive Oxygen Species in Inflammation and Tissue Injury. Antioxid. Redox Signal. *20*, 1126–1167.

Monchusi, B., and Ntwasa, M. (2017). Methyl pyruvate protects a normal lung fibroblast cell line from irinotecan-induced cell death: Potential use as adjunctive to chemotherapy. PLOS ONE *12*, e0182789.

Morisato, D., and Anderson, K.V. (1994). The spätzle gene encodes a component of the extracellular signaling pathway establishing the dorsal-ventral pattern of the Drosophila embryo. Cell *76*, 677–688.

Morrison, D.C., and Jacobs, D.M. (1976). Binding of polymyxin B to the lipid A portion of bacterial lipopolysaccharides. Immunochemistry *13*, 813–818.

Mostafa, M.H., Sheweita, S.A., and O'Connor, P.J. (1999). Relationship between Schistosomiasis and Bladder Cancer. Clin. Microbiol. Rev. *12*, 97–111.

Mostafavi, S., Ray, D., Warde-Farley, D., Grouios, C., and Morris, Q. (2008). GeneMANIA: a real-time multiple association network integration algorithm for predicting gene function. Genome Biol. *9*, S4–S4.

Mühl, H., Nold, M., Chang, J.H., Frank, S., Eberhardt, W., and Pfeilschifter, J. (1999). Expression and release of chemokines associated with apoptotic cell death in human promonocytic U937 cells and peripheral blood mononuclear cells. Eur. J. Immunol. *29*, 3225–3235.

Münger, K., Baldwin, A., Edwards, K.M., Hayakawa, H., Nguyen, C.L., Owens, M., Grace, M., and Huh, K. (2004). Mechanisms of Human Papillomavirus-Induced Oncogenesis. J. Virol. *78*, 11451–11460.

Murooka, T.T., Wong, M.M., Rahbar, R., Majchrzak-Kita, B., Proudfoot, A.E.I., and Fish, E.N. (2006). CCL5-CCR5-mediated Apoptosis in T Cells requirement for glycosaminoglycan binding and CCL5 aggregation. J. Biol. Chem. *281*, 25184–25194.

Muzio, M., Bosisio, D., Polentarutti, N., D'amico, G., Stoppacciaro, A., Mancinelli, R., van't Veer, C., Penton-Rol, G., Ruco, L.P., Allavena, P., et al. (2000). Differential Expression and Regulation of Toll-Like Receptors (TLR) in Human Leukocytes: Selective Expression of TLR3 in Dendritic Cells. J. Immunol. *164*, 5998.

Newsholme, P., Gordon, S., and Newsholme, E.A. (1987). Rates of utilization and fates of glucose, glutamine, pyruvate, fatty acids and ketone bodies by mouse macrophages. Biochem. J. *242*, 631.

Nishi, K., Oda, T., Takabuchi, S., Oda, S., Fukuda, K., Adachi, T., Semenza, G.L., Shingu, K., and Hirota, K. (2008). LPS Induces Hypoxia-Inducible Factor 1 Activation in Macrophage-Differentiated Cells in a Reactive Oxygen Species–Dependent Manner. Antioxid. Redox Signal. *10*, 983–996.

Noble, C.L., Abbas, A.R., Cornelius, J., Lees, C.W., Ho, G.-T., Toy, K., Modrusan, Z., Pal, N., Zhong, F., Chalasani, S., et al. (2008). Regional variation in gene expression in the healthy colon is dysregulated in ulcerative colitis. Gut *57*, 1398–1405.

Obach, M., Navarro-Sabaté, À., Caro, J., Kong, X., Duran, J., Gómez, M., Perales, J.C., Ventura, F., Rosa, J.L., and Bartrons, R. (2004). 6-Phosphofructo-2-kinase (pfkfb3) Gene Promoter Contains Hypoxia-inducible Factor-1 Binding Sites Necessary for Transactivation in Response to Hypoxia. J. Biol. Chem. *279*, 53562–53570.

O'Connor, P.M., Lapointe, T.K., Beck, P.L., and Buret, A.G. (2010). Mechanisms by which inflammation may increase intestinal cancer risk in inflammatory bowel disease. Inflamm. Bowel Dis. *16*, 1411–1420.

Oka, Y., Asano, T., Shibasaki, Y., Lin, J.-L., Tsukuda, K., Katagiri, H., Akanuma, Y., and Takaku, F. (1990). C-terminal truncated glucose transporter is locked into an inward-facing form without transport activity. Nature *345*, 550.

Olsson Inge, Bergh Gösta, Ehinger Mats, and Gullberg Urban (1996). Cell differentiation in acute myeloid leukemia. Eur. J. Haematol. *57*, 1–16.

O'Neill, L.A., and Pearce, E.J. (2016). Immunometabolism governs dendritic cell and macrophage function. J. Exp. Med. *213*, 15–23.

O'Neill, L.A.J., Bryant, C.E., and Doyle, S.L. (2009). Therapeutic Targeting of Toll-Like Receptors for Infectious and Inflammatory Diseases and Cancer. Pharmacol. Rev. *61*, 177–197.

Palsson-McDermott, E.M., Doyle, S.L., McGettrick, A.F., Hardy, M., Husebye, H., Banahan, K., Gong, M., Golenbock, D., Espevik, T., and O'Neill, L.A.J. (2009). TAG, a splice variant of the adaptor TRAM, negatively regulates the adaptor MyD88–independent TLR4 pathway. Nat. Immunol. *10*, 579.

Pannone, G., Zamparese, R., Pace, M., Pedicillo, M.C., Cagiano, S., Somma, P., Errico, M.E., Donofrio, V., Franco, R., De Chiara, A., et al. (2014). The role of EBV in the pathogenesis of Burkitt's Lymphoma: an Italian hospital-based survey. Infect. Agent. Cancer *9*, 34.

Parkin, D.M. (2006). The global health burden of infection-associated cancers in the year 2002. Int. J. Cancer J. Int. Cancer *118*, 3030–3044.

Pastorino, J.G., Shulga, N., and Hoek, J.B. (2002). Mitochondrial Binding of Hexokinase II Inhibits Bax-induced Cytochrome c Release and Apoptosis. J. Biol. Chem. *277*, 7610–7618.

Patra, K.C., Wang, Q., Bhaskar, P.T., Miller, L., Wang, Z., Wheaton, W., Chandel, N., Laakso, M., Muller, W.J., Allen, E.L., et al. (2013). Hexokinase 2 is required for tumor initiation and maintenance and its systemic deletion is therapeutic in mouse models of cancer. Cancer Cell *24*, 213–228.

Pattle, S.B., and Farrell, P.J. (2006). The role of Epstein–Barr virus in cancer. Expert Opin. Biol. Ther. *6*, 1193–1205.

Peek, R.M., and Crabtree, J.E. (2006). Helicobacter infection and gastric neoplasia. J. Pathol. *208*, 233–248.

Peña-Castillo, L., Tasan, M., Myers, C.L., Lee, H., Joshi, T., Zhang, C., Guan, Y., Leone, M., Pagnani, A., Kim, W.K., et al. (2008). A critical assessment of Mus musculus gene function prediction using integrated genomic evidence. Genome Biol. *9*, S2–S2.

Perry, S.W., Norman, J.P., Barbieri, J., Brown, E.B., and Gelbard, H.A. (2011). Mitochondrial membrane potential probes and the proton gradient: a practical usage guide. BioTechniques *50*, 98–115.

Petitjean, A., Achatz, M.I.W., Borresen-Dale, A.L., Hainaut, P., and Olivier, M. (2007). TP53 mutations in human cancers: functional selection and impact on cancer prognosis and outcomes. Oncogene *26*, 2157–2165.

Pfeiffer, T., Schuster, S., and Bonhoeffer, S. (2001). Cooperation and competition in the evolution of ATP-producing pathways. Science *292*, 504–507.

Pinheiro, C., Reis, R.M., Ricardo, S., Longatto-Filho, A., Schmitt, F., Baltazar, F., Pinheiro, C., Reis, R.M., Ricardo, S., Longatto-Filho, A., et al. (2010). Expression of Monocarboxylate Transporters 1, 2, and 4 in Human Tumours and Their Association with CD147 and CD44, Expression of Monocarboxylate Transporters 1, 2, and 4 in Human Tumours and Their Association with CD147 and CD44. BioMed Res. Int. BioMed Res. Int. *2010*, *2010*, e427694.

Plummer, M., de Martel, C., Vignat, J., Ferlay, J., Bray, F., and Franceschi, S. (2016). Global burden of cancers attributable to infections in 2012: a synthetic analysis. Lancet Glob. Health *4*, e609–e616.

Poteet, E., Choudhury, G.R., Winters, A., Li, W., Ryou, M.-G., Liu, R., Tang, L., Ghorpade, A., Wen, Y., Yuan, F., et al. (2013). Reversing the Warburg Effect as a Treatment for Glioblastoma. J. Biol. Chem. *288*, 9153–9164.

Prêle, C.M., Woodward, E.A., Bisley, J., Keith-Magee, A., Nicholson, S.E., and Hart, P.H. (2008). SOCS1 regulates the IFN but not NFκB pathway in TLR-stimulated human monocytes and macrophages. J. Immunol. Baltim. Md 1950 *181*, 8018–8026.

Principe, M., Ceruti, P., Shih, N.-Y., Chattaragada, M.S., Rolla, S., Conti, L., Bestagno, M., Zentilin, L., Yang, S.-H., Migliorini, P., et al. (2015). Targeting of surface alpha-enolase inhibits the invasiveness of pancreatic cancer cells. Oncotarget *6*, 11098–11113.

Pugin, J., Schürer-Maly, C.C., Leturcq, D., Moriarty, A., Ulevitch, R.J., and Tobias, P.S. (1993). Lipopolysaccharide activation of human endothelial and epithelial cells is mediated by lipopolysaccharide-binding protein and soluble CD14. Proc. Natl. Acad. Sci. *90*, 2744.

Puram, R.V., Kowalczyk, M.S., de Boer, C.G., Schneider, R.K., Miller, P.G., McConkey, M., Tothova, Z., Tejero, H., Heckl, D., Järås, M., et al. (2016). Core circadian clock genes regulate leukemia stem cells in AML. Cell *165*, 303–316.

Puzio-Kuter, A.M. (2011). The Role of p53 in Metabolic Regulation. Genes Cancer *2*, 385–391.

Qureshi, S.T., Larivière, L., Leveque, G., Clermont, S., Moore, K.J., Gros, P., and Malo, D. (1999). Endotoxin-tolerant Mice Have Mutations in Toll-like Receptor 4 (Tlr4). J. Exp. Med. *189*, 615–625.

Rahman, S., Al-hallaj, A.-S., Nedhi, A., Gmati, G., Ahmed, khadega, Jama, H.A., Trivilegio, T., Mashour, A., Askar, A.A., and Boudjelal, M. (2017). Differential Expression of Circadian Genes in Leukemia and a Possible Role for Sirt1 in Restoring the Circadian Clock in Chronic Myeloid Leukemia. J. Circadian Rhythms *15*, 3.

Ramaswamy, S., Tamayo, P., Rifkin, R., Mukherjee, S., Yeang, C.H., Angelo, M., Ladd, C., Reich, M., Latulippe, E., Mesirov, J.P., et al. (2001). Multiclass cancer diagnosis using tumor gene expression signatures. Proc. Natl. Acad. Sci. U. S. A. *98*, 15149–15154.

Rambau, P.F., Chalya, P.L., and Jackson, K. (2013). Schistosomiasis and urinary bladder cancer in North Western Tanzania: a retrospective review of 185 patients. Infect. Agent. Cancer *8*, 19–19.

Reczek, C.R., and Chandel, N.S. (2017). The Two Faces of Reactive Oxygen Species in Cancer. Annu. Rev. Cancer Biol. *1*, 79–98.

Rieger, K.E., Hong, W.-J., Tusher, V.G., Tang, J., Tibshirani, R., and Chu, G. (2004). Toxicity from radiation therapy associated with abnormal transcriptional responses to DNA damage. Proc. Natl. Acad. Sci. U. S. A. *101*, 6635–6640.

Rijksen, G., Staal, G.E.J., Beks, P.J., Streefkerk, M., and Akkerman, J.W.N. (1982). Compartmentation of hexokinase in human blood cells characterization of soluble and particulate enzymes. Biochim. Biophys. Acta BBA - Gen. Subj. *719*, 431–437.

Rogatzki, M.J., Ferguson, B.S., Goodwin, M.L., and Gladden, L.B. (2015). Lactate is always the end product of glycolysis. Front. Neurosci. *9*, 22.

Roth, R.B., Hevezi, P., Lee, J., Willhite, D., Lechner, S.M., Foster, A.C., and Zlotnik, A. (2006). Gene expression analyses reveal molecular relationships among 20 regions of the human CNS. Neurogenetics *7*, 67–80.

Rutz, H.P., and Little, J.B. (1995). Exogenous lactate interferes with cell-cycle control in Balb3T3 mouse fibroblasts. Int. J. Radiat. Oncol. *31*, 525–528.

Sag, D., Carling, D., Stout, R.D., and Suttles, J. (2008). Adenosine 5′-Monophosphate-Activated Protein Kinase Promotes Macrophage Polarization to an Anti-Inflammatory Functional Phenotype. J. Immunol. *181*, 8633.

Samoszuk, M., and Nansen, L. (1990). Detection of interleukin-5 messenger RNA in Reed-Sternberg cells of Hodgkin's disease with eosinophilia. Blood *75*, 13.

Sanchez, X., Suetomi, K., Cousins-Hodges, B., Horton, J.K., and Navarro, J. (1998). CXC Chemokines Suppress Proliferation of Myeloid Progenitor Cells by Activation of the CXC Chemokine Receptor 2. J. Immunol. *160*, 906.

Sato, F., Bhawal, U.K., Yoshimura, T., and Muragaki, Y. (2016). DEC1 and DEC2 Crosstalk between Circadian Rhythm and Tumor Progression. J. Cancer *7*, 153–159.

Schadt, E.E., Edwards, S.W., GuhaThakurta, D., Holder, D., Ying, L., Svetnik, V., Leonardson, A., Hart, K.W., Russell, A., Li, G., et al. (2004). A comprehensive transcript index of the human genome generated using microarrays and computational approaches. Genome Biol. *5*, R73.

Schneider, D.S., Jin, Y., Morisato, D., and Anderson, K.V. (1994). A processed form of the Spatzle protein defines dorsal-ventral polarity in the Drosophila embryo. Development *120*, 1243.

Schwartzenberg-Bar-Yoseph, F., Armoni, M., and Karnieli, E. (2004). The tumor suppressor p53 down-regulates glucose transporters GLUT1 and GLUT4 gene expression. Cancer Res. *64*, 2627–2633.

Segura, M., Vadeboncoeur, N., and Gottschalk, M. (2002). CD14-dependent and -independent cytokine and chemokine production by human THP-1 monocytes stimulated by Streptococcus suis capsular type 2. Clin. Exp. Immunol. *127*, 243–254.

Semenza, G.L., Jiang, B.-H., Leung, S.W., Passantino, R., Concordet, J.-P., Maire, P., and Giallongo, A. (1996). Hypoxia Response Elements in the Aldolase A, Enolase 1, and Lactate Dehydrogenase A Gene Promoters Contain Essential Binding Sites for Hypoxia-inducible Factor 1. J. Biol. Chem. *271*, 32529–32537.

Shi, M., Chen, X., Ye, K., Yao, Y., and Li, Y. (2016). Application potential of toll-like receptors in cancer immunotherapy: Systematic review. Medicine (Baltimore) *95*, e3951.

Shim, H., Dolde, C., Lewis, B.C., Wu, C.S., Dang, G., Jungmann, R.A., Dalla-Favera, R., and Dang, C.V. (1997). c-Myc transactivation of LDH-A: implications for tumor metabolism and growth. Proc. Natl. Acad. Sci. U. S. A. *94*, 6658–6663.

Shime, H., Yabu, M., Akazawa, T., Kodama, K., Matsumoto, M., Seya, T., and Inoue, N. (2008). Tumor-secreted lactic acid promotes IL-23/IL-17 proinflammatory pathway. J. Immunol. Baltim. Md 1950 *180*, 7175–7183.

Shiraishi, T., Verdone, J.E., Huang, J., Kahlert, U.D., Hernandez, J.R., Torga, G., Zarif, J.C., Epstein, T., Gatenby, R., McCartney, A., et al. (2015). Glycolysis is the primary bioenergetic pathway for cell motility and cytoskeletal remodeling in human prostate and breast cancer cells. Oncotarget *6*, 130–143.

Shukla, S., MacLennan, G.T., Hartman, D.J., Fu, P., Resnick, M.I., and Gupta, S. (2007). Activation of PI3K-Akt signaling pathway promotes prostate cancer cell invasion. Int. J. Cancer *121*, 1424–1432.

Siddiqui, I.A., Sanna, V., Ahmad, N., Sechi, M., and Mukhtar, H. (2015). Resveratrol nanoformulation for cancer prevention and therapy. Ann. N. Y. Acad. Sci. *1348*, 20–31.

Simon, F., and Fernández, R. (2009). Early lipopolysaccharide-induced reactive oxygen species production evokes necrotic cell death in human umbilical vein endothelial cells. J. Hypertens. *27*.

Simon, H.U., Haj-Yehia, A., and Levi-Schaffer, F. (2000). Role of reactive oxygen species (ROS) in apoptosis induction. Apoptosis Int. J. Program. Cell Death *5*, 415–418.

Singh, S.K., Mishra, M.K., Eltoum, I.-E.A., Bae, S., Lillard, J.W., and Singh, R. (2018). CCR5/CCL5 axis interaction promotes migratory and invasiveness of pancreatic cancer cells. Sci. Rep. *8*, 1323.

Smith, T.A.D. (2000). Mammalian hexokinases and their abnormal expression in cancer. Br. J. Biomed. Sci. *57*, 170–178.

Spirig, R., Djafarzadeh, S., Regueira, T., Shaw, S.G., von Garnier, C., Takala, J., Jakob, S.M., Rieben, R., and Lepper, P.M. (2010). Effects of TLR agonists on the hypoxia-regulated transcription factor HIF-1α and dendritic cell maturation under normoxic conditions. PLoS ONE *5*.

Straus, D.S. (2013). TNFα and IL-17 cooperatively stimulate glucose metabolism and growth factor production in human colorectal cancer cells. Mol. Cancer *12*, 78.

Suganuma, K., Miwa, H., Imai, N., Shikami, M., Gotou, M., Goto, M., Mizuno, S., Takahashi, M., Yamamoto, H., Hiramatsu, A., et al. (2010). Energy metabolism of leukemia cells: glycolysis versus oxidative phosphorylation. Leuk. Lymphoma *51*, 2112–2119.

Sullivan, K.E., Reddy, A.B.M., Dietzmann, K., Suriano, A.R., Kocieda, V.P., Stewart, M., and Bhatia, M. (2007). Epigenetic regulation of tumor necrosis factor alpha. Mol. Cell. Biol. *27*, 5147–5160.

Sun, Q., Chen, X., Ma, J., Peng, H., Wang, F., Zha, X., Wang, Y., Jing, Y., Yang, H., Chen, R., et al. (2011). Mammalian target of rapamycin up-regulation of pyruvate kinase isoenzyme type M2 is critical for aerobic glycolysis and tumor growth. Proc. Natl. Acad. Sci. *108*, 4129–4134.

Suzuki, T., Kobayashi, M., Isatsu, K., Nishihara, T., Aiuchi, T., Nakaya, K., and Hasegawa, K. (2004). Mechanisms Involved in Apoptosis of Human Macrophages Induced by Lipopolysaccharide from Actinobacillus actinomycetemcomitans in the Presence of Cycloheximide. Infect. Immun. *72*, 1856–1865.

Takeda, K., and Akira, S. (2005). Toll-like receptors in innate immunity. Int. Immunol. *17*, 1–14.

Takeda, K., Kaisho, T., and Akira, S. (2003). Toll-Like Receptors. Annu. Rev. Immunol. *21*, 335–376.

Takeuchi, O., Sato, S., Horiuchi, T., Hoshino, K., Takeda, K., Dong, Z., Modlin, R.L., and Akira, S. (2002). Cutting edge: Role of Toll-like receptor 1 in mediating immune response to microbial lipoproteins. J. Immunol. *169*, 10–14.

Taylor, D.J., Faragher, E.B., and Evanson, J.M. (1992). Inflammatory cytokines stimulate glucose uptake and glycolysis but reduce glucose oxidation in human dermal fibroblasts in vitro. Circ. Shock *37*, 105–110.

Tedla, N., Palladinetti, P., Wakefield, D., and Lloyd, A. (1999). Abundant expression of chemokines in malignant and infective human lymphadenopathies. Cytokine *11*, 531–540.

TeSlaa, T., and Teitell, M.A. (2014). Techniques to Monitor Glycolysis. Methods Enzymol. *542*, 91–114.

The Cancer Association of South Africa. (2018). World Cancer Statistics. Accessed: 8 January 2019 https://www.cansa.org.za/global-cancer-statistics/

Thompson, M.P., and Kurzrock, R. (2004). Epstein-Barr Virus and Cancer. Clin. Cancer Res. *10*, 803.

Tobias, P.S., Soldau, K., Kline, L., Lee, J.D., Kato, K., Martin, T.P., and Ulevitch, R.J. (1993). Cross-linking of lipopolysaccharide (LPS) to CD14 on THP-1 cells mediated by LPS-binding protein. J. Immunol. *150*, 3011.

Tsuchiya, S., Yamabe, M., Yamaguchi, Y., Kobayashi, Y., Konno, T., and Tada, K. (1980). Establishment and characterization of a human acute monocytic leukemia cell line (THP-1). Int. J. Cancer *26*, 171–176.

Tsukishiro, S., Suzumori, N., Nishikawa, H., Arakawa, A., and Suzumori, K. (2006). Elevated serum RANTES levels in patients with ovarian cancer correlate with the extent of the disorder. Gynecol. Oncol. *102*, 542–545.

Tzeng, Y.-L., Datta, A., Kolli, V.K., Carlson, R.W., and Stephens, D.S. (2002). Endotoxin of Neisseria meningitidis Composed Only of Intact Lipid A: Inactivation of the Meningococcal 3-Deoxy-d-Manno-Octulosonic Acid Transferase. J. Bacteriol. *184*, 2379–2388.

Ushio-Fukai, M., and Nakamura, Y. (2008). Reactive Oxygen Species and Angiogenesis: NADPH Oxidase as Target for Cancer Therapy. Cancer Lett. *266*, 37–52.

Valente, L.J., Gray, D.H.D., Michalak, E.M., Pinon-Hofbauer, J., Egle, A., Scott, C.L., Janic, A., and Strasser, A. (2013). p53 Efficiently Suppresses Tumor Development in the Complete Absence of Its Cell-Cycle Inhibitory and Proapoptotic Effectors p21, Puma, and Noxa. Cell Rep. *3*, 1339–1345.

Valle, A., Oliver, J., and Roca, P. (2010). Role of Uncoupling Proteins in Cancer. Cancers *2*, 567–591.

Vander Heiden, M.G., Cantley, L.C., and Thompson, C.B. (2009). Understanding the Warburg effect: the metabolic requirements of cell proliferation. Science *324*, 1029–1033.

Vats, D., Mukundan, L., Odegaard, J.I., Zhang, L., Smith, K.L., Morel, C.R., Greaves, D.R., Murray, P.J., and Chawla, A. Oxidative metabolism and PGC-1β attenuate macrophage-mediated inflammation. Cell Metab. *4*, 13–24.

Vattimo, M. de F.F., Watanabe, M., da Fonseca, C.D., Neiva, L.B. de M., Pessoa, E.A., and Borges, F.T. (2016). Polymyxin B Nephrotoxicity: From Organ to Cell Damage. PLoS ONE *11*, e0161057.

Vaughan, R.A., Garcia-Smith, R., Dorsey, J., Griffith, J.K., Bisoffi, M., and Trujillo, K.A. (2013). Tumor necrosis factor alpha induces Warburg-like metabolism and is reversed by anti-inflammatory curcumin in breast epithelial cells. Int. J. Cancer *133*, 2504–2510.

Vetrano, S., Borroni, E.M., Sarukhan, A., Savino, B., Bonecchi, R., Correale, C., Arena, V., Fantini, M., Roncalli, M., Malesci, A., et al. (2010). The lymphatic system controls intestinal inflammation and inflammation-associated Colon Cancer through the chemokine decoy receptor D6. Gut *59*, 197–206.

Vicari, A.P., and Caux, C. (2002). Chemokines in cancer. Cytokines Tumor Immun. Immunother. *13*, 143–154.

Viljanen, P., and Vaara, M. (1984). Susceptibility of gram-negative bacteria to polymyxin B nonapeptide. Antimicrob. Agents Chemother. *25*, 701–705.

Vogelstein, B., Lane, D., and Levine, A.J. (2000). Surfing the p53 network. Nature *408*, 307–310.

Vousden, K.H., and Ryan, K.M. (2009). p53 and metabolism. Nat. Rev. Cancer *9*, 691–700.

Wang, D., and Richmond, A. (2001). Nuclear Factor-κB Activation by the CXC Chemokine Melanoma Growth-stimulatory Activity/Growth-regulated Protein Involves the MEKK1/p38 Mitogen-activated Protein Kinase Pathway. J. Biol. Chem. *276*, 3650–3659.

Wang, I.X., Ramrattan, G., and Cheung, V.G. (2015). Genetic variation in insulin-induced kinase signaling. Mol. Syst. Biol. *11*, 820.

Wang, K., Wang, P., Shi, J., Zhu, X., He, M., Jia, X., Yang, X., Qiu, F., Jin, W., Qian, M., et al. (2010). PML/RARα Targets Promoter Regions Containing PU.1 Consensus and RARE Half Sites in Acute Promyelocytic Leukemia. Cancer Cell *17*, 186–197.

Wang, Q., Diskin, S., Rappaport, E., Attiyeh, E., Mosse, Y., Shue, D., Seiser, E., Jagannathan, J., Shusterman, S., Bansal, M., et al. (2006). Integrative genomics identifies distinct molecular classes of neuroblastoma and shows that multiple genes are targeted by regional alterations in DNA copy number. Cancer Res. *66*, 6050–6062.

Wang, T., Marquardt, C., and Foker, J. (1976). Aerobic glycolysis during lymphocyte proliferation. Nature *261*, 702.

Wang, X., Zhang, F., and Wu, X.-R. (2017). Inhibition of Pyruvate Kinase M2 Markedly Reduces Chemoresistance of Advanced Bladder Cancer to Cisplatin. *7*, 45983.

Wang, Y., Liu, T., Yang, N., Xu, S., Li, X., and Wang, D. (2016). Hypoxia and macrophages promote glioblastoma invasion by the CCL4-CCR5 axis. Oncol. Rep. *36*, 3522–3528.

Warburg, O. (1956). On the origin of cancer cells. Science *123*, 309–314.

Ward, P.S., and Thompson, C.B. (2012). Metabolic Reprogramming: A Cancer Hallmark Even Warburg Did Not Anticipate. Cancer Cell *21*, 297–308.

Warde-Farley, D., Donaldson, S.L., Comes, O., Zuberi, K., Badrawi, R., Chao, P., Franz, M., Grouios, C., Kazi, F., Lopes, C.T., et al. (2010). The GeneMANIA prediction server: biological network integration for gene prioritization and predicting gene function. Nucleic Acids Res. *38*, W214–W220.

Waris, G., and Ahsan, H. (2006). Reactive oxygen species: role in the development of cancer and various chronic conditions. J. Carcinog. *5*, 14–14.

Wataha, J.C., Ratanasathien, S., Hanks, C.T., and Sun, Z. (1996). In vitro IL-1β and TNF-α release from THP-1 monocytes in response to metal ions. Dent. Mater. *12*, 322–327.

Waugh, D.J.J., and Wilson, C. (2008). The Interleukin-8 Pathway in Cancer. Clin. Cancer Res. *14*, 6735.

Weinhouse, S. (1976). The Warburg hypothesis fifty years later. Z. Für Krebsforsch. Klin. Onkol. Cancer Res. Clin. Oncol. *87*, 115–126.

Werth, N., Beerlage, C., Rosenberger, C., Yazdi, A.S., Edelmann, M., Amr, A., Bernhardt, W., von Eiff, C., Becker, K., Schäfer, A., et al. (2010). Activation of Hypoxia Inducible Factor 1 Is a General Phenomenon in Infections with Human Pathogens. PLoS ONE *5*, e11576.

West, A.P., Brodsky, I.E., Rahner, C., Woo, D.K., Erdjument-Bromage, H., Tempst, P., Walsh, M.C., Choi, Y., Shadel, G.S., and Ghosh, S. (2011). TLR signalling augments macrophage bactericidal activity through mitochondrial ROS. Nature *472*, 476–480.

Wise, D.R., and Thompson, C.B. (2010). Glutamine Addiction: A New Therapeutic Target in Cancer. Trends Biochem. Sci. *35*, 427–433.

Wiseman, H., and Halliwell, B. (1996). Damage to DNA by reactive oxygen and nitrogen species: role in inflammatory disease and progression to cancer. Biochem. J. *313*, 17–29.

Wolf, A., Agnihotri, S., Micallef, J., Mukherjee, J., Sabha, N., Cairns, R., Hawkins, C., and Guha, A. (2011). Hexokinase 2 is a key mediator of aerobic glycolysis and promotes tumor growth in human glioblastoma multiforme. J. Exp. Med. *208*, 313.

Wolpaw, A.J., and Dang, C.V. (2018). Exploiting Metabolic Vulnerabilities of Cancer with Precision and Accuracy. Trends Cell Biol. *28*, 201–212.

Wong, A.K., Park, C.Y., Greene, C.S., Bongo, L.A., Guan, Y., and Troyanskaya, O.G. (2012). IMP: a multi-species functional genomics portal for integration, visualization and prediction of protein functions and networks. Nucleic Acids Res. *40*, W484–W490.

Wong, A.K., Krishnan, A., Yao, V., Tadych, A., and Troyanskaya, O.G. (2015). IMP 2.0: a multi-species functional genomics portal for integration, visualization and prediction of protein functions and networks. Nucleic Acids Res. *43*, W128–W133.

Wong, C.C.-L., Au, S.L.-K., Tse, A.P.-W., Xu, I.M.-J., Lai, R.K.-H., Chiu, D.K.-C., Wei, L.L., Fan, D.N.-Y., Tsang, F.H.-C., Lo, R.C.-L., et al. (2014). Switching of Pyruvate Kinase Isoform L to M2 Promotes Metabolic Reprogramming in Hepatocarcinogenesis. PLOS ONE *9*, e115036.

World Health Organisation. (2018). Cancer: Statistics. Accessed: 8 January 2019. https://www.who.int/news-room/fact-sheets/detail/cancer

Wouters, B.J., Löwenberg, B., Erpelinck-Verschueren, C.A.J., van Putten, W.L.J., Valk, P.J.M., and Delwel, R. (2009). Double CEBPA mutations, but not single CEBPA mutations, define a subgroup of acute myeloid leukemia with a distinctive gene expression profile that is uniquely associated with a favorable outcome. Blood *113*, 3088.

Wu, X., Wang, J., Cui, X., Maianu, L., Rhees, B., Rosinski, J., So, W.V., Willi, S.M., Osier, M.V., Hill, H.S., et al. (2007). The effect of insulin on expression of genes and biochemical pathways in human skeletal muscle. Endocrine *31*, 5–17.

Wu, Y., Antony, S., Meitzler, J.L., and Doroshow, J.H. (2014). Molecular mechanisms underlying chronic inflammation-associated cancers. Cancer Lett. *345*, 164–173.

Xaus, J., Comalada, M., Valledor, A.F., Lloberas, J., López-Soriano, F., Argilés, J.M., Bogdan, C., and Celada, A. (2000). LPS induces apoptosis in macrophages mostly through the autocrine production of TNF-α. Blood *95*, 3823.

Xia, L., Wang, X.-R., Wang, X.-L., Liu, S.-H., Ding, X.-W., Chen, G.-Q., and Lu, Y. (2016). A Novel Role for Pyruvate Kinase M2 as a Corepressor for P53 during the DNA Damage Response in Human Tumor Cells. J. Biol. Chem. *291*, 26138–26150.

Ying, M.-Z., Wang, J.-J., Li, D.-W., Yu, G.-Z., Wang, X., Pan, J., Chen, Y., and He, M.-X. (2010). The p300/CBP - associated factor is frequently down-regulated in intestinal-type gastric carcinoma and constitutes a biomarker for clinical outcome. Cancer Biol. Ther. *9*, 312–320.

Yoeli-Lerner, M., and Toker, A. (2006). Akt/PKB Signaling in Cancer: A Function in Cell Motility and Invasion. Cell Cycle *5*, 603–605.

Yokochi, T., Kato, Y., Sugiyama, T., Koide, N., Morikawa, A., Jiang, G.-Z., Kawai, M., Yoshida, T., Fukada, M., and Takahashi, K. (1996). Lipopolysaccharide induces apoptotic cell death of B memory cells and regulates B cell memory in antigen-nonspecific manner. FEMS Immunol. Med. Microbiol. *15*, 1–8.

Yoshimura, A., Naka, T., and Kubo, M. (2007). SOCS proteins, cytokine signalling and immune regulation. Nat. Rev. Immunol. *7*, 454–465.

Younes, M., Brown, R.W., Stephenson, M., Gondo, M., and Cagle, P.T. (1997). Overexpression of Glut1 and Glut3 in stage I nonsmall cell lung carcinoma is associated with poor survival. Cancer *80*, 1046–1051.

Yu, X., and Li, S. (2016). Non-metabolic functions of glycolytic enzymes in tumorigenesis. Oncogene *36*, 2629.

Yu, H., Pardoll, D., and Jove, R. (2009a). STATs in cancer inflammation and immunity: A leading role for STAT3. Nat. Rev. Cancer *9*, 798–809.

Yu, S.-T., Chen, L., Wang, H.-J., Tang, X.-D., Fang, D.-C., and Yang, S.-M. (2009b). hTERT promotes the invasion of telomerase-negative tumor cells in vitro. Int. J. Oncol. *35*, 329–336.

Yuan, Z., Guan, Y., Wang, L., Wei, W., Kane, A.B., and Chin, Y.E. (2004). Central Role of the Threonine Residue within the p+1 Loop of Receptor Tyrosine Kinase in STAT3 Constitutive Phosphorylation in Metastatic Cancer Cells. Mol. Cell. Biol. *24*, 9390–9400.

Yun, B., Zhang, T., Azad, M.A.K., Wang, J., Nowell, C.J., Kalitsis, P., Velkov, T., Hudson, D.F., and Li, J. (2018). Polymyxin B causes DNA damage in HK-2 cells and mice. Arch. Toxicol.

Yuneva, M., Zamboni, N., Oefner, P., Sachidanandam, R., and Lazebnik, Y. (2007). Deficiency in glutamine but not glucose induces MYC-dependent apoptosis in human cells. J. Cell Biol. *178*, 93–105.

Zamzami, N., and Kroemer, G. (2001). The mitochondrion in apoptosis: how Pandora's box opens. *2*, 67.

Zhang, J.-M., and An, J. (2007). Cytokines, Inflammation and Pain. Int. Anesthesiol. Clin. *45*, 27–37.

Zhang, X.-Y., Zhang, M., Cong, Q., Zhang, M.-X., Zhang, M.-Y., Lu, Y.-Y., and Xu, C.-J. (2018). Hexokinase 2 confers resistance to cisplatin in ovarian cancer cells by enhancing cisplatin-induced autophagy. Int. J. Biochem. Cell Biol. *95*, 9–16.

Zhao, T., Zhu, Y., Morinibu, A., Kobayashi, M., Shinomiya, K., Itasaka, S., Yoshimura, M., Guo, G., Hiraoka, M., and Harada, H. (2014). HIF-1-mediated metabolic reprogramming reduces ROS levels and facilitates the metastatic colonization of cancers in lungs. Sci. Rep. *4*, 3793.

Zhao, Y.H., Zhou, M., Liu, H., Ding, Y., Khong, H.T., Yu, D., Fodstad, O., and Tan, M. (2009). Upregulation of lactate dehydrogenase A by ErbB2 through heat shock factor 1 promotes breast cancer cell glycolysis and growth. Oncogene *28*, 3689–3701.

Zhong, J.-T., and Zhou, S.-H. (2017). Warburg effect, hexokinase-II, and radioresistance of laryngeal carcinoma. Oncotarget *8*, 14133–14146.

Zhou, M., Bracci, P.M., McCoy, L.S., Hsuang, G., Wiemels, J.L., Rice, T., Zheng, S., Kelsey, K.T., Wrensch, M.R., and Wiencke, J.K. (2015). Serum macrophage-derived chemokine/CCL22 levels are associated with glioma risk, CD4 T cell lymphopenia and survival time. Int. J. Cancer J. Int. Cancer *137*, 826–836.

Zinkernagel, A.S., Johnson, R.S., and Nizet, V. (2007). Hypoxia inducible factor (HIF) function in innate immunity and infection. J. Mol. Med. *85*, 1339–1346.

456991:Inline_Submission

ORIGINALITY REPORT

9%	5%	7%	%
SIMILARITY INDEX	INTERNET SOURCES	PUBLICATIONS	STUDENT PAPERS

PRIMARY SOURCES

1	Systems Biology of Free Radicals and Antioxidants, 2014. Publication	1%
2	pt.scribd.com Internet Source	1%
3	es.scribd.com Internet Source	<1%
4	Mitochondria The Anti- cancer Target for the Third Millennium, 2014. Publication	<1%
5	d-nb.info Internet Source	<1%
6	Zuberi, K., M. Franz, H. Rodriguez, J. Montojo, C. T. Lopes, G. D. Bader, and Q. Morris. "GeneMANIA Prediction Server 2013 Update", Nucleic Acids Research, 2013. Publication	<1%
7	www.jove.com Internet Source	<1%